The Dissertation Committee for Christina Elisa Bonsell Certifies that this is the approved version of the following Dissertation:

Factors that influence the distribution of the Arctic endemic kelp, *Laminaria solidungula* (J. Agardh 1868)

Committee:

Kenneth H. Dunton, Supervisor

Craig Aumack

Bryan Black

Deana Erdner

Factors that influence the distribution of the Arctic endemic kelp, *Laminaria solidungula* (J. Agardh 1868)

by

Christina Elisa Bonsell

Dissertation

Presented to the Faculty of the Graduate School of

The University of Texas at Austin

in Partial Fulfillment

of the Requirements

for the Degree of

Doctor of Philosophy

The University of Texas at Austin

May 2019

Dedication

To Etta, Gralinda, and Lilo, who gave me the will to make a path.

Acknowledgements

Many people contributed to this research and my growth as a scientist. First, I want to thank my advisor Ken Dunton for providing guidance, support and energy throughout this project. My committee gave constructive feedback and advice that improved the quality of my research and writing. Discussion with and instruction by Dean Erdner and Ingrid Sassenhagen were essential to the kelp genetics research. Susan Schonberg lent taxonomic expertise and taught me how to be an Arctic field biologist. Phil Bucolo and Arely Muth provided generous mentorship and collaboration, even when conditions were less than mint. I am indebted to Ted Dunton and John Dunton, whose unrivaled technical expertise and good humor kept me and my science going during long, hiccupy field seasons. I am also extremely grateful for the logistical support by personnel from Endicott Production Facility and Service Area 10. This project would not have happened without instrumental assistance and emotional support from my labmates and fellow Arctic graduate students: Kim Jackson, Carrie Harris, Sara Wilson, Victoria Congdon, Meaghan Cuddy, Craig Connolly, Claire Griffin, and Nathan McTigue. Sarah Brown, Joe Ripley, Clay McClure, and Liz Murphy aided with lab work and logistics. Statistical analyses, particularly of current data, were strengthened with the help from Lindsay Scheef and Erin Frolli. Carpenters on the UTMSI Facilities staff helped design and build settling plate moorings. Andrew Esbaugh and Patrick Larkin provided essential lab space for molecular work after Hurricane Harvey.

In my first Arctic field season, fate stuck me on an icebreaker with Jordann Young, whose invaluable friendship has given me strength ever since. Kiley Seitz enriched my graduate school experience and answered many silly molecular biology questions. I can now call myself a scientist thanks to three key people who encouraged me early on: Scott Simon, who opened the door; Shannon Jarrell, who guided me into research; and Paul Dayton, who gave me many things to aspire to, but emphasized that being a good human is the most important. I am also especially thankful for Nick Reyna's patient support and

positive encouragement. Finally, I would like to thank my parents for giving me the opportunity to succeed. I am very fortunate.

Funding for this research was provided by BOEM Award Number M12AS00001, a Phycological Society of America Student Grant-In-Aid, and various fellowships from UT Austin and UTMSI. Field research took place in Iñupiat ancestral territory.

Abstract

Factors that influence the distribution of the Arctic endemic kelp, *Laminaria solidungula* (J. Agardh 1868)

Christina Elisa Bonsell, Ph.D.

The University of Texas at Austin, 2019

Supervisor: Kenneth H. Dunton

Foundation species, including kelps, have a disproportionate effect on ecosystems by exerting strong influence on food webs and community structure. Shifts in kelp species' distributions are occurring worldwide, and are especially anticipated in the Arctic due to habitat modification by climate change. On Arctic inner shelves, the kelp *Laminaria solidungula* (J. Agardh 1868) can dominate nearshore rocky areas, and provide physical structure and subsidies of year-round primary production in a highly seasonal region. However, controls over the distribution of this Arctic endemic species are not well understood. A species' interactions with the abiotic and biotic environment, its dispersal dynamics, and evolutionary history all control its ultimate range and spatial arrangement. This work describes how these factors impact *L. solidungula* distribution across multiple scales, with focus on the Stefansson Sound Boulder Patch, Beaufort Sea, Alaska. First, although the Stefansson Sound open-water season has lengthened by ~17 days since 1979, annual kelp growth shows no long-term trends because attenuation by suspended sediments causes pervasive low-light conditions during summer (mean light attenuation: 0.5-0.8 m^{-1}), negating any positive impacts of decreased ice-cover. Second, the abiotic environment of the Boulder Patch undergoes significant seasonal changes, mediated by physiography and bathymetry, which impact the spatial arrangement of *L. solidungula* and other epilithic

species. A site within 4 km of river inputs experiences salinity drops of ~30 corresponding to the spring freshet. Crustose coralline algae (0-19% average cover) is completely absent at this site, but cover increases with distance from river inputs. Red algae (47-79%) and kelp (2-19%) cover shows no clear environmental correlations, and are likely regulated by multiple factors. Importantly, no *L. solidungula* recruited to settlement tiles after three years of deployment. Finally, population genetics suggest Beaufort Sea *L. solidungula* is one large interbreeding population (population differentiation as global F_{ST}: 0.01) assisted by the regional current regime, though smaller scale differentiation occurs within the Boulder Patch. Additionally, Beaufort Sea *L. solidungula* is genetically distinct from those in other areas of the Western Arctic Ocean Basin. This work represents an important baseline in ecological and genetic characteristics of *L. solidungula* in the rapidly changing Arctic Ocean.

Table of Contents

List of Tables

List of Figures

Introduction

Kelp are large brown algae in the order Laminariales that provide vital services to coastal ecosystems worldwide. By dominating rocky marine habitats, kelp act as foundation species that offer structural complexity and habitat that increases local biodiversity and biomass (Christie et al. 2009; Teagle et al. 2017). Through primary production, kelp capture carbon and introduce it to both local food webs and adjacent ecosystems via direct grazing, fragmentation, and drift (Vetter 1995; Polis and Hurd 1996; Fredriksen 2003). In highly seasonal environments, kelp can act as an important basal food source in winter months and thereby contribute to regional food web stability (Dunton and Schell 1987; McMeans et al. 2015). Kelps can also alter the surrounding physiochemical environment by attenuating currents (e.g. Kitching et al. 1934; Jackson and Winant 1983; Gaylord et al. 2007, 2012), taking up nutrients (e.g. Probyn and Mcquaid 1985), and altering the chemical environment (e.g. Delille et al. 2009; Krause-Jensen et al. 2016). Some hypothesize that kelp distribution in the Northeast Pacific, and associated distribution of marine resources, shaped human migration patterns into North America ("the kelp highway hypothesis", Erlandson et al. 2007).

Due to their use by humans and their general charisma (Jackson et al. 2016), western scientists have studied kelps for centuries. Baseline data on kelp distribution dating back to the early 20th century contributes to the knowledge that many regions of the world are experiencing decadal-scale changes in kelp distribution (Steneck et al. 2002; Krumhansl et al. 2016). The ultimate reason for the majority of these shifts is altered climate conditions due to the anthropogenic input of greenhouse gases into the atmosphere (Steneck et al. 2002). Warmer oceans push kelp distributions poleward and contribute to kelp decline in lower-latitudes, but enhance kelp biomass in higher latitudes (Krause-Jensen and Duarte 2014; Wernberg et al. 2015; Vergés et al. 2016; Pessarrodona et al. 2018). In the Arctic, increases in kelp biomass are expected due to warming and decreased ice extent (Krause-Jensen et al. 2012; Krause-Jensen and Duarte 2014). However, the

invasion of boreal kelp species may coincide with declines in Arctic-adapted kelp species and their associated biota. Redistribution of foundation species, such as kelps, will profoundly affect the rearrangement of biodiversity and ecosystem functions in the emerging Arctic. Knowledge of Arctic kelp distribution, dispersal patterns, and environmental interactions is key to predict and evaluate future ecosystem change. Scientific investigation of these topics also reveals ecosystem dynamics of the rapidly changing Arctic coastal ocean.

Baseline biological and ecological knowledge of high Arctic kelp is scarce due to the logistical challenges associated with working in the region (Wilce 2016; Krumhansl et al.; Filbee-Dexter et al. 2019). Current awareness of Arctic kelp distribution relies heavily on observations that are decades old (Filbee-Dexter et al. 2019). Nevertheless, naturalists associated with the "Heroic Age" of Arctic exploration (mid 19th to early 20th century) contributed important foundational work to the body of Arctic phycology. The 1858 Torell Expedition to Svalbard led to the description of the Arctic endemic kelp species *Laminairia solidungula* by J. G. Agardh (1862), who depicted the annual growth cycle that leads to the species' undulating blade morphology (Fig. 1). Kjellman (1883) published "The Algae of the Arctic Sea", the first significant treatise on the topic, which described distribution and natural history from expeditions throughout the European-Russian Arctic including the Vega Expedition through the Northeast Passage. Therein, he explains how sea ice and the darkness of the polar night limits benthic algae distribution. He further postulates that the low salinities near the mouths of large Arctic rivers do not "offer tolerable or suitable conditions for the development of… the majority of arctic algae" (Kjellman 1883 p. 28). Technological advances afford the modern scientist the ability to investigate the mechanisms of Kjellman's observations and test his hypotheses linking Arctic environmental conditions to macroalgal growth and distribution.

Arctic marine ecosystems can be classified based on environmental regime, defined by current flows, regional river influence, ice conditions, and the nature of the coastline (Carmack and Wassmann 2006). Much of the current scientific understanding about rocky

subtidal areas in the Arctic, including kelp beds, comes from continued research in the glacial archipelago of Svalbard. However, erosional coastlines make up the majority of arctic nearshore areas (Lantuit et al. 2012) and can host large kelp beds where rocky substrate is available (Dunton et al. 1982; Filbee-Dexter et al. 2019). These inner shelf regions, such as the Alaskan Beaufort Sea, are characterized by significant erosion and freshwater input (Carmack and Wassmann 2006; Lantuit et al. 2012). In winter, the coastal ocean is covered by landfast sea ice, which breaks up in spring with help from an intense pulse of land-derived freshwater (the freshet) (Barry et al. 1979). Estuarine conditions persist throughout the summer, as freshwater from land and melted sea ice mixes with marine water masses (Carmack and Wassmann 2006; McClelland et al. 2012). In fall, the water column homogenizes as freezing conditions set in and the sea ice forms again (Weingartner et al. 2017). The shallow, estuarine, and soft-sediment nature of these areas expose local kelp beds to a suite of environmental conditions that are distinct from those of glacial fjords. The benthic community afforded by these habitats represent "hotspots" of regional diversity (Dunton and Schonberg 2000) and contribute important lower trophic level organisms to a regional food web that supports andromymous fishes, marine mammals, and native peoples (Connors 1984; Craig et al. 1984; Craig 1984; Frost and Lowry 1984).

The kelp *L. solidungula*, the only Arctic endemic kelp, is a dominant species in Arctic inner shelf kelp beds, including those in Alaska (Dunton et al. 1982; Filbee-Dexter et al. 2019). This species provides biogenic structure and a subsidy of year-round primary production in a highly seasonal region (Dunton et al. 1982; Dunton and Schell 1987). The macroscopic sporophyte of this species consists of a single, thick blade, a short stipe, and a discoid holdfast ("soli-": solitary/single, "-ungula": hoof/foot). Due to the alternating seasonal cycles of light and nitrogen in this environment, the sporophyte undergoes an annual growth cycle: carbohydrate reserves created via photosynthesis during light periods to fuel growth of a new blade segment in the dark winter when nitrate is available (Chapman and Lindley 1980; Dunton 1984; Dunton 1985). Growth is mainly controlled by

light, which is related to the annual solar cycle as well as dynamics of sediment-laden ice and summer wind-derived turbidity (Dunton 1990; Aumack et al. 2007). *L. solidungula* is distributed across the Arctic as well as in deep, cold waters of subpolar areas including Newfoundland. This environmental affinity may inhibit local persistence in the face of warming Arctic waters.

The Arctic is warming at a faster rate than any other region (IPCC 2014), with significant effects on the marine environment. Sea ice cover has decreased at a rate of ~13.3% per decade since the 1970s (Serreze and Stroeve 2015). Rates of precipitation and river discharge have also increased (McClelland et al. 2006, Rawlins et al. 2010). Arctic-wide, coastal erosion rates are 0.5 m yr^{-1}, but have been measured up to 25 m yr^{-1} at certain inner shelf locations (Jones et al. 2008; Lantuit et al. 2012; Gunther et al. 2015). As a result, ecosystems are undergoing a suite of transformations, including shifts in primary production, species distributions, and biodiversity (Michel et al. 2012; Bluhm et al. 2011; Grebmeier 2012). The northward range expansion of species of diatoms (Reid et al. 2007), bivalves (Berge et al. 2005), and fish demonstrate that "the coming Arctic invasion" (Vermeij and Roopnarine 2008) is occurring across all taxonomic groups. Overall, warming is hypothesized to enhance diversity in the Arctic and thereby increase the importance of interspecific interactions such as predation and competition (Vermeij and Roopnarine 2008; Michel et al. 2012). Furthermore, direct anthropogenic impacts on species ranges will only compound over time, as ensured by continuous oil exploration and the opening of the Northwest Passage for shipping routes. Arctic change thus includes alterations to biotic and abiotic environments as well as species' dispersal vectors, which will reshape distributions of native species. Arctic ecosystems are especially prone to perturbations caused by alterations to the local species pool because of their overall lack of functional redundancy in (Post et al. 2009). Understanding the regulation of Arctic species distributions and evaluate them for baselines is integral for comparing future changes. This is especially important for foundation species such as *L. solidungula*, whose presence or absence could have substantial repercussions for ecosystem function.

A species' interactions with the abiotic and biotic environment, its dispersal dynamics, and its evolutionary history all control its ultimate distribution. This work describes how these factors determine *L. solidungula* distribution across multiple scales in the Alaskan Arctic. In Chapter 1, I use multidecadal timeseries to test the hypothesis that length of the open water season, which has increased with warming, has positive impacts on *L. solidungula* growth in the Stefansson Sound Boulder Patch, a kelp bed adjacent to Prudhoe Bay, Alaska. Chapter 2 describes the seasonal cycle in physiochemical conditions in Stefansson Sound in the context of setting the environmental stage for Boulder Patch community ecology. These data are paired with Boulder Patch benthic community structure data in Chapter 3 to hypothesize mechanisms for spatial differences in the benthic assemblage. Additionally, this chapter explores the role of early life history in community development by examining the timescale and spatial variability of recruitment and succession dynamics. Finally, Chapter 4 examines *L. solidungula* through the lens of population genetics to describe connectivity and relatedness both within the Beaufort Sea and across the Western Arctic Ocean Basin.

Chapter One: Long-term patterns of benthic irradiance and kelp production in the central Beaufort Sea reveal implications of warming for Arctic inner shelves[1]

ABSTRACT

This study synthesizes a multidecadal dataset of annual growth of the Arctic endemic kelp *Laminaria solidungula* and corresponding measurements of *in situ* benthic irradiance from Stefansson Sound in the central Beaufort Sea. We incorporate long-term data on sea ice concentration (National Sea Ice Data Center) and wind (National Weather Service) to assess how ice extent and summer wind dynamics affect the benthic light environment and annual kelp production. We find evidence of significant changes in sea ice extent in Stefansson Sound, with an extension of the ice-free season by approximately 17 days since 1979. Although kelp elongation at 5-7 m depths varies significantly among sites and years (3.8 to 49.8 cm yr^{-1}), there is no evidence for increased production with either earlier ice break-up or a longer summer ice-free period. This is explained by very low light transmittance to the benthos during the summer season (mean daily percent surface irradiance ±SD: 1.7±3.6 to 4.5±6.6, depending on depth, with light attenuation values ranging from 0.5 to 0.8 m^{-1}), resulting in minimal potential for kelp production on most days. Additionally, on month-long timescales (35 days) in the ice-free summer, benthic light levels are negatively related to wind speed. The frequent, wind-driven resuspension of sediments following ice break-up significantly reduce light to the seabed, effectively nullifying the benefits of an increased ice-free season on annual kelp growth. Instead, benthic light and primary production may depend substantially on the 1-3 week period surrounding ice break-up when intermediate sea ice concentrations reduce wind-driven sediment resuspension. These results suggest that both benthic and water column primary

[1] Based on prior publication: Bonsell, C., and K. H. Dunton. 2018. Long-term patterns of benthic irradiance and kelp production in the central Beaufort Sea reveal implications of warming for Arctic inner shelves. Prog. Oceanogr. 162: 160–170. Author contribution statement: CB and KHD preformed and oversaw data collection. CB analyzed and interpreted results. CB conceptualized the study and wrote the manuscript with input from KD.

production along the inner shelf of Arctic marginal seas may decrease, not increase, with reductions in sea ice extent.

INTRODUCTION

Seasonal sea ice cover plays a prominent role in marine primary productivity in high-latitude ecosystems, as it can set the timing of peak production and determine annual light budgets (Kahru et al. 2011; Clark et al. 2013; Ji et al. 2013; Post et al. 2013). In the Arctic Ocean, there has been a striking decline in sea ice extent since the onset of observations via satellite measurements, at a rate of approximately 13.3% loss in area per decade (Serreze and Stroeve 2015). Despite on-going efforts by scientists to investigate the effects of sea ice loss on pelagic production (reviewed in Wassmann and Reigstad 2011), only a few studies to date have addressed the direct consequences on benthic production (Krause-Jensen et al. 2012; Clark et al. 2013; Krause-Jensen and Duarte 2014). In coastal Arctic systems, benthic primary production by macro- and micro-algae in Arctic waters is important to ecosystem production, elemental cycling, and food web dynamics, especially during times of limited pelagic production (Dunton and Schell 1987; Glud et al. 2009; McMeans et al. 2015; Renaud et al. 2015). Additionally, bio-physical processes in shallow, nearshore Arctic areas, where much of this production takes place, remain understudied due to logistical constraints (e.g. Fritz et al. 2017). Changes to production in these areas would have broad consequences for Arctic ecosystem function.

Because of the strong annual cycle of solar irradiance in polar regions, seasonal sea ice and solar energy models predict that earlier dates of ice break-up will result in exponential increases in benthic light budgets (Clark et al. 2013). For instance, Krause-Jensen et al. (2012) and Clark et al. (2013) used existing gradients in seasonal ice cover in Greenland and Antarctica, respectively, to link lengthened ice-free seasons with increases in macroalgal production and hypothesized that future warming-driven reductions in seasonal sea ice extent and duration will enhance annual production by benthic macrophytes. These predictions contribute to the idea that Arctic coastal habitats will become increasingly macrophyte-dominated as Arctic warming continues, with

consequences for Arctic food webs and seawater chemistry (Clark et al. 2013; Krause-Jensen and Duarte 2014; Krause-Jensen et al. 2016). However, variations in underwater optical properties, which have a profound influence on light transmittance to the benthos and demonstrable impacts on benthic primary production (Van Duin et al. 2001), are largely overlooked in these analyses. Bartsch et al. (2016) hypothesized that enhanced sediment inputs from glacial melt caused a narrower euphotic zone during the open water season, leading to observed shallowing of peak biomass and shallower depth limit of kelps in Svalbard over the past two decades. The links between ice loss, irradiance at depth, and primary production appear to be multifaceted and warrant further investigation.

While ice cover determines irradiance at the water's surface, irradiance at depth depends on light attenuation in the water column. In the coastal Arctic Ocean, summer water transparency is influenced by concentrations of phytoplankton and sediments suspended in the water column. Concentrations of suspended sediments during the open-water summer in the coastal Beaufort Sea have been directly linked to increased light attenuation and decreased annual production by benthic macroalgae (Aumack et al. 2007). Many Arctic inner shelf areas (depth <10 m), such as the Alaskan Beaufort Sea coast, have particularly high suspended sediment concentrations due to shallow depth, persistence of unconsolidated sediments, and significant inputs by numerous rivers and streams (notably, the Arctic Ocean receives 11% of global river discharge, but only constitutes 1% or global ocean volume; McClelland et al. 2011). These sediments originate from coastal erosion, resuspension due to water motion, and fluvial inputs by Arctic rivers, which discharge the large majority of their annual suspended sediments loads by the end of the spring melt (Wegner et al. 2003; O'Brien et al. 2006; Walker et al. 2008). Because most river fluxes occur before the end of ice-break up, changes in wind direction and/or speed during the open-water period are the main drivers of temporal variability in underwater irradiance in the nearshore areas, as they are in other shallow aquatic systems (Van Duin et al. 2001). Annual benthic light budgets may consequently have a negative relationship with wind speeds during the ice-free season.

The primary objective of this paper is to examine how sea ice extent and wind dynamics affect variation in the annual benthic light budget and production by the Arctic endemic kelp *Laminaria solidungula* in the central Beaufort Sea. Since 1979, sea ice duration in the Beaufort Sea has decreased at an accelerating rate, while summertime easterly winds have increased in speed and frequency across the coastal region (Wood et al. 2013, 2015; Frey et al. 2015). These long-term environmental changes may have significant, but opposing, effects on long-term primary production patterns. Although lengthened ice-free season results in increased irradiance at the waters' surface, enhanced summer winds may degrade the underwater light climate. Frond elongation in *L. solidungula*, is entirely dependent on the utilization of photosynthetically derived carbon reserves produced the previous summer (Dunton and Schell 1986). The resulting annual growth has a strong correlation with the light budget of the preceding ice-free season (Dunton 1990). This species is ideal for assessing the biological effects of changes to the Arctic underwater light environment due to its enhanced capacity to respond to small changes in irradiance compared to other kelp species, particularly evident in its low saturating irradiance for photosynthesis (38 µmol photons sec^{-1}; Dunton and Jodwalis 1988).

Multidecadal time series that document biological responses to variations in regional climate in Arctic marine systems are rare, but critical for the development of accurate projections of future ecosystem change (Wassmann et al. 2011). Here, we synthesize a multidecadal dataset (collected from 1977-1992 and 2002-2008) and incorporate previously unpublished data (2012-2016), on benthic irradiance and kelp growth from Stefansson Sound in the central Beaufort Sea (Dunton 1990; Dunton et al. 1992, 2009; Aumack et al. 2007) to demonstrate the combined influence of seasonal ice extent and wind dynamics on the annual light budget, and annual kelp production. Additionally, we assess whether annual variations in *L. solidungula* growth relate to seasonal ice extent and summer wind dynamics. In doing so, this work highlights the importance of including factors that affect underwater light transmittance in projecting changes in primary productivity and ecosystem structure in Arctic marine ecosystems.

METHODS

Study Site

The Stefansson Sound Boulder Patch (hereafter 'the Boulder Patch') is an isolated rocky zone of boulders and cobbles covering an area of approximately 63 km^2 in a region dominated by soft sediment (Barnes and Reimnitz 1974; Fig. 1). Located in relatively shallow water (4-8 m) within 15 kilometers of the coast, the Boulder Patch remains a non-depositional environment despite its proximity to the Sagavanirktok River, which has a 1-2 week period of peak discharge in late May and early June (Dunton et al. 1982; Rember and Trefry 2004)

The epilithic community in the Boulder Patch is dominated by the kelp *L. solidungula* and represents a regional biodiversity hotspot. Research conducted in the area since the 1970s has focused primarily on characterizing the underwater light environment and the biological production of *L. solidungula* (Dunton 1985; Dunton and Schell 1986, 1987, Dunton et al. 1992, 2009; Henley and Dunton 1995; Aumack et al. 2007). Field studies have been nearly continuous since 1978 except for a single seven-year lapse (1993-2000), with ten long-term study sites occupied since 1984 (Fig. 1).

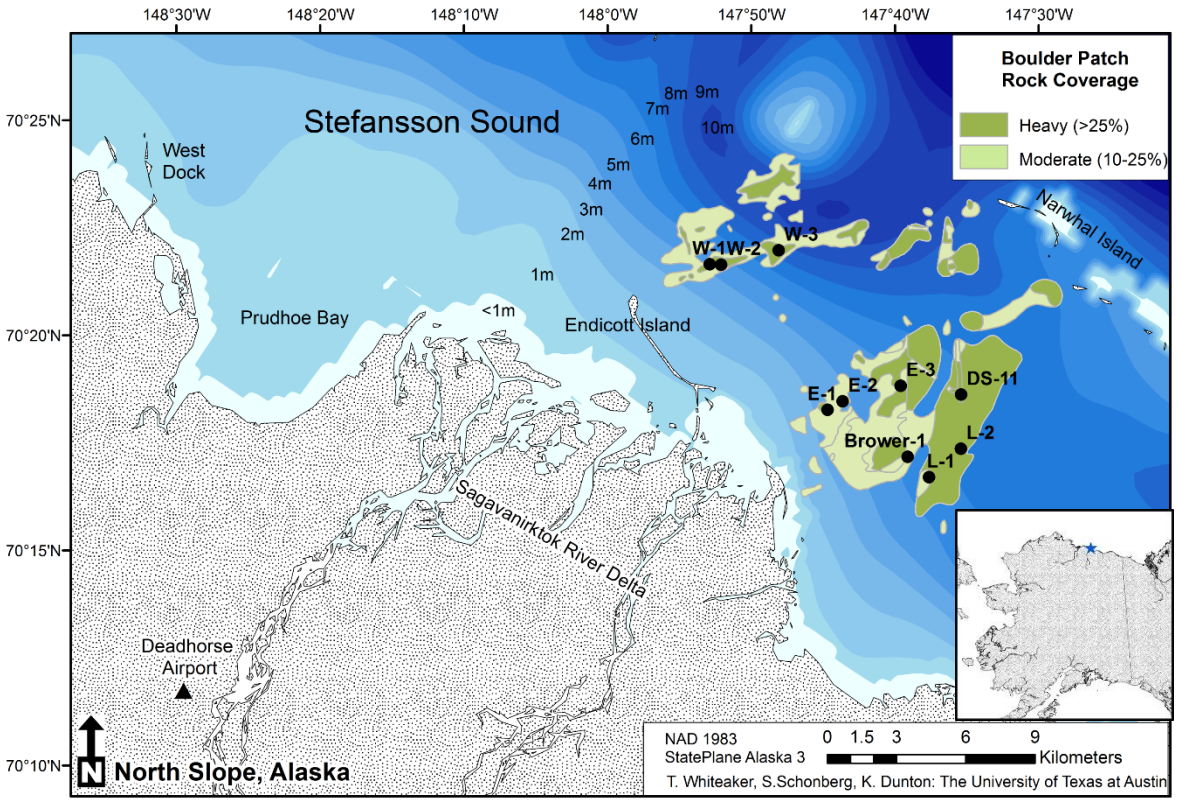

Figure 1.1: The Stefansson Sound Boulder Patch, showing location of long-term study sites in relation to percent rock cover in Stefansson Sound. Inset shows location of Stefansson Sound (blue star) in reference to Alaska.

Kelp production

Laminaria solidungula individuals from long-term study sites were collected by SCUBA divers at one- or two-year intervals. The thallus of this species consists of a single blade with multiple ovate growth sections, each representing one year of production. The blade section closest to the stipe represents production from the most recent year and the immediate distal section represents growth from the previous year. Because multiple years

of production can be measured from a single individual, this dataset spans from 1976 to 1990 and 1996 to 2015.

Benthic and surface irradiance

Spherical quantum sensors (LI-193SA, LI-COR Inc.), placed ~0.5 m above the benthos, were deployed for measurements of photosynthetically active radiation (PAR) at sites across the Boulder Patch (Fig. 1, Supp. Table 1). Sensors were deployed in conjunction with either CR21 (Campbell Scientific), LI-1000, LI-1400, or LI-1500 dataloggers (LI-COR Inc.), depending on the site and study year (Supp. Table 1). Cosine PAR sensors (LI-192SA, LI-COR Inc.) deployed in line with a LI-1000 datalogger collected continuous surface light measurements at East Dock in Prudhoe Bay (1986-1987) and Endicott Island (1987-2016; Fig. 1). Sensors were cleaned between deployments (once a year), as bio-fouling in this environment is negligible. Sensors made instantaneous measurements every minute and logged the average every 1 or 3 hours, depending on site and study year (Supp. Table 1). All PAR measurements were converted into total daily photon flux rate (mol m^{-2} day^{-1}) for analysis. Daily hours of saturating irradiance for *L. solidungula* (H_{sat}: hours with average photon flux rate ≥38 µmol photon m^{-2} sec^{-1}; Dunton and Jodwalis 1988) were also calculated, as this metric is more closely related to annual production than photon flux rate (Dunton 1990). For years with irradiance data for >90% of the year, annual H_{sat} was calculated at each site.

Sea Ice

Sea ice concentration from 1979-2016, measured via passive microwave data, was obtained from the National Sea Ice Data Center via the Arctic Data Integration Portal (http://portal.aoos.org) for the two 25 km^2 grid areas that contain the Boulder Patch. Values from the two areas mirrored each other closely over time and were therefore averaged daily. Dates of key events in the ice season (break-up start, break-up end, freeze-up start, and freeze-up end) were calculated using the algorithms described by Johnson and Eicken (2016). These events define the seasonality of direct incident solar radiation to the sea

surface. The length of the ice-free season was calculated as freeze-up start minus break-up end.

Wind

Wind speed and direction for West Dock in western Stefansson Sound (National Climate Data Center ID 9497645), spanning 1993-2016, were obtained from the National Weather Service Cooperative Observer Program (COOP) via the R package "r-noaa" (Chamberlain et al. 2016). Wind speed and direction for Deadhorse Airport, spanning 1973-2016, were obtained from the Alaska Airport Weather Observations Network (mesonet.agron.iastate.edu/ASOS/) and underwent quality control procedures before analysis. Coastal wind speed was estimated from the Deadhorse data using the linear relationship between wind speed at Deadhorse and West Dock (see *Results*). For consistency, we only use the estimated coastal wind speed in analyses relating to irradiance and kelp growth. To examine changes in summer winds over time, we used data confined by the dates of start of break-up and start of freeze-up for each year; for analyses relating wind to benthic light or kelp growth, we focused on wind data confined by the dates of end of break-up and start of freeze-up for each year. In concurrence with other studies in the region, storm events were defined as >6 consecutive hours of average wind speeds over 10 m/s, with direction defined by primary cardinal direction (e.g. winds from NNE were defined as N winds; Manson and Solomon 2007).

To assess the effect of wind speed on underwater light transmittance, we plotted the relationship between mean daily coastal wind speed (as estimated from Deadhorse) and daily percent surface irradiance. Due to noisy data, wind speeds were binned by rounding to the nearest whole number.

Production model

To assess the effects of ice extent and wind speed on annual kelp production, we used the model developed by Aumack et al (2007) to calculate daily production rates under given depth and suspended sediment concentrations. Briefly, this model uses incident radiation

and a suspended sediment concentration-specific light attenuation coefficient to estimate benthic irradiance to calculate *L. solidungula* production over the open-water season. We estimated incident radiation on each day of the year by averaging values for each day from all the years of surface irradiance measurements. We incorporated daily wind speeds by using estimates of suspended sediment concentrations under given wind speeds obtained in this region (Trefry et al. 2009, Aumack and Dunton *unpublished data*; Supp. Table 2). We confined the model to ice-free dates only and used daily average coastal wind speed. Annual carbon production was estimated for the average size of individuals from our long-term dataset (22.5 cm basal blade length). Modelled carbon production was compared to the long-term kelp growth dataset, with measured kelp growth converted into g C yr^{-1} based on previously derived relationships (Dunton and Jodwalis 1988; Aumack 2003).

Statistical analysis

Trends in ice events, wind speed, and kelp growth over time were assessed using linear regression analyses. The relative effects of year and site, and the interaction between the two terms, on kelp growth were determined using ANOVA. We tested the relationships between kelp growth (linear elongation in centimeters) and date of ice break up and length of ice free season by linear regression.

For years and sites with irradiance data for >90% of the summer period (July-September), we tested if ice break-up date and length of ice-free season predicted the annual benthic irradiance budget using linear models. For these data, cumulative H_{sat} was calculated for each day by inclusively summing H_{sat} from all previous days to determine the seasonality of potential kelp production.

For all years of irradiance data, the longest portion of the year with representative data for multiple sites and years from multiple decades is 27 July – 31 August. There were not adequate redundancies in sites across years for these dates, so separate one-way ANOVAs were conducted to test the individual effects of site and year on three irradiance variables: a) total annual irradiance, b) mean irradiance, and c) total H_{sat}. The relative effects of mean daily sea ice concentration and mean daily maximum wind speed, and the

interaction between the two terms, on the three irradiance variables for this 36-day period were determined by linear regressions. As westerly winds entrain turbid coastal water in the nearshore in this region, we also tested the effects of wind direction and proportion of westerly winds on the three irradiance variables using linear regression. We defined westerly wind as within 45^o of due west (270^o). To test the relative importance of this period of time to annual kelp production, the relationships between site-specific annual kelp growth and total irradiance, as well as between site-specific annual kelp growth and total H_{sat}, were each tested by linear regression.

All analyses were carried out using R (R Core Team, 2016). Directional data was analyzed and plotted using the R package "circular" (Lund and Agostinelli 2015).

RESULTS

Physical drivers: sea ice and winds

We found that the ice-free season in Stefansson Sound (end of break-up to start of freeze-up) lengthened during the period of this study. Dates between ice break-up and freeze-up increased from 74 days in 1979 to 132 days in 2016 (Fig. 2-3, Supp. Table 3). Duration of ice break-up, however, does not show any change (Fig. 3, Supp. Table 3).

Coastal wind speeds directly measured at West Dock and estimated from Deadhorse show no trends over time (linear regressions on daily summer wind speed and fraction of hours with wind speeds > 10 m/s, $p>0.05$, $R^2<0.1$). We also did not find evidence for a strengthening of easterly or westerly winds over time (linear regressions, $p>0.05$, $R^2<0.1$). From the 1993-2016 data, we calculated the linear relationship between West Dock and Deadhorse daily wind speeds as

(Eq. 1) $$Speed_{West\ Dock} = 1.40 + 1.04 * Speed_{Deadhorse}$$

where speeds are in m s^{-1} (linear regression, $p<0.05$, $R^2=0.63$). Wind direction data for both stations are not vonMises distributed and therefore could not be analyzed statistically for

trends over time. We discerned that mean wind direction at each station varies between years (particularly at Deadhorse), but typically originates from the east at West Dock and from the northeast at Deadhorse (Fig. 4).

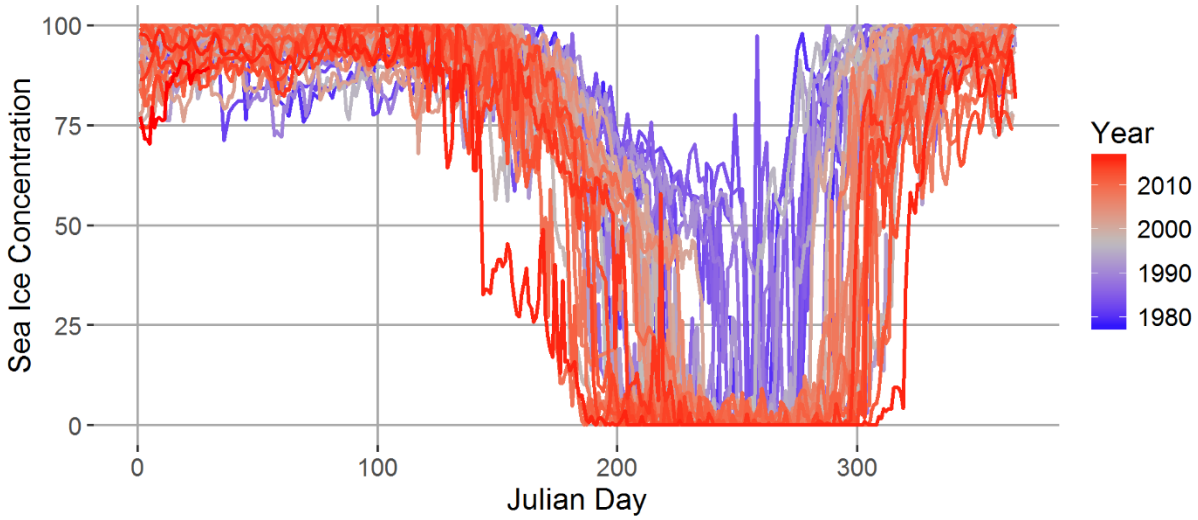

Figure 1.2: Sea ice concentration by Julian Day in Stefansson Sound over a 38-year period (January 1979-2017) illustrates the lengthening of the open water season and the decrease in summer ice concentration over time.

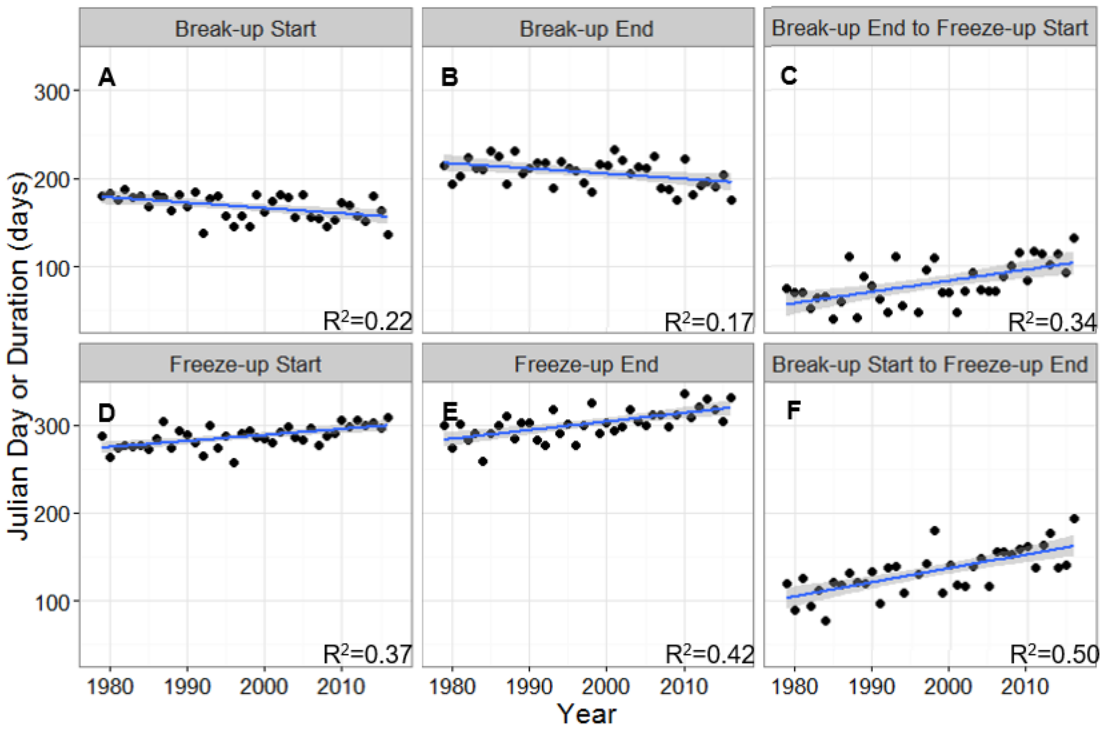

Figure 1.3: Key events related to freeze-up and break-up by Julian Day (A-B,D-E) or duration of event in days (C,F). Generally, break-up is occurring earlier and freeze-up later over the 38-year period. Blue line represents the linear relationship ±SE (grey shading).

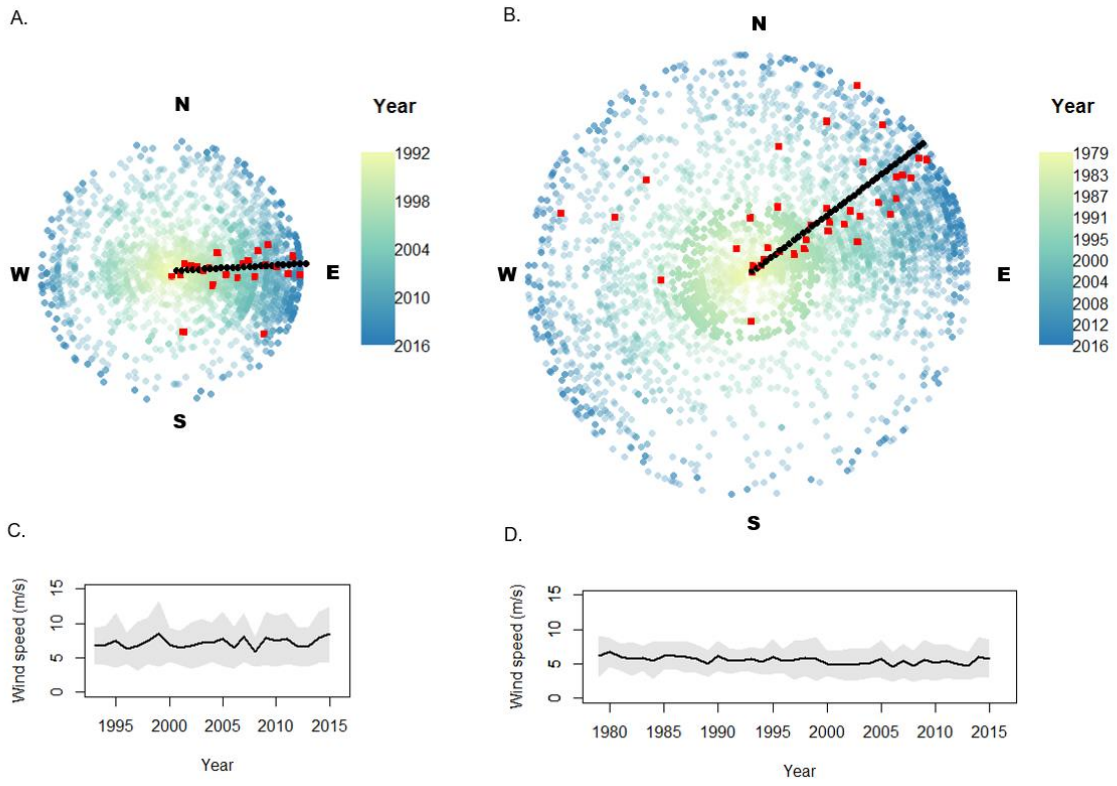

Figure 1.4: Daily summer wind variables over time for West Dock (A,C) and Deadhorse Airport (B,D). The distributions of daily mean wind direction (A,B) show that winds tend to originate from the east. The earliest year of measurement is the most interior circle of points, the latest year is the most exterior. Semi-transparent points indicate daily average wind direction, colored by year. Opaque red squares indicate annual mean direction. Black line indicates overall mean direction for all years. Daily wind speeds (C,D) are shown as annual means ±SD (black line and grey shading). Wind speed varies between summers, but shows no long-term trends.

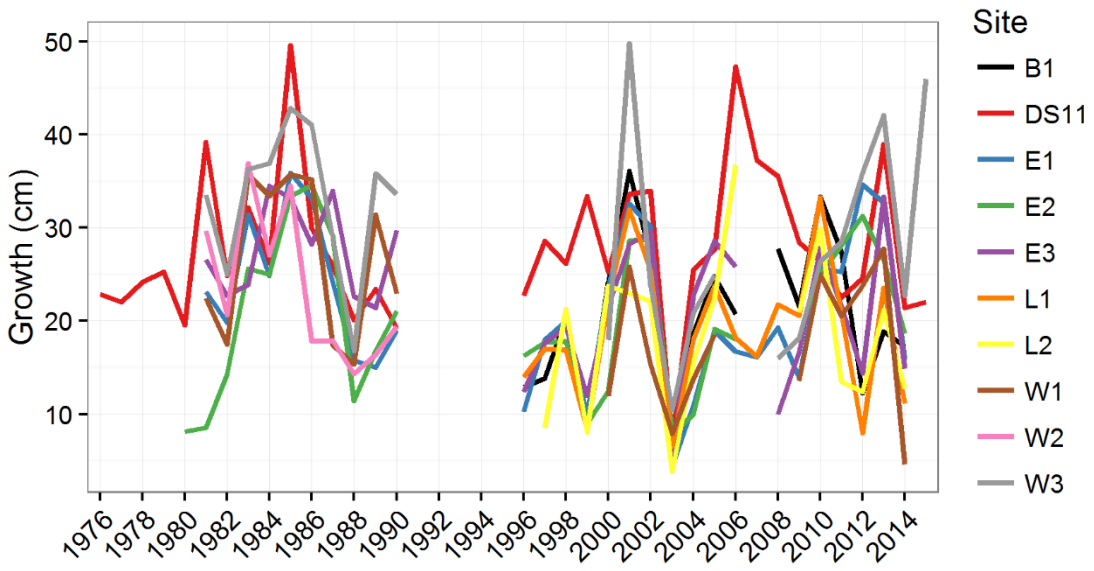

Figure 1.5: Mean Laminaria solidungula growth (cm) varies between sites and years, with some years showing strong annual patterns (e.g. 2001 and 2003).

In situ kelp growth and benthic irradiance: relationships to sea ice and wind

Analysis of the long-term data shows that kelp growth (as measured by blade elongation) in the Boulder Patch fluctuates over time and between sites (Fig. 5), although there is more variation in growth between sites than between years (SS_{Site}=80127, $F_{Site}(9,8936)$=105, -p<0.01 SS_{Year}=442890, $F_{Year}(34,8936)$=153, p<0.01). The relationship between annual kelp growth across the Boulder Patch and the length of the open-water season is not significant (linear regression, p>0.05, R^2<0.1).

Benthic irradiance at all sites displays strong seasonality, with some variation in maximum daily photon flux per year (Fig. 6). We only have data for the entire summer for a couple of years, confined mostly to the late 1980s and early 1990s, but we did not find any trends over time in the annual maximum daily photon flux rate (linear regressions performed for each site, p>0.05, R^2<0.1). Under ice cover, no measurable light occurs except at some sites in some years in the spring under "clean ice" (Dunton 1984), until around the time of the freshet when irradiance levels return to zero (Fig. 6). The first significant light transmittance occurs after ice break-up has begun (Figs. 6 and 7). Overall

summer light levels are low, with the majority of days lacking light levels that approach saturation irradiance for *Laminaria solidungula* (Table 1). Interestingly, these data show that the days surrounding ice break up contribute strongly to annual H_{sat} for a given site, sometimes over 50% of the annual value (Fig. 7).

Our analysis of data from 27 July – 31 August showed no significant differences between sites for mean daily benthic irradiance (MDI), total benthic irradiance (TBI), or total H_{sat} (TH). However, we detected significant differences between years for this period ($SS_{MDI\sim Year}$=10.58, $F_{MDI\sim Year}$ (6,18)=9.95, p <0.01; $SS_{TBI\sim Year}$=12102, $F_{TBI\sim Year}$ (6,18)=10.54, p<0.01; $SS_{TH\sim Year}$=85591, $F_{TH\sim Year}$ (6,18)=11.8, p<0.01). TBI and TH from this period do not predict annual kelp growth (linear regressions, p>0.05, R^2<0.1). We did not find significant effects of mean daily sea ice concentration, or the interaction between ice concentration and mean daily maximum wind speed on MDI, TBI, or TH. However, mean daily maximum wind speed alone significantly affects MDI (linear regression, p<0.05, R^2=0.24), TBI (linear regression, p<0.05, R^2=0.24), and TH (linear regression, p<0.05, R^2=0.19). This effect of wind is always negative. Plots of binned mean daily wind speed compared to percent surface irradiance for all ice-free dates at each site echo this negative relationship (Fig. 8). In contrast, there is no linear relationship between daily percent surface irradiance and sea ice concentration in the summer, with high irradiance values possible at high ice concentrations (Fig. 9). Although there is no relationship between mean wind direction and MDI, TBI, or TH for the 27 July – 31 August data, the proportion of westerly winds has a significant, negative effect on each of these irradiance variables (linear regressions, p<0.05, R^2_{MDI}=0.21, R^2_{TBI}=0.20, R^2_{TH}=0.19).

Modelled kelp production based on wind during the ice-free summer is more variable between sites than measured production, and shows a general increase over time in annual production (Fig 10). Compared to measured production, the model is conservative, often underestimating annual kelp production, and has a high incidence of predicting zero production, especially for shallower sites.

Table 1.1: Summary of underwater daily light values for ice-free summer (end of break-up to the start of freeze-up). Differences in mean daily surface irradiance between sites are due to differences in benthic light data coverage over time (Supp. Table 1).

Site	Depth (m)	Mean daily surface irradiance (mol photons m^{-2} day^{-1}))	Mean daily percent surface irradiance ±SD	Mean light attenuation, k (m^{-1})	Percent of days with benthic photon flux of 0	Mean daily hours H_{sat}	Percent of days with 0 hours H_{sat}
DS11	6.1	15.5	4.1±6.2	0.52	20.9	1.9±4.0	77.8
E1	4.4	15.1	3.2±6.4	0.78	29.9	1.7±4.0	81.5
E2	4.3	13.8	3.1±6.2	0.81	38.1	1.5±3.6	82.8
E3	5.5	12.7	3.6±6.6	0.60	35.4	1.7±3.9	78.8
L1	5.5	17.0	1.9±3.8	0.72	35.3	1.4±3.7	82.7
W1	6.0	12.5	1.9±3.7	0.66	39.3	0.8±2.5	87.0
W2	6.2	13.3	2.2±4.2	0.62	41.2	0.9±2.9	87.9
W3	6.6	12.2	2.3±4.3	0.57	43.9	1.1±2.8	84.2

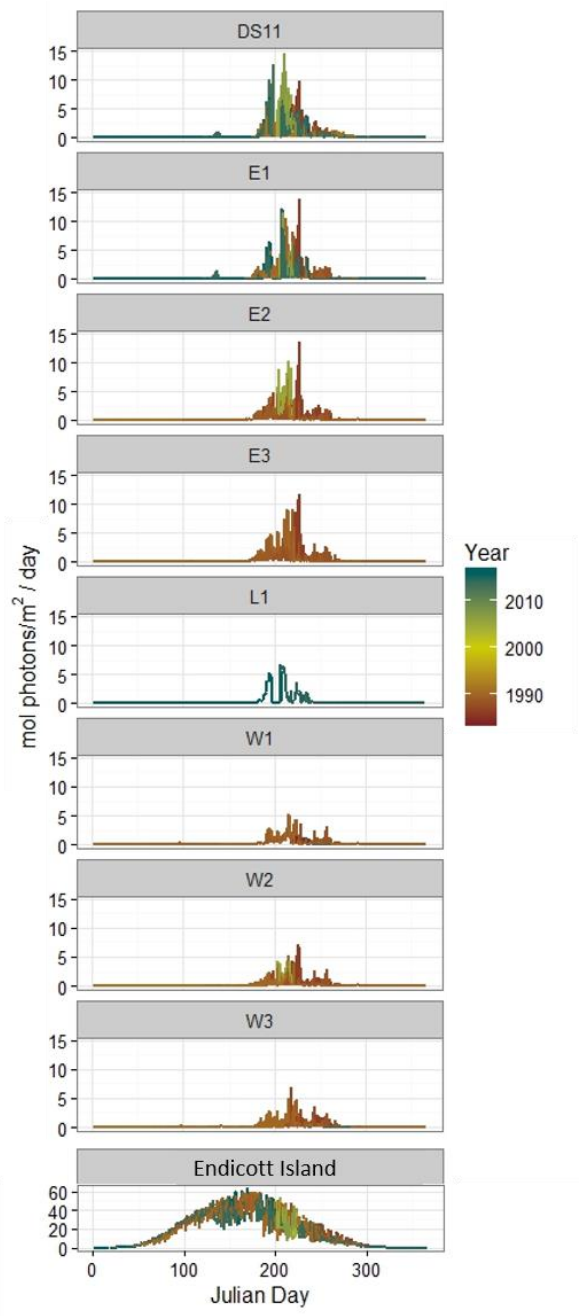

Figure 1.6: Seasonal pattern of both incident (Endicott Island) and underwater irradiance (mol photons m^{-2} day^{-1}) on the seabed at eight locations in Stefansson Sound by year. Note change in scale for surface irradiance.

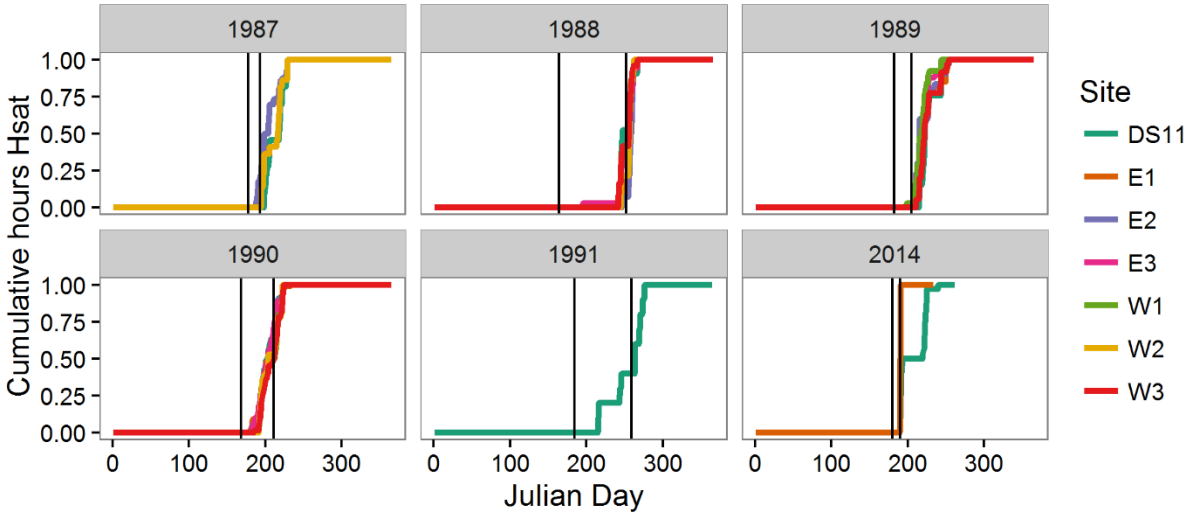

Figure 1.7: Cumulative H_{sat}, as proportion of annual H_{sat}, illustrates the rapid accumulation of hours of saturating irradiance during and directly following the period of ice break-up, based on available in situ irradiance data from each site from July through September. Pairs of black vertical lines frame the period between start of break-up and when sea ice concentration reaches 15%.

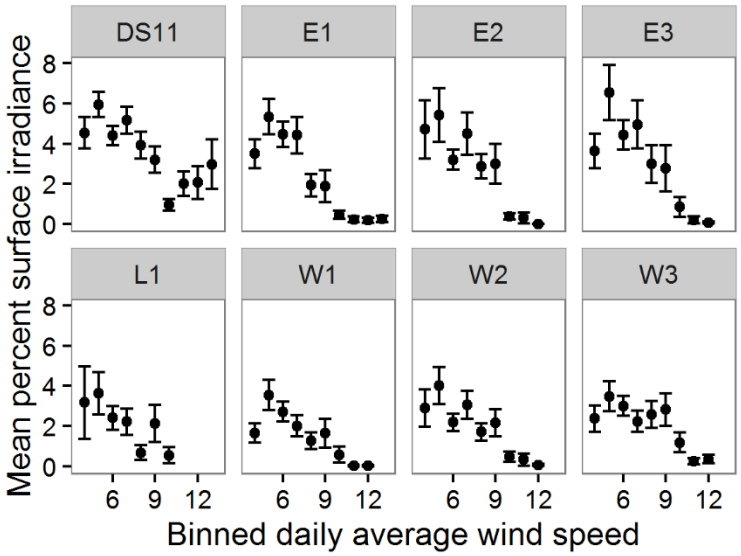

Figure 1.8: Mean daily underwater irradiance, as percent surface irradiance, at each site in relation to coastal wind speed calculated from the Deadhorse Airport station (Eq. 1).

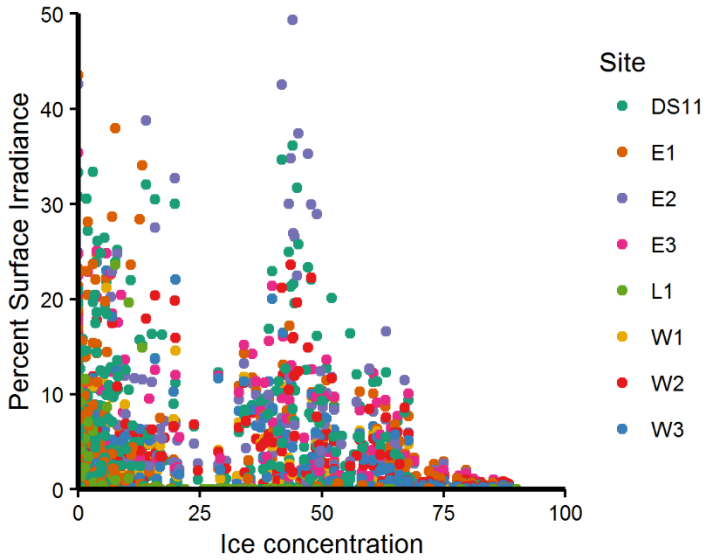

Figure 1.9: Distribution of daily underwater irradiance values (as percent of surface irradiance) as a function of ice concentration during the period from the start of ice break-up to the start of freeze-up. Note that high irradiance values are possible at relatively high ice concentrations.

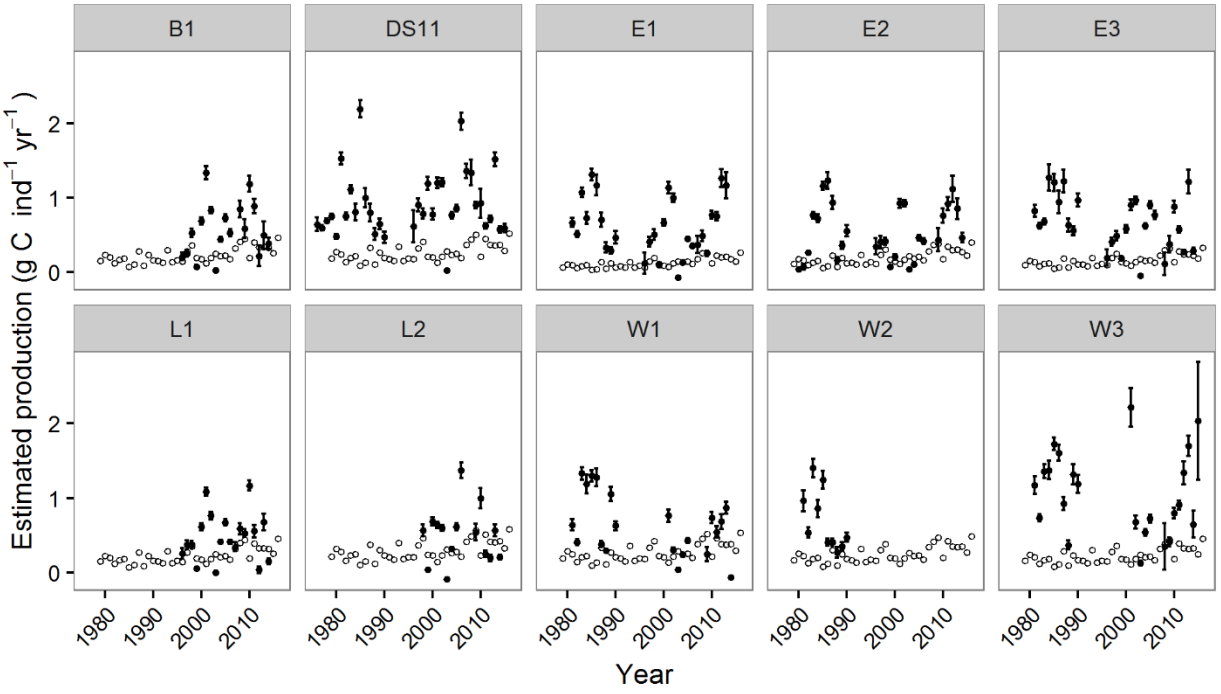

Figure 1.10: Modelled kelp production (white circles), calculated for an average-sized individual (22.5 cm basal blade length) based on the relationship between wind velocity, total suspended soilds, and light attenuation during the ice-free period, compared to measured mean kelp production (black circles ±SE) calculated from blade elongation.

DISCUSSION

Although the ice-free season has lengthened over time in Stefansson Sound, we found no evidence of increased kelp production. Low light conditions prevail during the summer, suggesting that suspended sediments, often derived from wind-driven water motion, are integral in controlling light transmittance in shallow, nearshore regions of the Arctic. However, annual kelp production and long-term trends were not accurately predicted by our model, which relied on established relationships between wind speed and light attenuation during the ice-free summer. Instead, annual benthic light budgets – and therefore annual kelp production – appear to rely heavily on enhanced light transmittance

in the days surrounding ice break-up. Overall, our results suggest that sea ice presence in these systems has a net positive effect on underwater light transmittance and marine primary production by attenuating swell and wave action.

Laminaria solidungula in Stefansson Sound survive at impressively low quantum budgets, reported previously by Dunton et al. (1990) at 45 mol photons m^{-2} yr^{-1}, the lowest measured for any kelp population (Lüning and Dring 1979 reported boreal *Laminaria hyperborea* at 71 mol photons m^{-2} yr^{-1}). In addition, *L. solidungula* exhibits saturation (E_k) and compensation (E_c) irradiance at 38 µmol photons m^{-2} sec^{-1} and 0.5-3 µmol photons m^{-2} sec^{-1}, respectively (Chapman and Lindley 1980; Dunton and Jodwalis 1988), among the lowest reported for marine macroalgae (Wiencke et al. 2006), and well below that of other cold water kelp species (*Laminaria digitata*: E_k and E_c =150 µmol photons m^{-2} sec^{-1} and 6 µmol photons m^{-2} sec^{-1}, respectively; *Saccharina latissima*: E_k and E_c =150 µmol photons m^{-2} sec^{-1} and 5 µmol photons m^{-2} sec^{-1}, respectively; *L. hyperborea* E_k and E_c =90 µmol photons m^{-2} $sec^{-}1$ and 9 µmol photons m^{-2} sec^{-1}, respectively; King and Schramm 1976, Lüning 1971). Consequently, because *L. solidungula* is very responsive to the low irradiance with an annual growth pattern strongly linked to summer open-water conditions (Dunton 1990), the species is an excellent indicator of interannual variations in the underwater light climate.

Ice concentration, wind dynamics, benthic irradiance, and kelp growth

Summer sea ice concentrations in Stefansson Sound have declined considerably since the 1980s (Fig. 2). Our analysis indicates that the open-water season (break up end to freeze up start) of the Boulder Patch area has gained approximately 17 days between 1979 and 2016 (Fig. 3). This rate of change is considerably less than that measured for the western coastal Beaufort Sea (~54 days over 34 years, Johnson and Eicken 2016) and the Beaufort Sea as a whole (~36 days over 30 years, Markus et al. 2009; ~31 days over 34 years, Stroeve et al. 2014; ~41 days over 33 years Frey et al. 2015). However, the Beaufort Sea is a region characterized by considerable variability compared to other Arctic regions (Markus et al. 2009; Stroeve et al. 2014), and the rate of change for Stefansson Sound is similar to the

trend for the entire Arctic (~20 days over 30 years, Markus et al. 2009; ~15 days over 34 years, Parkinson 2014). While some of these differences may be attributed to varied definitions of "ice covered", geomorphology is likely the main cause of disparity. Stefansson Sound is largely protected by a chain of barrier islands which affects the dynamics of landfast ice compared to pack ice. Landfast ice forms first in protected areas, such as lagoons and sheltered bays, and the timing of its freeze and melt are closely tied to the onset of freezing and thawing temperatures, respectively (Barry et al. 1979; Mahoney et al. 2014). As a result, ice presence in sheltered coastal waters such as Stefansson Sound may respond to different forcing and exhibit more moderate long-term trends than in exposed and offshore waters.

One expected outcome of decreased seasonal ice is an increase in underwater light and annual production in *L. solidungula* over time (i.e. Krause-Jensen et al. 2012; Clark et al. 2013), as demonstrated by our productivity model (Fig. 10). Our data, however, do not show such a trend (Figs. 4 and 10). Previous research has demonstrated that while there is a strong correlation between annual benthic irradiance and *L. solidungula* production, there is no correlation between daily surface and underwater irradiance in Stefansson Sound (Dunton 1990). Additionally, the timing of ice dynamics has no direct impact on annual kelp production. Instead, annual benthic light budgets in Stefansson Sound are primarily limited by resuspension of sediments by wind-induced water motion (Aumack et al. 2007). This is partially demonstrated by the considerable accumulation of H_{sat} during the dates surrounding ice break-up (Fig. 7), when wind-driven water motion is limited by high sea ice concentrations. The negative relationship between wind speed and benthic irradiance over month-long periods, and the prevalence of low light conditions during the ice-free season (Table 1), further emphasize the link between wind and light attenuation.

The lack of a significant relationship between ice concentration and benthic light during late July through August indicates that the negative effects of wind outweigh the potentially remediating effects of any sea ice that lingers in the nearshore area after the open water season is underway. As in other shallow aquatic systems, rates of particle settlement and transport of suspended sediments confound the connection between benthic

irradiance and wind (Van Duin et al. 2001). The effect of wind direction on the entrainment or advection of turbid coastal waters adds additional complexity to this relationship. It appears that the frequency of short-term increases in underwater light transmittance, under favorable wind and ice conditions ultimately determine the annual benthic light budget in this system.

The temporal accumulation of H_{sat} suggests that the days surrounding ice break-up contribute significantly (as much as 75-100%; Fig. 7) to annual benthic light budgets and annual kelp production. Underwater irradiance during this time depends on the amount of sediments contained within the ice (Dunton et al. 1982; Kempema et al. 1989), as well as ice dynamics during break-up, which are difficult to predict, and therefore not included in our production model. The omission of the break-up period may explain why the ice- and wind-based production model often underestimated kelp growth (Fig. 10). The drastically reduced light levels during the ice-free summer and the lack of relationship to annual kelp growth demonstrate that light conditions during the ice-free summer are usually poor. Consequently, contracted sea ice extent may simply contribute to wind-driven mixing of the water column and increased suspended sediments earlier in the year, effectively diminishing benthic irradiance and kelp production during the ice-free summer.

Reduced sea ice coverage in the coastal Beaufort Sea has increased wave fetch and intensified wave energy (Thomson and Rogers 2014; Thomson et al. 2016) that can substantially increase suspended sediments (Trefry 2009). Other studies in this region show that wave height is related to wind speed, as well as ice concentration (Manson and Solomon 2007). Therefore the strengthening of easterly winds in the region since the mid-2000s may also contribute to enhanced sediment resuspension (Wood et al. 2013, 2015), though this trend was not reflected in the wind measurements recorded at the Prudhoe Bay weather stations.

Current projections for macrophyte communities in Arctic marine systems assume that benthic irradiance will increase as sea ice extent contracts (i.e. Clark et al. 2013, Krause-Jensen and Duarte 2014). The long-term data presented here show that this assumption may not apply to inner shelf regions, especially marginal Arctic seas that

receive substantial river inputs during the summer open-water period. This also agrees with results from a glacially-influenced site, where sediment-laden glacial meltwater is thought to have shrank the euphotic zone over time (Bartsch et al. 2016). Light attenuation by suspended sediments demonstrably affects irradiance available for primary production, both in the water column (Van Duin et al. 2001) and in the benthos (Anthony et al. 2004; Aumack et al. 2007), and should be considered for Arctic ecosystem change scenarios.

The Arctic inner shelf under future climate change

Shallow inner shelf zones make up 20% of the area of Arctic shelves (Fritz et al. 2017). Outside of Greenland and the Canadian Archipelago, these systems experience considerable inputs from Arctic rivers during the melt season that contribute to total suspended sediment (TSS) concentrations (Gordeev et al. 1996; Holmes et al. 2002; Gordeev 2006; McClelland et al. 2012). Coastal erosion also significantly contributes to elevated TSS levels in inner shelf zones (Reimnitz et al. 1988; Hill and Nadeau 1989), which are often maintained by wind events that resuspend unconsolidated sediments on shallow shelves (Hill and Nadeau 1989). The reduction in water transparency in response to increased TSS, which is accentuated by expanded fetch and diminished ice extent, demonstrates the effects of a warming Arctic on primary production, especially on the coast and inner shelf. Consequently, we should expect that coastal ecosystems will respond differently to climate change than deeper, offshore seasonal ice zones.

As warming continues, multiple environmental factors in nearshore Arctic areas will cause average summer light attenuation to surpasses current levels (~0.8 m^{-1}; Table 1). The persistence of these high attenuation conditions, which match the turbid conditions previously measured in Stefansson Sound (Dunton 1990; Dunton et al. 2009), will alter regimes of underwater light transmittance and primary productivity (Fig. 11). First, the reduction of sea ice will increase the incident sunlight to the ocean, leading to enhanced capacity for primary productivity at the surface. However, this reduction in sea ice will also lead to lengthened fetch, larger swell, stronger wave activity in the nearshore, and higher incidence of sediment resuspension (Wegner et al. 2003; Walker et al. 2008;

Thomson and Rogers 2014; Thomson et al. 2016). Nearshore wave activity also intensifies coastal erosion, aided by melting permafrost and sea level rise (ACIA 2005, Overeem et al. 2011). Currently, both sheltered mainland-lagoon and open-ocean exposed coastlines of the Beaufort Sea are eroding at rates of 0.9 to 1.8 m y^{-1}, respectively (Gibbs and Richmond 2015). Globally, rates have been measured as high as 25 m y^{-1} (Jones et al. 2009; Gunther et al. 2015). Beaufort Sea Coast erosion rates appear to have increased, or even doubled over the past five decades (Jones et al. 2008, 2009). As the climate continues to warm, most Arctic coastlines are expected to experience accelerated coastal erosion (Fritz et al. 2017, ACIA 2005). River discharge to the Arctic Ocean is also increasing, with measured increase of ~11% from 1964-2000 (McClelland et al. 2006). This will contribute to intensified fluvial sediment flux, estimated to rise by 30-122% for the six largest Arctic rivers by the end of the century (Gordeev 2006).

The additive effects of sea ice loss, coastal erosion, and enhanced fluvial inputs will ultimately increase suspended sediments in Arctic inner shelf waters during the open-water season (Fig. 11). Our research suggests that as summer ice concentrations continue to decrease, the annual benthic light budget in nearshore areas will progressively depend on light transmitted through the ice and water before and during break-up. It also shows that primary production may shift in unexpected ways in the future, depending on local characteristics. In areas with high suspended sediments, benthic production may not be enhanced by ice loss, but will increasingly rely on light transmittance during break up. Phytoplankton productivity in the nearshore Arctic will also depend on the balance between light attenuation by suspended sediments and nutrient concentrations in the upper water column, which are similarly determined by sediment resuspension, erosion, and fluvial inputs. Decreased light transmission during summer will shallow the critical depth of growth, altering depth distributions of benthic and planktonic primary producers. Our work demonstrates that environmental factors that characterize Arctic inner shelves, particularly suspended sediments, should be considered in projections that evaluate the response of Arctic ecosystems to climate change.

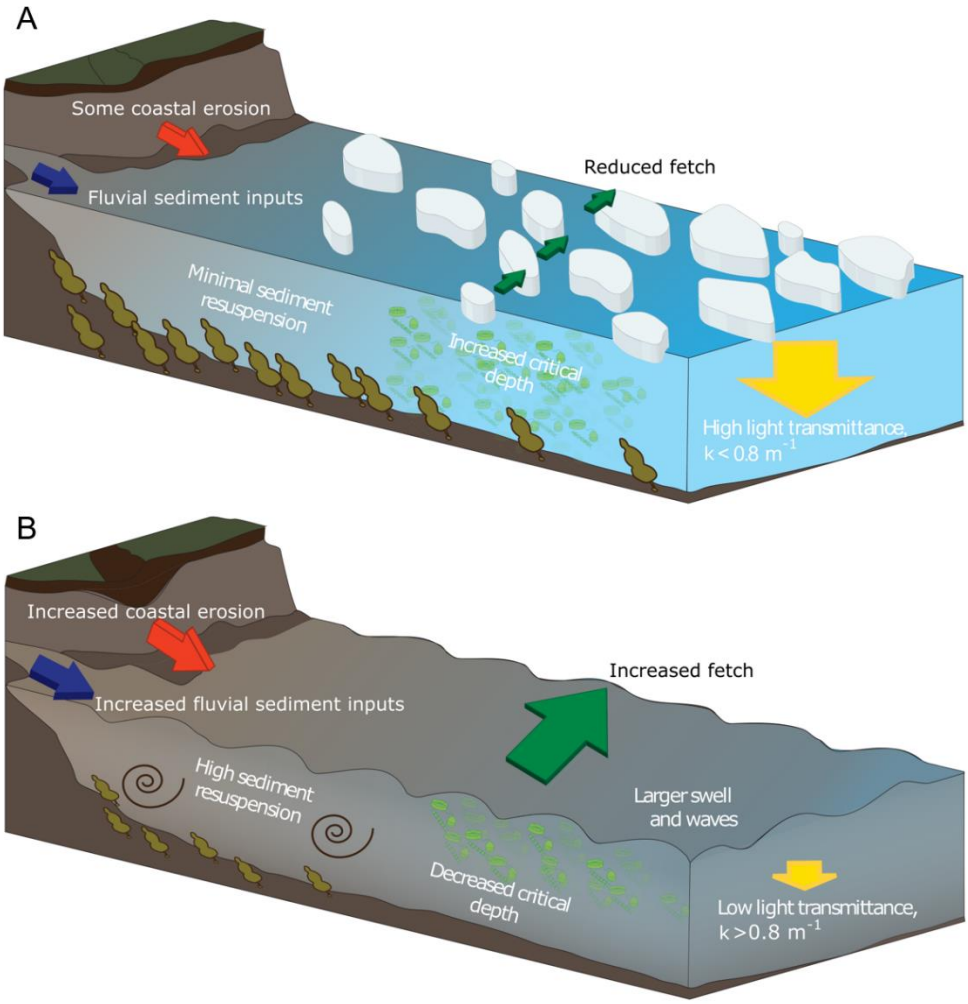

Figure 1.11: Conceptual diagram of the effects of a) summer ice cover versus b) reduced summer ice cover on processes affecting the underwater light environment in shallow inshore (<10 m) Arctic ecosystems. Reduced ice will increase coastal erosion, lead to larger swell, and increase sediment resuspension, which will combine with enhanced fluvial sediment inputs to ultimately increase light attenuation (k). This will decrease annual growth of benthic macrophytes, and shift depth distributions of pelagic and benthic primary producers by shallowing the critical depth.

Chapter Two: Seasonality and change near the mouth of an Arctic river: Environmental variability in Stefansson Sound, Alaska

ABSTRACT

On Arctic inner shelves, seasonal spatial gradients in abiotic conditions caused by bathymetry and distance from freshwater inputs influence biological characteristics and biogeochemical processes. I examined spatial variations in near-benthic temperature, salinity, currents, and light over seasonal and annual timescales (2011-2017) in Stefansson Sound, a shallow embayment (<15 m) at the mouth of the Sagavanirktok River on the North Slope of Alaska. Stable temperature and salinity conditions prevailed in the study area throughout the winter (-1.9--1.8 ^{o}C, salinity 33-35). However, spatial abiotic differences developed from May-October. During these months, temperature and salinity exhibited strong cross-shelf gradients, especially in June-September when nearshore sites reached 6 ^{o}C or more and exhibited salinities below 20, while offshore sites averaged 2 ^{o}C and salinities of 28-29. Under the cover of landfast ice and coincident with the spring freshet, coastal waters near the mouth of the Sagavanirktok River experienced salinities below 10 at 4 m depths in one of the sampled years. Currents are generally alongshore and bi-directional from November-May, but flow direction becomes wind-driven and variable following ice break-up. In all seasons, currents were faster and more variable at sites adjacent to deep, inter-island passes, reflecting influence by strong offshore currents. Underwater light levels were highest in July and August, but extremely variable in space and time (0.0-12.6 mol photon m^{-2} day^{-1}) in response to wind-driven resuspension events. The timing of ice break-up appears to determine mean annual conditions, as it separates the cold, dark, high salinity, low variance winter from the warmer, fresher, high variance summer. These measurements imply that a considerable portion of the benthos is regularly exposed to low salinity conditions before the beginning of ice break-up. Our results reinforce the estuarine nature of Arctic nearshore systems and provides the hydrographic setting that determines the strong seasonal nature of the coupled benthic and pelagic ecosystem of the Beaufort Sea.

INTRODUCTION

Shallow, predominantly soft-sediment habitats, which characterize the benthic nearshore areas of the Alaskan Arctic, are important settings for marine life and ecological processes. These ecosystems are also locations of ongoing and proposed industrial activity. Numerous river and stream inputs define the inner shelf area as an estuarine environment (Carmack and Wassman 2006). Benthic organisms in the inner shelf are key primary producers or consumers that link autochthonous and allochthonous production to higher trophic levels by assimilating organic matter originating from the terrestrial realm, offshore, and the nearshore zone (Craig et al. 1984, Dunton et al. 2012, Harris et al. 2018). Migratory birds, marine and anadromous fishes, and marine mammals take advantage of the food and habitat provided by these environments (Connors 1984, Craig et al. 1984, Craig 1984, Dickovy 1984, Frost and Lowry 1984). The strong seasonality of Arctic coastal ecosystems defines the timing and magnitude of freshwater inflows, sea ice dynamics, and water exchange with the ocean, which in turn shapes their estuarine nature.

Seasonal changes in the physiochemical environment of these systems is largely event-driven, dominated by annual cycles of river inputs and ice cover (McClelland et al. 2012; Weingartner et al. 2017). Rivers draining the North Slope of Alaska discharge over half of their annual flow in a short, two-week spring melt period between late May and early June (i.e. the "spring freshet") (McClelland et al. 2012, 2014). This flow initially occurs above and beneath the sea ice, creating a relatively stable stratified layer of river water that can reach up to ~ 3 m deep (Reimnitz 2000; Alkire and Trefry 2006; Kasper and Weingartner 2015) until sea ice break-up commences and wind mixing strengthens (Weingartner et al. 2017). Depending on winds, currents, and flow conditions, ice break up can occur over a period of days or weeks. In the Beaufort Sea, the ice-free summer is then characterized by wind-mixing and higher current speeds, especially late in the season (Weingartner et al. 2017). Ice formation begins as the amount solar energy that reaches Arctic latitudes decreases in the fall, further homogenizing the water column. Landfast ice forms along the shore, then spreads offshore, with freeze-up complete in nearshore areas

by late-October (Barry et al. 1979; Mahoney et al. 2014). As ice formation continues, both salinity and inorganic nutrient levels increase within the underlying waters through the respective processes of brine rejection and remineralization (Chapman and Lindley 1980; Matthews 1981; Dunton et al. 1982; Macdonald and Yu 2006).

In the marine realm of Arctic nearshore systems, bathymetry and proximity to river inputs mediate seasonal variation in abiotic conditions, and thereby impart "zones" of ecological characteristics and biogeochemical processes. For example, greater sediment resuspension at shallow depths due to summer wind-mixing can reduce benthic primary productivity relative to deeper, more offshore areas (Aumack et al. 2007). Additionally, stratification in the spring and early summer exposes nearshore, near-river benthos to a distinct, river-derived water mass. Associated organic matter, freshwater, and heat inputs may result in profound differences between nearshore and offshore benthic diversity and biogeochemical processes (Bonsell 2019, Chap. 3; Muth *pers. comm.*).

Understanding year-round *in situ* conditions is a critical knowledge gap linking Arctic abiotic factors to biological characteristics and biogeochemical processes. As seasonal transitions can vary from year to year (e.g. Harris et al. 2017), multiple years of data are necessary to assess the magnitude and spatial extent of abiotic changes. Logistical constraints and ice risks discourage long-term mooring deployments in shallow areas, meaning that underwater conditions during the freshet and ice break up are not well characterized for most Arctic estuaries. Recent technological advances have made affordable *in situ* instrumentation more readily available, and researchers more willing to risk equipment for the chance of acquiring valuable environmental data.

The goals of this study are to: 1) Define the seasonal cycle in temperature, salinity, currents, and underwater light in the nearshore environment of Stefansson Sound; 2) Determine the influence of bathymetric and physiogeographic characteristics (distance from river inputs and coastline orientation) on spatial differences in the marine environment; 3) Discuss the influence of regional wind patterns on temporal variability

and current dynamics; and 4) Assess evidence for long-term change in temperature and salinity in Stefansson Sound. As a whole, this work depicts the environmental setting for nearshore biological processes on Arctic inner shelves.

Weingartner et al. (2017) recently described seasonal abiotic conditions in the nearshore landfast ice zone of the central Beaufort Sea coast, with moorings as shallow as 7 m in Stefansson Sound. Their study provides important environmental context for ecological studies and proposed development scenarios related to oil and gas extraction. My work extends shoreward to 4 m within Stefansson Sound, where stratified fluvial inputs interact with benthic processes that affect local production, diversity, and biogeochemical cycling. Observations of temperature, salinity, and currents collected in this study were compared to offshore measurements, as well as to data collected in previous decades (1970s and 1980s). Comparisons to historical datasets are important since the changes occurring over sub-decadal time scales can be masked by innate interannual variability. I consider the effects of bathymetric and physiogeographic characteristics on the abiotic environment, and how those may impact marine life. Our dataloggers were within 60 cm of the benthos, providing an opportunity to describe how benthic biota experience seasonality adjacent to river inputs.

METHODS

Study Area

Stefansson Sound is a shallow (<10 m) embayment on the central Beaufort Sea coast, partially protected by barrier islands. The Sagavanirktok River, with headwaters in the Brooks Range, empties into the Stefansson Sound via numerous delta channels (Fig. 2.1). Like most of the Beaufort Sea coast, the benthos is primarily composed of silty sediments, but a large deposit of boulders and cobbles, termed the "Boulder Patch", gives rise to a unique benthic bed community in the eastern portion (Fig. 2.1; Dunton et al. 1982). The Endicott Causeway, completed in 1985, extends into the sound past the Sagavanirktok

River delta. Development of the adjacent Prudhoe Bay oilfield resulted in intense study of Stefansson Sound relative to other Arctic inner shelf habitats. As a result, changes to the marine environment over time can be evaluated from historical *in situ* datasets.

Over the course of the study period (2011-2017), we occupied five long-term monitoring sites within the Boulder Patch area of Stefansson Sound. Sites differed in depth and distance from Sagavanirktok River channels (Fig. 2.1, Table 2.1). These included three nearshore sites (E1, L1, and W1), and two sites further offshore (DS11, W3).

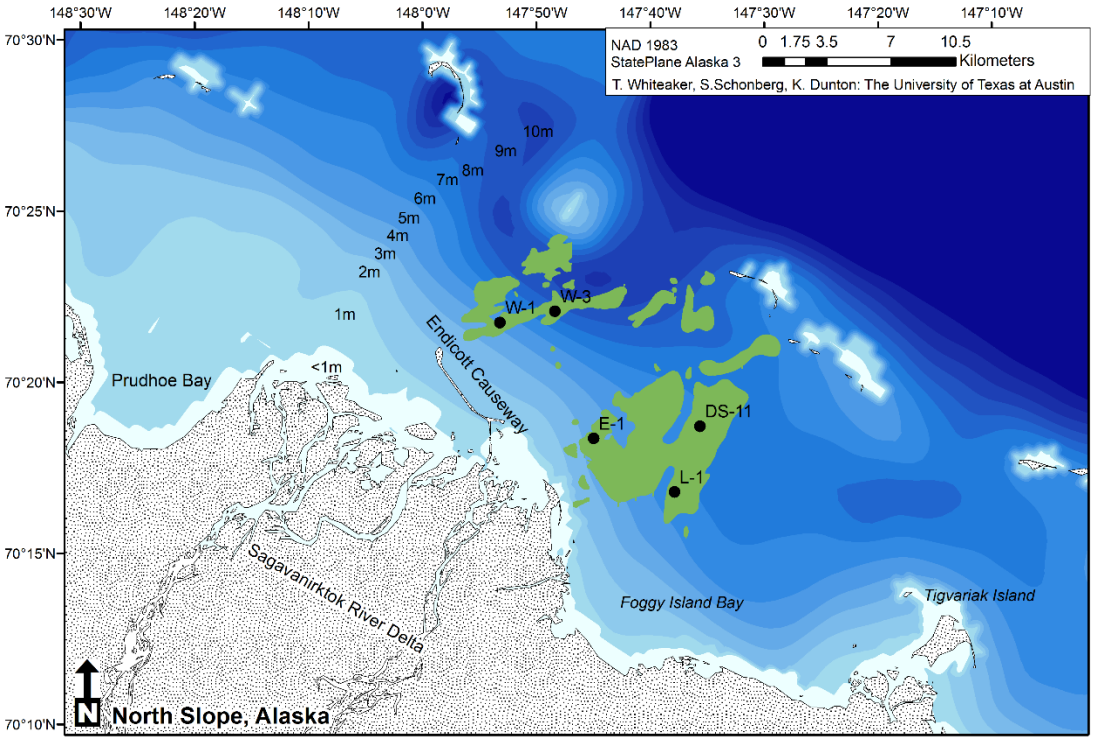

Figure 2.1: Map of the Stefansson Sound area, with the five long-term study sites used in this study: W1, W3, E1, L1, and DS11. The green area symbolizes the Boulder Patch.

Mooring description

Benthic moorings, composed of a variety of *in situ* data loggers (described bleow), collected continuous environmental data at each of our sites. These were retrieved each summer (July or August) and redeployed within two weeks after downloading the data. Photosynthetically active radiation (PAR) was recorded ~ 50 cm above the seabed using a LI-COR LI-193SA spherical quantum sensor (accuracy: ±5%) connected to LI-1000, LI-1400, or LI-1500 dataloggers. Some of this data has been incorporated in previous studies to examine multidecadal underwater light patterns in the Boulder Patch (Bonsell and Dunton 2018). Continuous *in situ* measurements of conductivity and temperature were collected with HOBO U24 Conductivity/Temperature Loggers (hourly sample interval) and Star Oddi DST loggers (half-hour sample interval; accuracy for both loggers: ± 0.1 ^{o}C, ±1.0 salinity). Instantaneous measurements of temperature and conductivity were measured upon deployment and retrieval of loggers using a YSI Data Sonde and used to calibrate records at each site. Temperature and conductivity were used to calculate salinity using the 1983 UNESCO equation. Measurements of temperature, current velocity and current bearing within ~1.2 m of the bottom were collected using SeaHorse Tilt Current meter fitted with a MAT-1 accelerometer or with a Lowell MAT-1 Tilt Current Meter (half-hour sample intervals, accuracy: ± 1^{o}).

Our mooring design placed conductivity cells within 30 cm of the benthos. This exposed them to fouling by resuspended sediments during fall storms, a known problem in these environments (Weingartner et al. 2017). As a result, conductivity data was removed for portions of the record at some sites. Additionally, some moorings were lost to damage by deep-draft ice, though the large majority survived deployment (Fig. 2.2).

Data analyses

After undergoing quality control, summary statistics were generated for each data type at each site overall and separated by season: ice-covered winter (December through

April), pre-ice-break-up spring (May through June), open-water summer (July through September), and fall freeze-up (October through November). This definition corresponds with the timing of key hydrologic events: the spring freshet (late May to early June), landfast ice break up (July), and sea ice freeze-up (early to mid-November). The four-season model has been used by others to describe Arctic annual cycles in connection to biological activity (Carmack and Macdonald 2002). To directly assess how abiotic conditions differed among sites over time, daily mean values for each continuous variable (temperature, salinity, PAR, current velocity) were calculated for each day where there was data for >1 site and compared using a blocked-ANOVA approach using time (day) as a block. Post-hoc pairwise comparisons assessed differences in least-squared means, with Tukey-adjusted p-values for multiple comparisons. Daily mean current direction and summary statistics were determined to the nearest degree using the R package 'circular' (Agostinelli and Lund 2017). Average daily wind speed and fastest five-minute wind direction from the Deadhorse Airport were downloaded from the National Climate Data Center (National Weather Service) and plotted against mean daily current conditions at each site. All data analysis was carried out using R v. 3.3.3 (R Core Team, 2016).

Table 2.1: Site locations, bathymetric, and physiographic information.

Site	Latitude (DD)	Longitude (DD)	Depth (m)	Dist. to river input (km)
DS11	70.32228	-147.579	6.1	9.03
E1	70.31495	-147.732	4.4	3.54
L1	70.28993	-147.613	5.5	7.20
W1	70.37003	-147.873	6.0	3.54
W3	70.37627	-147.794	6.6	7.31

RESULTS

Our data show the strong seasonal pattern of environmental conditions in the Arctic, with relatively consistent temperature, salinity, light, and currents during the winter and a

much more variable environment during the rest of the year (Table 2.2, Figs. 2.2-2.5). Generally, sites experienced synchronous variations in all parameters except salinity, though the magnitude of change could vary significantly between sites (Figs. 2.2, 2.5) Signatures of the annual sea ice cycle and the spring freshet are apparent in the underwater physiochemical record.

Salinity on the seabed reached its highest average (33-36) in the winter, and its lowest average in summer (below 30) at all sites (Table 2.2). Winter temperatures were stable at ~-1.9 to -1.8 ^{o}C, but reached upwards of 5 ^{o}C in the summer (Table 2.2, Figs. 2.2-2.4). Shallow, inshore sites experienced the greatest range in salinities, with E1 and W1 fresher than the other sites in the spring and summer (Table 2.2, Figs. 2.2-2.3). The site closest to the river mouth (E1) also exhibited the greatest riverine influence: temperatures rose earlier and a springtime pulse of low salinity was noted in some years that was not seen at the offshore sites (Figs. 2.2, 2.4). E1 also had significantly higher temperatures than the other sites during spring and summer, and was the warmest site overall (Tables 2.2-2.3). While the freshet signal was strongest at E1, it could also be seen at other sites as a small (<1 ^{o}C) rise in temperature in the spring (Fig. 2.2). The subsequent onset of sea-ice melt was marked by a rapid, large (> 2 ^{o}C) increase in temperature and a decrease in salinity (>3) across Stefansson Sound (Fig. 2.2). Temperatures were maximal in August, then decreased gradually through the early fall until dropping rapidly by more than 2 ^{o}C leading up to sea ice freeze-up (Fig. 2.2).

Photon flux was extremely variable across sites in the summer, but most notably at E1 (Table 2.2, Figs. 2.2-2.3). Underwater light levels hit their annual maximum in July (above 5 mol photons m^{-2} day^{-1}), with the rest of the summer characterized by smaller, sporadic spikes of measurable light levels (Fig. 2.2). In summer, DS11 and E1 tended to have higher underwater light levels than other sites (Table 2.3). PAR dropped to zero in the fall, then increased briefly in the spring in two of the four years (2014 and 2017), before dropping to zero again (Fig. 2.2).

At all sites, near-bottom current velocities were much lower and less variable under ice cover during the winter and spring (<2 cm/s, Table 2.2, Figs. 2.2-2.3,2.5). Similar to temperature, current speeds accelerated slightly (<2 cm s^{-1}) with the freshet, then strengthened considerably as sea ice cover decreased in the Beaufort Sea during summer (Fig. 2.2). Average velocity at all sites was highest in the summer and fall (average >3 cm s^{-1}, Table 1.2, Figs. 2.2-2.3,2.5). The shallow, within-bay sites E1 and L1 experienced their maximum seasonal current velocity in the summer, while currents were fastest in the fall at the more exposed and deeper sites (DS11, W1, W3; Table 2.2, Figs. 2.2-2.3,2.5). On average, velocity was greater at these three sites, while E1 and L1 had significantly lower velocities, and lower variability (as measured by standard deviation) across seasons (Tables 2.2-2.3, Fig. 2.3). The onset of sea ice freeze-up in October (2014-2015) or November (2016) caused current speed to plummet (Figs. 2.2,2.5).

Current direction data failed to meet the assumptions for statistical comparisons between sites and seasons as it was not Von Mises distributed (Watson test for continuous probability distribution on the circle, α=0.1). Currents were primarily bi-directional: east-west for W1 and W3, northwest-southeast for L1 and DS11 (Figs. 2.5-2.7). Unlike the other sites, currents at E1 were more unidirectional and tended to be toward the south (Figs. 2.5-2.7, Table 2.3). At all sites, the strongest currents typically had a northwest bearing (Figs. 2.5,2.7). During summer and fall, strong along-shore flows developed throughout the Boulder Patch (Fig. 2.6). Currents bearing south became more frequent during the winter and pre-break up spring (Fig. 2.5-2.6).

Table 2.2: Mean and standard deviation of daily benthic environmental conditions measured at each site, split by season, of entire data record (Fig. 2.2). Subscripts refer to number of observations (days). Superscripts indicate that there were significant differences between sites, with letter indicating group affinity within each season (α=0.05, Supp. Table B1). * Differences in mean current direction could not be analyzed statistically.

Season	Site	Temp. (°C)	Salinity	Current vel. (cm s^{-1})	Current direction (degrees)*	PAR (mol photons m^{-2} day^{-1})
Ice-covered (Dec-Apr)	DS11	-1.8±0.1 $^{a}_{908}$	34±1 $^{a}_{908}$	1.7±1.3 $^{a}_{151}$	180±83 $_{151}$	0.013±0.025 $_{605}$
	E1	-1.9±0.1 $^{b}_{605}$	34±2 $^{b}_{598}$	1.3±0.6 $^{bd}_{454}$	236±64 $_{454}$	0.014±0.034 $_{454}$
	L1	-1.8±0.1 $^{a}_{605}$	36±1 $^{c}_{240}$	0.7±0.4 $^{c}_{454}$	194±108 $_{454}$	0.012±0.025 $_{302}$
	W1	-1.9±0.1 $^{b}_{454}$	33±1 $^{d}_{151}$	1.3±1.0 $^{b}_{303}$	144±48 $_{303}$	Instrument failed
	W3	-1.8±0.1 $^{c}_{485}$	34±1 $^{ab}_{302}$	1.6±0.8 $^{ad}_{151}$	162±100 $_{302}$	0.017±0.024 $_{151}$
Pre-break-up spring (May-Jun)	DS11	-1.6±0.2 $^{a}_{366}$	33±1 $^{a}_{366}$	1.7±1.2 $^{a}_{61}$	96±83 $_{61}$	0.082±0.178 $_{244}$
	E1	-1.3±0.7 $^{b}_{244}$	31±6 $^{b}_{243}$	1.5±0.8 $^{b}_{183}$	199±69 $_{183}$	0.070±0.186 $_{183}$
	L1	-1.5±0.2 $^{c}_{244}$	35±1 $^{c}_{132}$	0.7±0.5 $^{c}_{183}$	198±91 $_{183}$	0.065±0.113 $_{122}$
	W1	-1.6±0.2 $^{ad}_{183}$	31±0 $^{b}_{77}$	1.4±0.9 $^{b}_{122}$	149±47 $_{122}$	Instrument failed
	W3	-1.7±0.2 $^{d}_{183}$	34±1 $^{a}_{122}$	1.6±0.7 $^{a}_{61}$	166±68 $_{122}$	0.082±0.103 $_{61}$
Open water summer (Jul-Sep)	DS11	2.0±2.2 $^{a}_{519}$	29±3 $^{a}_{519}$	7.3±4.9 $^{ab}_{108}$	353±97 $_{109}$	1.062±1.878 $^{a}_{336}$
	E1	3.2±2.5 $^{b}_{377}$	27±3 $^{b}_{377}$	5.3±3.7 $^{c}_{248}$	266±90 $_{248}$	0.812±1.789 $^{ab}_{247}$
	L1	2.0±2.1 $^{a}_{326}$	29±4 $^{c}_{246}$	3.9±2.6 $^{c}_{250}$	279±87 $_{250}$	0.620±1.314 $^{b}_{222}$
	W1	1.7±2.2 $^{a}_{232}$	26±4 $^{d}_{148}$	7.7±5.5 $^{a}_{215}$	193±75 $_{217}$	0.102±0.236 $^{b}_{27}$
	W3	1.6±2.1 $^{a}_{334}$	28±3 $^{a}_{270}$	6.5±4.0 $^{b}_{201}$	206±71 $_{219}$	0.534±1.188 $^{b}_{126}$
Fall freeze-up (Oct-Nov)	DS11	-1.4±1.0 $_{366}$	31±2 $^{ab}_{322}$	8.8±8.4 $^{a}_{61}$	235±80 $_{61}$	0.014±0.053 $_{244}$
	E1	-1.3±1.1 $_{244}$	31±2 $^{bc}_{221}$	4.3±4.8 $^{b}_{183}$	271±73 $_{183}$	0.013±0.040 $_{183}$
	L1	-1.4±0.9 $_{244}$	32±2 $^{c}_{124}$	3.5±4.3 $^{b}_{183}$	285±86 $_{183}$	0.002±0.005 $_{124}$
	W1	-1.4±0.9 $_{183}$	29±2 $^{a}_{49}$	7.7±7.5 $^{a}_{142}$	215±68 $_{142}$	Instrument failed
	W3	-1.4±0.9 $_{244}$	31±3 $^{abc}_{98}$	8.0±5.9 $^{a}_{108}$	228±97 $_{132}$	0.001±0.002 $_{70}$

Table 2.3: Daily, year-round mean (±SD) benthic environmental conditions at each site of entire data record (Fig. 2.2). Superscripts indicate that there were significant differences between sites, with letter indicating group affinity (α=0.05, Supp. Table B1). * Differences in mean current direction could not be analyzed statistically.

Site	Temperature (°C)	Salinity	Current velocity (cm s^{-1})	Current direction (degrees)*	PAR (mol photons m^{-2} day^{-1})
DS11	-0.78±1.96 $^{a}_{2159}$	32±3 $^{a}_{2115}$	4.4±5.3 $^{a}_{381}$	181±77 $_{382}$	0.271±1.013 $_{1429}$
E1	-0.41±2.50 $^{b}_{1470}$	31±4 $^{b}_{1439}$	2.8±3.2 $^{b}_{1068}$	239±66 $_{1068}$	0.208±0.925 $_{1067}$
L1	-0.82±1.89 $^{a}_{1419}$	33±4 $^{a}_{742}$	1.9±2.7 $^{c}_{1070}$	251±76 $_{1070}$	0.194±0.756 $_{772}$
W1	-0.95±1.84 $^{a}_{1052}$	30±4 $^{c}_{425}$	4.3±5.4 $^{d}_{782}$	164±61 $_{784}$	0.102±0.236 $_{27}$
W3	-0.80±1.88 $^{a}_{1246}$	32±3 $^{b}_{792}$	4.8±4.6 $^{a}_{521}$	189±71 $_{775}$	0.184±0.700 $_{408}$

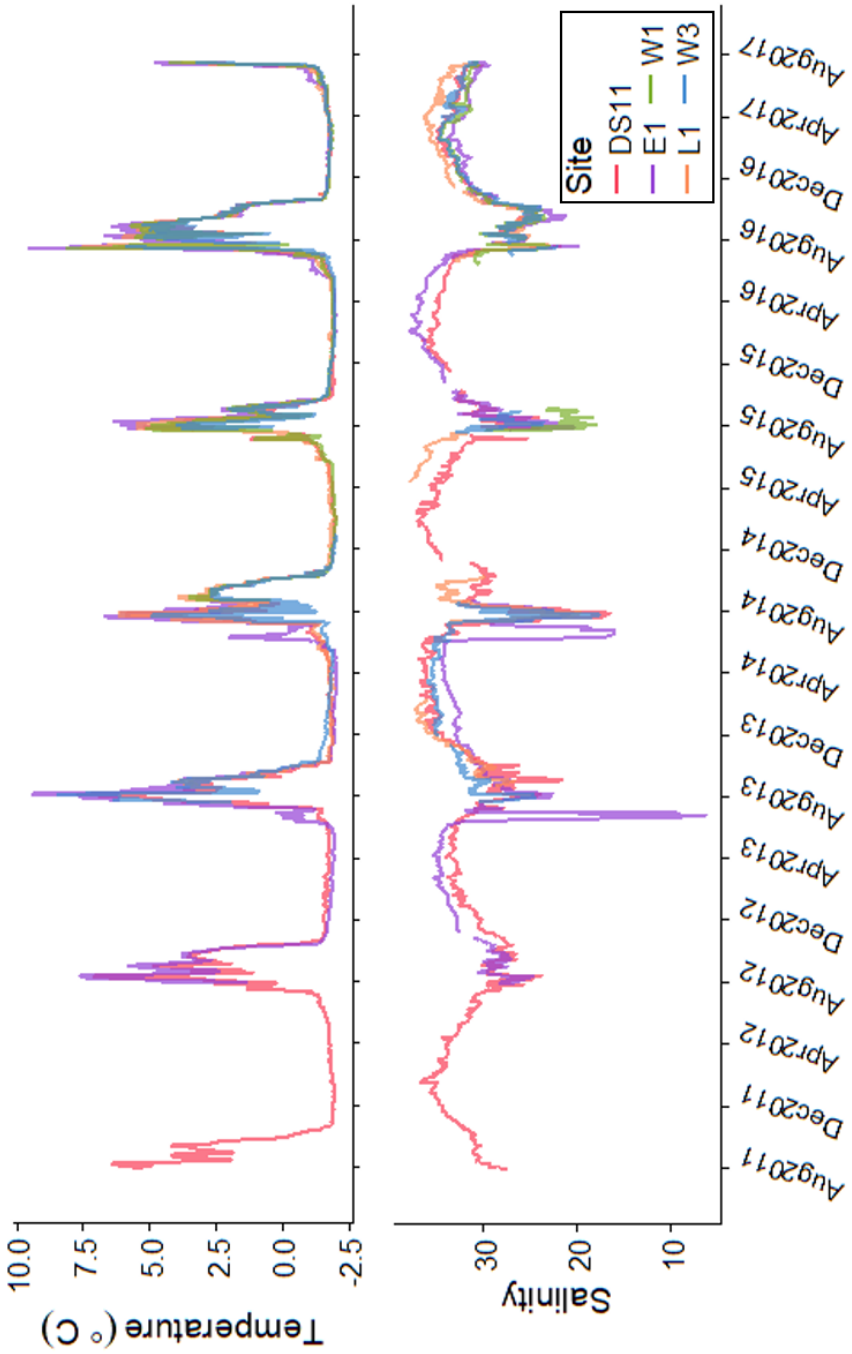

Figure 2.2: Timeseries of daily mean temperature, salinity, photon flux, and current velocity at each site.

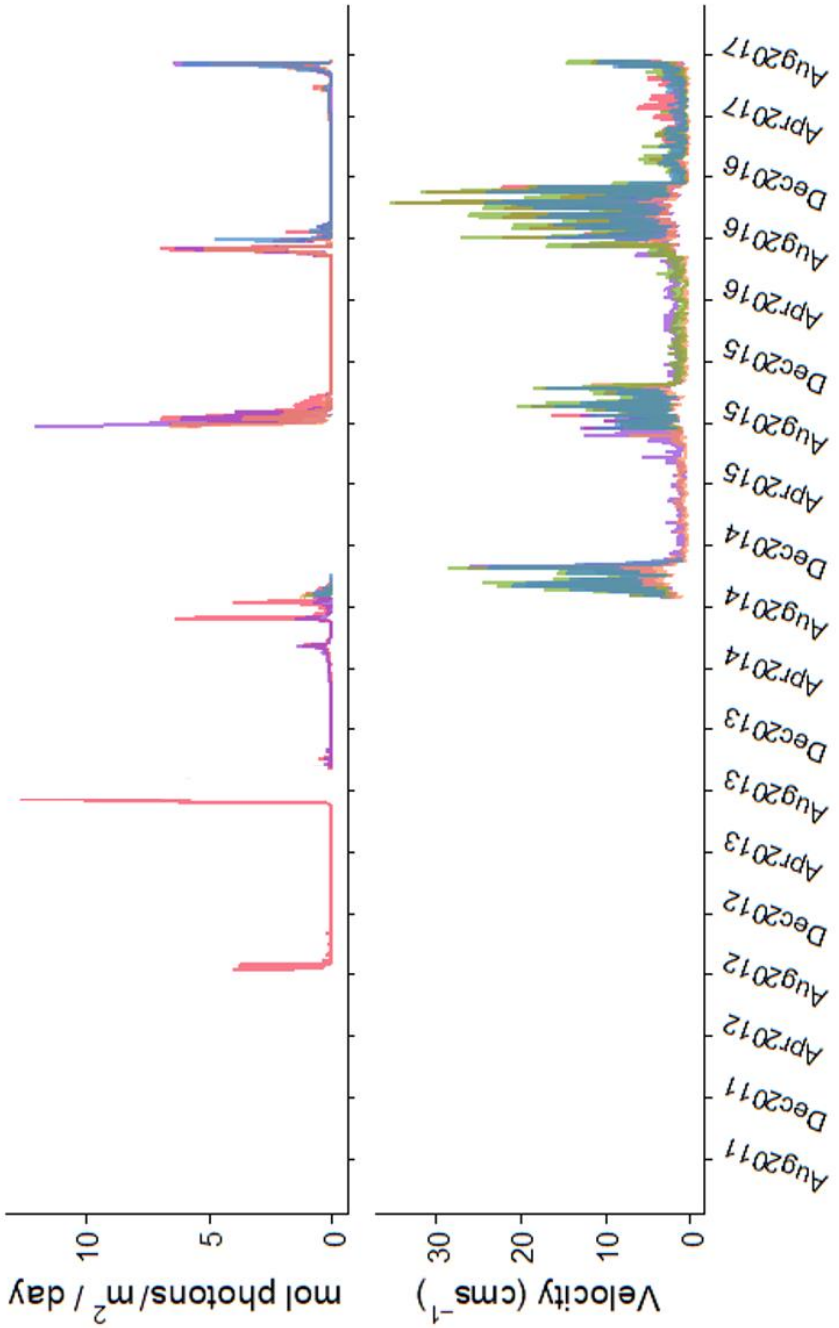

Figure 2.2 cont.: Timeseries of daily mean temperature, salinity, photon flux, and current velocity at each site.

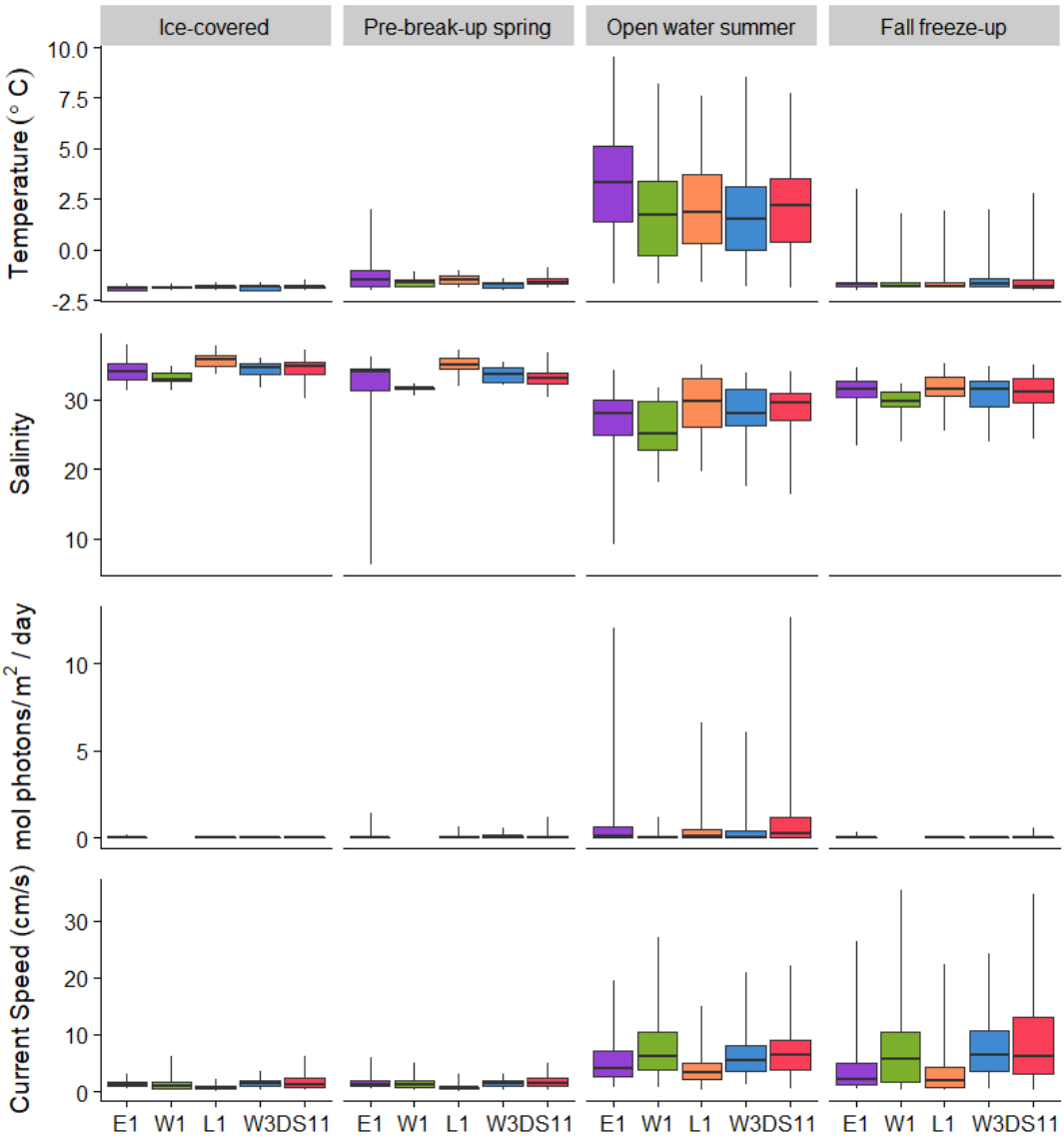

Figure 2.3: Distribution of measurements for each variable by site and season for entire data record (Fig. 2.2). Sites are ordered by increasing distance offshore. Central horizontal line indicates the median, upper and lower limits of the box indicate interquartile range, vertical lines indicate the overall range of values. See Table 2.2 for significant group affinities. This figure differs from Table 2.2 in that it shows median values, so less weight is given to rare observations at the edge of the range.

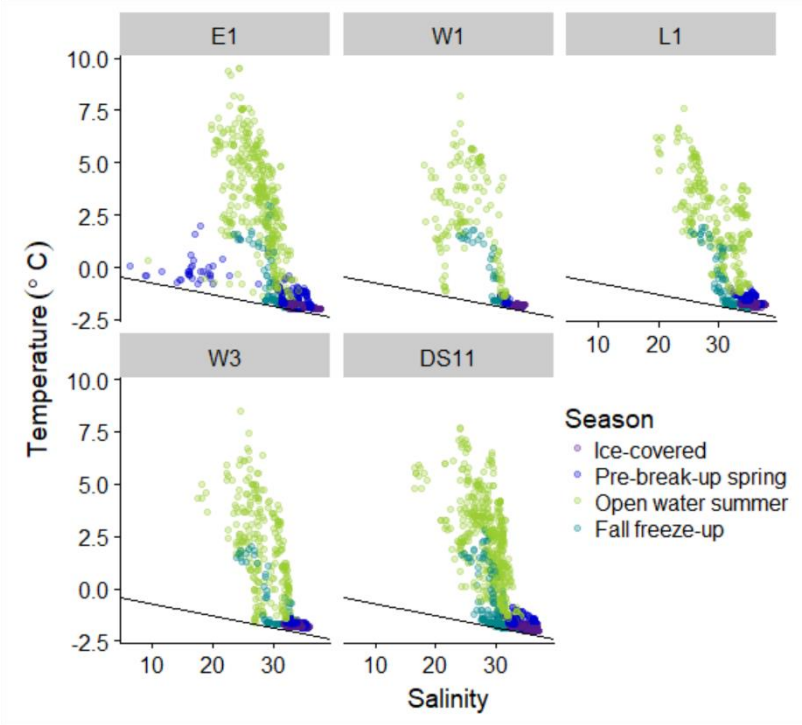

Figure 2.4: Temperature vs. salinity plots at each site for entire data record (Fig. 2.2), color-coded by season. Purple: ice-covered; blue: spring; green: summer; teal: fall. Black line indicates the freezing point of water.

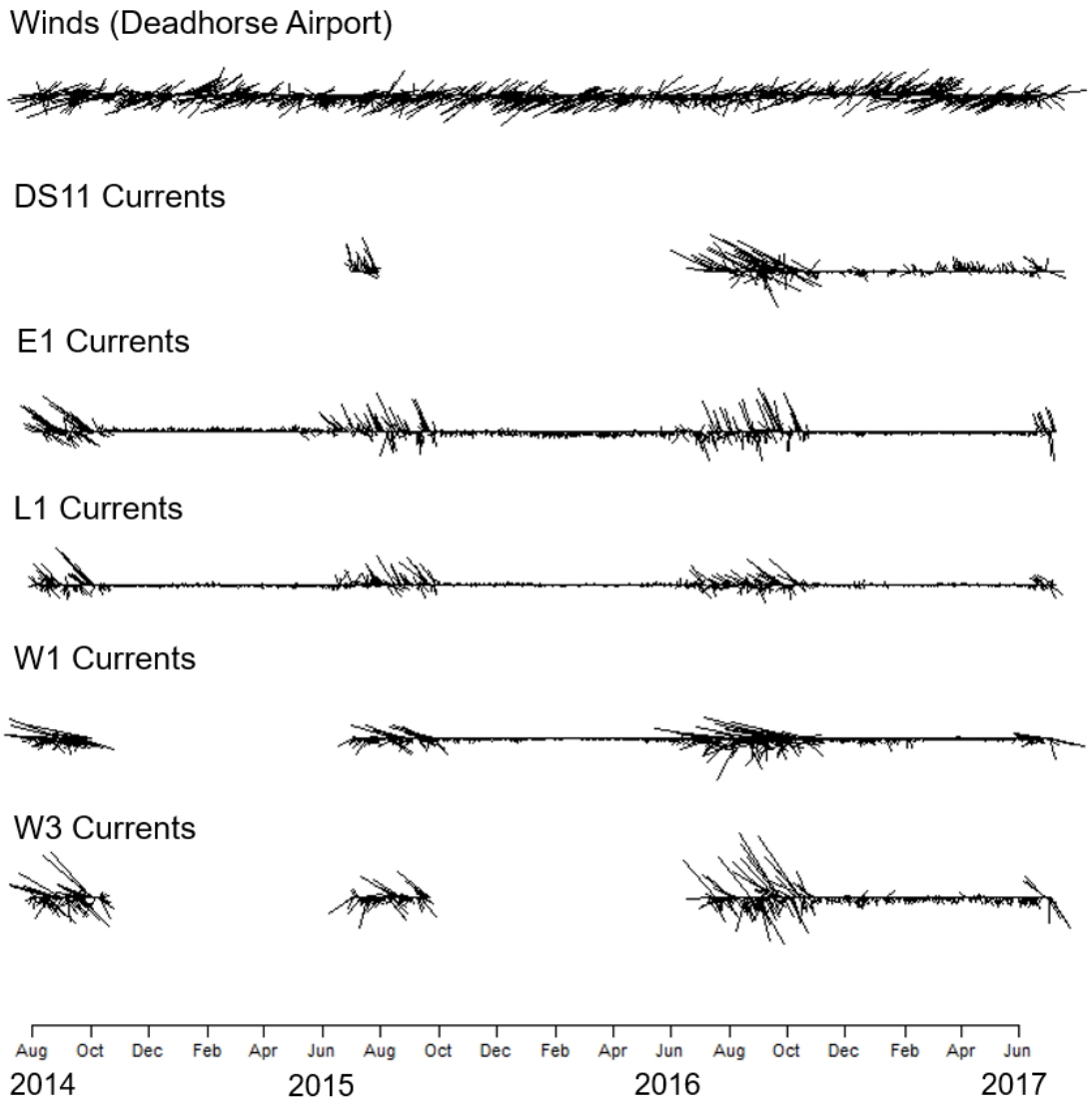

Figure 2.5: Timeseries of direction and relative speed of wind at Deadhorse Airport (NWS) and currents at each site. North is positive in the y-axis, east is positive in the x-axis.

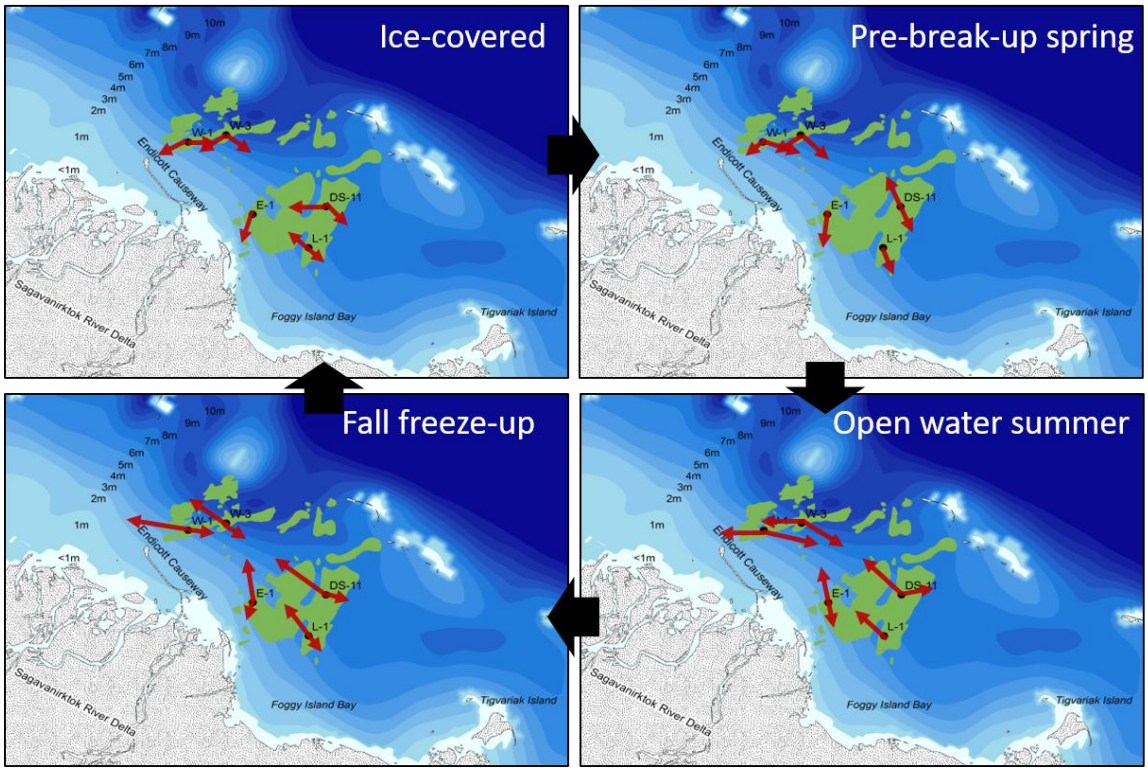

Figure 2.6: Seasonal flow patterns over the Boulder Patch. Vectors display the principal uni- or bi-directionality and relative velocity, based on circular histograms of current data.

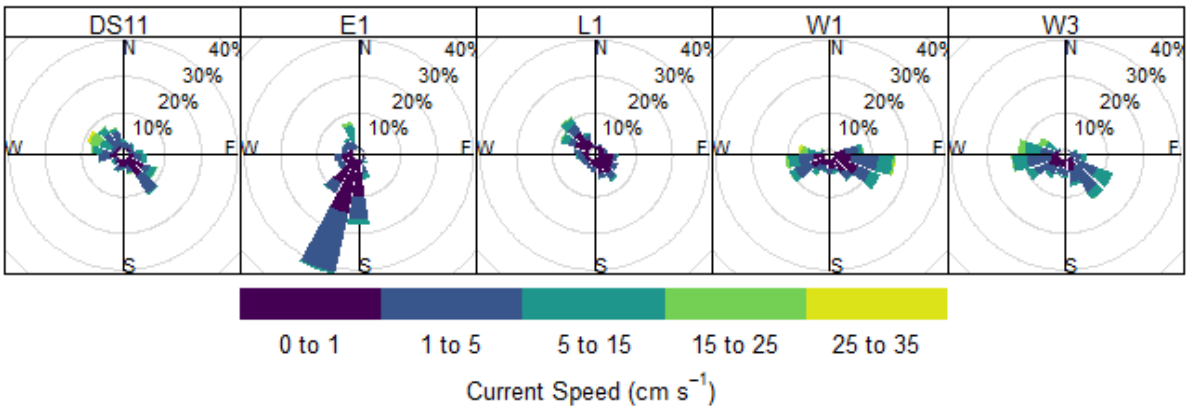

Figure 2.7: Distribution of mean daily current velocity and direction for each site for the entire dataset. Arc sections indicate the frequency of currents of a particular velocity and bearing, binned by 20^{o}

DISCUSSION

Spatiotemporal variability

Temporal abiotic variability in Stefansson Sound is primarily driven by sea-ice dynamics. On annual timescales, the timing of ice break-up and freeze-up determines the magnitude of current velocity, as well as temperature and salinity variation (Figs. 2.2,2.5). This timing also significantly influences underwater light levels (Dunton et al. 1992). Since tides along the Beaufort Sea coast are minimal, higher-frequency variations are caused by atmospheric forcing, which drives nearshore water mass movement (Dunton et al. 2006; Weingartner et al. 2017). In the absence of ice cover, this effect is amplified, leading to higher environmental variability in the summer. Much of the temperature and salinity variation at offshore sites (DS11 and W3) from July-October can be explained by upwelling due to easterly winds, which transports cold, saline shelf bottom waters further onto the inner shelf (Dunton et al. 2006). Westerly winds, on the other hand, entrain warm, fresh nearshore water into Stefansson Sound (Sellmann et al. 1992). These drivers are strengthened in the absence of sea ice, so most of the major spatial abiotic variability exists outside of the ice-covered winter months.

Spatial abiotic variation is linked to bathymetry and distance from the Sagavanirktok River. While our salinity record is inconsistent due to sediment fouling, some key trends emerge. By mid-November, after fall freeze-up, equivalent bottom temperature and salinity conditions prevail throughout Stefansson Sound. Winter minimum temperatures of ~-1.9, just above the freezing point (Fig. 2.4), as reported by Matthews (1981) and Sellmann et al. (1992), persist until May. Salinity increases to above 33 through the beginning of winter as a result of ion exclusion by the growing sea ice (Matthews 1981). With the advancement of spring, river runoff and sea ice melt begin to influence salinity and temperature in shallow areas (Figs. 2.2-2.3). Low salinities (mean ≤ 32) at E1 and W1 suggest greater riverine influence at these sites through the spring and summer (Table 3, Figs. 2.3-2.4). This is especially evident at E1, where the freshet was documented each year in June (Figs. 2.2-2.4), as predicted by modelling studies which showed that stratified fluvial plumes are retrained in the nearshore during ice cover (Kasper and Weingartner 2015). Elevated bottom temperatures at the shallow, nearshore site (E1; annual mean -0.47 ^{o}C) indicate frequent position above the thermocline, and exposure to warmer, inshore waters throughout the summer, when the mean temperature at this site is ~ 1 ^{o}C above that of the other sites (Tables 2.2-2.3, Figs. 2.3-2.4; Sellmann et al. 1992). While the timing of these events corresponds to Weingartner et al. (2017), comparison of the two studies emphasizes the cross-shore estuarine gradient in Stefansson Sound, with nearshore waters generally warmer by a few degrees and fresher than those further offshore.

Underwater light levels in the Boulder Patch are negligible for most of the year. In the winter, ice cover and the polar night keep the benthos in darkness. Sediments in the sea ice, which become entrained during fall storms (Osterkamp and Gosnik 1984) can further attenuate light at the sea surface. In some years (2014 and 2017), underwater light briefly rose in the spring, likely due to the presence of an ice canopy relatively free of these sediments, which allows light to penetrate into the water column. In spring of 2014, the year with the highest under-ice light levels, the return to darkness corresponded with the pulse of low salinity at E1 (Fig. 2.2), indicating that sediment and debris accompanying

spring runoff either wash over or spread under the ice, causing light levels to drop again. Underwater light levels increase dramatically during ice break-up, the time when they reach their maximum annual value (Bonsell and Dunton 2018). After ice break-up, wind and runoff events suspend sediments in the water column and light levels decrease until the sediments settle (Aumack et al. 2007; Bonsell and Dunton 2018). Comparisons between sites agree with past studies that showed daily underwater light levels are often elevated at the deep, offshore sites (Table 2.3) where concentrations of suspended sediment are reduced (Aumack et al. 2007; Bonsell and Dunton 2018).

Unlike other variables, current velocity and direction show large spatial variability in both summer and into winter, connected to the bathymetry and physiography of Stefansson Sound (Tables 2.2-2.3, Figs. 2.3,2.5-2.6). In winter, currents are minimal at most shallow sites (E1, L1; <2 cm s^{-1}). Offshore circulation patterns may influence sites adjacent to deep areas (W1, DS11 and W3, Fig. 2.1), and result in larger variability in winter current velocities, though overall velocities remained low (<3 cm s^{-1}), similar to winter measurements made by Matthews (1981) at DS11. Without direct influence from surface winds, currents appear more tidally-influenced during winter and spring (Figs. 2.5-2.6). After ice break up, flow direction becomes much more variable, as water motion becomes influenced by surface winds (Weingartner et al. 2017). Alongshore currents dominate across the Boulder Patch (Figs. 2.5-2.6). Wind-driven flows periodically reach above 15 cm s^{-1}, usually associated with easterly winds (Figs. 2.5, 2.7). Spatial variability in current velocity and direction is related to geomorphology and bathymetry: W1, which is less protected and closer to a deep inter-island pass than the other shallow sites (Fig. 2.1), has the highest mean current velocity in summer and fall (> 8 cm s^{-1}; Table 2.2, Fig. 2.3). The nearby deep site, W3, also experiences elevated flow velocity during summer and fall, as does DS11 (means >6 cm s^{-1}). Flow speeds are less than those measured north of Stefansson Sound at 17 m depth, which can reach above 50 cm s^{-1} in the fall (Weingartner et al. 2017), and the shallow sites closer to Foggy Island Bay have even lower mean current speeds (≤5 cm s^{-1}). Strong east wind events during late summer and fall result in elevated

current velocity, often bearing northwest, until freeze up is complete (Figs. 2.2,2.5). The W3 site mooring was lost to ice scour during one such fall storm in 2015. I was able to reconstruct the event to the day (11 October 2015) by a sudden increase in current speeds across Stefansson Sound leading up to instrument loss, which corresponded to a days-long easterly wind event (Figs. 2.2,2.5), which would have pushed drifting ice into and across Stefansson Sound (Fig. 2.6). This annual cycle of current velocity, driven by ice cover and wind, reflects previous studies in Stefansson Sound (Weingartner et al. 2017).

Long-term change

In Stefansson Sound, the ice-free season has lengthened by ~17 days over the past four decades (Bonsell and Dunton 2018). Comparisons to previous studies suggest that Stefansson Sound is warming as well: the average temperature at DS11 for August 1987-August 1988 was -1.25±1.42^{o}C (Sellmann et al. 1992), compared to our August 2011-July 2017 average of -0.76±1.97^{o}C (Fig. 2.8). The spring freshet signal was also absent from the 1988 temperature record, leading to a difference of 0.3 degrees in average May-June temperature (2012-2017 mean±SD: -1.58±0.20, 1988 mean±SD: -1.82±0.08, Fig. 2.8). Long-term warming may be confined to the spring and summer months, since our winter measurements of benthic temperature and salinity at DS11 mirror those collected at midwater depths from November 1978- February 1979 (-1.98--1.80 ^{o}C, salinity 32.5-34.3) (Matthews 1981b). The longer open-water season in the landfast ice zone during the recent decade is a result of temperatures increasing earlier and decreasing later in the year (Fig. 2.8; Mahoney et al. 2014). While the range of salinities appears similar, summertime salinities dropped later in the year in 1987 due to a later melt season.

A longer ice-free season would profoundly impact annual current dynamics. Of the variables we measured, currents responded most immediately to ice break-up and freeze-up, which confines the interaction between wind forcing and water motion (Figs. 2.2,2.5; Weingartner et al. 2017). Earlier melt and later freeze up would raise annual mean current velocity. Additionally, strengthened easterly winds in the Beaufort Sea region (Wood et al.

2013, 2015) would intensify advection from Stefansson Sound. This would potentially increase summer salinities at the benthos by transporting buoyant freshwater offshore.

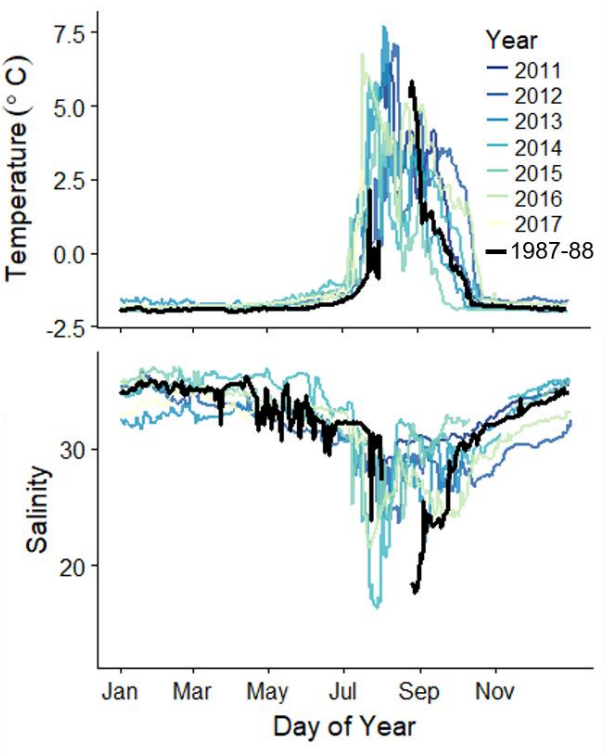

Figure 2.8: Temperature and salinity at DS11 for 2011-2017 (colored lines, this study) compared to 25 August 1987 to 11 August 1988 (black line, Sellmann et al. 1992).

Implications for the benthic ecosystem

In river-fed estuaries, the flow of freshwater can create gradients that affect ecological and biogeochemical processes. The extent and character of these gradients impact the ecosystem function of the estuary as a whole. In this study, I have demonstrated that the freshwater plume associated with the freshet can bathe shallow portions of Stefansson Sound in low-salinity water, reaching down to ~4 m in certain years (Figs. 2.2-2.3). Arctic river water differs from seawater not only in salinity, but in other chemical constituents, which could affect the physiology of benthic organisms underlying the

buoyant layer. Nutrient-depleted river water displaces seawater high in inorganic nutrients which have built up over the winter, which may result in significant nutrient stress for benthic autotrophs. Additionally, the organic composition of freshwater could create zones of differential biological activity and biogeochemical processes. For example, the dissolved organic matter associated with the freshet is highly labile (Holmes et al. 2008). If mixing is minimal (as it is under the ice), a nearshore zone with high concentrations of labile DOM could impact sediment microbial diversity and activity.

Current dynamics also influence the benthic realm by determining rates of sedimentation, as well as the delivery of food and nutrients to benthic organisms (e.g. Pequegnat 1964; Sebens 1984). High flow speeds can also mechanically stress or remove attached flora and fauna. Additionally, current dynamics determine the advection and transport of planktonic propagules, thereby impacting population connectivity and persistence within the region (e.g. Cowen and Sponaugle 2009; Coleman et al. 2011). The annual cycle of minimal currents in the winter and maximal currents in the fall imply that propagule transport for any given species greatly depends on the timing of its life cycle. Differences in current regime between the eastern Boulder Patch sites and the deep and western sites (Figs. 2.5-2.7) suggest that these locations may have differing rates of propagule advection and delivery, which could affect benthic community structure and genetic diversity. Intensified easterly winds (Wood et al. 2013, 2015) and a longer open-water season (Mahoney et al. 2014) in the Beaufort Sea would increase the advection of terrestrial material, nutrients, plankton, and propagules away from the coastal zone.

Studies that focus on estuarine processes within the Arctic are rare, and even fewer studies cover time periods outside of mid- to late-summer (McClelland et al. 2012). However, as demonstrated here, environmental variability occurs during periods outside the summer months that could profoundly affect nearshore ecosystems. Knowledge of the range and spatial patterns of abiotic conditions provide the conceptual basis to evaluate and understand ecosystem processes and function on Arctic inner shelves.

Chapter Three: Patterns and drivers of benthic community structure and early succession in an estuarine Arctic kelp bed

ABSTRACT

Benthic community structure in Arctic nearshore ecosystems may result from both seasonal abiotic variability and the processes of recruitment and succession, all of which could be mediated by physiographic and bathymetric characteristics. In this study, we compared spatial differences in community structure to environmental conditions (temperature, salinity, current speed, underwater light), and to bathymetry and physiography (depth, distance from river inputs) in a shallow Arctic kelp bed. Additionally, because propagule delivery and recruitment can overcome strictly abiotic effects on ecosystem structure, we monitored spatial and temporal patterns of recruitment and community development to assess the timescale and trajectory of ecological succession. The benthic community varied among sites, but was dominated by red algae (47-79% average cover at each site), prostrate kelps (2-19% average cover), and crustose coralline algae (0-19% average cover). Strong spatial distinctions among sites were particularly due to the positive correlation between distance to river inputs and cover by crustose coralline algae ($\rho = 1.0$), and larger proportions of invertebrates at a high flow site. However, there were no significant relationships between any single environmental characteristic and any functional group. Recruitment patterns indicated that successional processes are important to structuring the community, with foliose red algae as a key early successional group (up to ~60% of recruits at shallow sites). Greater variance in successional trajectory at sites near deep passes compared to more sheltered sites indicated that differential flow patterns affect community development by altering the local propagule pool. Succession also occurred extremely slowly, which would hinder ecosystem recovery after catastrophic disturbances. These results suggest that community development in the nearshore Beaufort Sea occurs over many years, and is influenced by combinations of abiotic and biotic factors. The benthic community, therefore, reflects an integration of abiotic conditions over timescales longer than most ecological studies. While seasonality exerts strong influence

on Arctic systems, ecologically-important environmental variability in the coastal zone can also occur over extended time periods. Climate-driven changes in Arctic Ocean wind dynamics, freshwater budgets, sea ice extent, and erosional inputs will alter the community structure and distribution of shallow kelp beds.

INTRODUCTION

Kelp bed communities in the Arctic are expected to change dramatically as climate warming reduces ice cover and warms temperatures. Boreal species are expected to shift distributions poleward into the Arctic realm and contribute to predicted increases in primary productivity and biomass in rocky nearshore habitats (Müller et al. 2009; Krause-Jensen et al. 2012; Krause-Jensen and Duarte 2014). However, the future of kelp beds adjacent to erosional coasts and rivers may be more uncertain than those along stable, rocky coasts (Filbee-Dexter et al. 2019). In these inner shelf areas, salinity stress from augmented freshwater inputs can reduce kelp photosynthetic capacity and recruitment (Karsten et al. 2001; McClelland et al. 2006; Fredersdorf et al. 2009). Increased sediments (Gordeev 2006; Lantuit et al. 2012; Fritz et al. 2017) that attenuate light (Van Duin et al. 2001; Aumack et al. 2007) and hinder recruitment (Devinny and Volse 1978; Zacher et al. 2016; Lind and Konar 2017; Traiger and Konar 2017) may further obstruct persistence of local kelps. As these habitats characterize a considerable portion of Arctic kelp beds, especially in Alaska and Russia (Lantuit et al. 2012; Filbee-Dexter et al. 2019), baseline data on the physical environment and biological patterns of shallow, river-influenced areas is vital to assess and evaluate the redistribution of Arctic biota and ecosystems .

The Boulder Patch is the largest of the discrete kelp beds scattered along the Alaskan Beaufort Sea coast, located in shallow (~4-7 m), nearshore waters of Stefansson Sound, east of Prudhoe Bay and adjacent to the Sagavanirktok River delta (Fig. 3.1). Influence from the Sagavanirktok River, and other large rivers (including the Mackenzie River) along the Beaufort Sea coast, make Stefansson Sound considerably estuarine in character (Bonsell 2019, Chap. 2). Boulder and cobble substrates that characterize the Boulder Patch support a rich epibenthic community with greater diversity than the

surrounding soft-sediment habitat (Dunton et al. 1982, Dunton and Schonberg 2000). Diversity and structure of this community varies across the kelp bed (Martin and Gallaway 1994). The community is dominated by the Arctic endemic kelp, *Laminaria solidungula*. The kelps *Saccharina latissimia* and *Alaria esculanta* are also present, though the latter is rare. Foliose red algae, including *Phyllophora trucatus*, *Dilsea socialis*, and *Phycodrus rubens* form a dense turf community throughout much of the Boulder Patch. Nestled amongst the turf are filter feeders: sponges (such as *Halichondria panacea* and *Semisubrites cribrosa*), bryozoans (such as *Eucratea loricata*), and hyrdoids (*Sertularia spp.*). The soft coral *Gersemia rubiformis* is a charismatic community member, and common in certain areas. At some sites, crustose coralline algae (likely *Leptophytum laeve* and *L. foecundum*) coats much of the rock surface unoccupied by the preceding groups, though it is completely absent in other areas. While the relationship between underwater light levels and kelp growth in the Boulder Patch is well established (Dunton 1990; Aumack et al. 2007; Dunton et al. 2009; Bonsell and Dunton 2018), the causes of these spatial variations in community structure are unknown.

The Arctic coastal ocean is distinctively seasonal – with strong influence from the cycles of terrestrial freshwater inflow and sea ice extent, the physiochemical marine environment transforms considerably from ice-covered winter, to spring melt, to open water summer. The range of conditions experienced over the year could have strong effects on ecosystem characteristics and processes. It is especially pertinent to establish linkages between abiotic variability and biological ecosystem characteristics because seasonal patterns are rapidly shifting in the Arctic due to increased surface air temperatures (~1^{o}C/decade, Christiansen et al. 2013) and the expansion of the summer open-water season (Markus et al. 2009; Parkinson 2014). These changes have already altered community structure and ecosystem function in Arctic marine habitats (e.g. Wassmann 2011; Kortsch et al. 2012). Shifts in sea ice extent and sea surface temperature – which can be measured remotely – have demonstrable effects on benthic community composition (Grebmeier et al. 2006; Beuchel et al. 2006; Kortsch et al. 2012). Linkages between year-round *in situ* environmental conditions and ecosystem characteristics, such as community

structure and recruitment, allows for stronger predictions of Arctic ecosystem change in the face of climactic warming and increased industrial activity.

Additionally, the drivers and spatiotemporal patterns of benthic recruitment and succession are currently understood via a handful of studies carried out in Svalbard and Eastern Greenland (Beuchel and Gulliksen 2008; Fricke et al. 2008; Kuklinski et al. 2013; Meyer et al. 2017), and one in the Beaufort Sea (Konar 2013). In some habitats, recruitment can occur relatively quickly, such as in shallow, Atlantic-influenced Svalbardian fjords (Meyer et al. 2017), while in other areas, recruitment and succession can proceed very slowly, taking over a decade for cleared experimental plots to resemble the benthic community (Konar 2013, Beuchel and Gulliksen 2008). Kortsch et al. (2012) hypothesized that climate-driven shifts in temperature and ice cover had reduced the resilience of benthic communities in Svalbard by altering patterns of recruitment and succession. These processes are a key component in the future persistence of Arctic kelp beds

The goal of the present study is to determine how seasonal variation in the physio-chemical environment, spatial variation in benthic community structure, and community development are related in a shallow (< 9 m), river-influenced Arctic kelp bed. I paired long-term environmental data (Bonsell 2019, Chap. 2) with benthic surveys to assess how benthic community composition may reflect spatial environmental variability. I also used *in situ* settlement tiles to evaluate whether community structure was simply an effect of larval supply. In particular, I examined if recruited community composition was different from established benthic community composition, but became more similar to the benthic community over time. The progression of ecological succession can reveal mechanisms that relate abiotic differences to community dissimilarity (Kroeker et al. 2012, 2013). Additionally, we were interested in the timescale of community development. Previous work indicates that recovery from disturbance can take a decade or more in the Boulder Patch (Konar 2013). However, climax community composition could be determined early on in succession due to abiotic restraints on species composition. This would especially be the case if the strength of competitive biotic interactions is low due to abiotic stress (Bertness and Callaway 1994). Therefore, this study also indirectly addresses the role of

abiotic versus biotic variables in determining community structure in Arctic nearshore ecosystems.

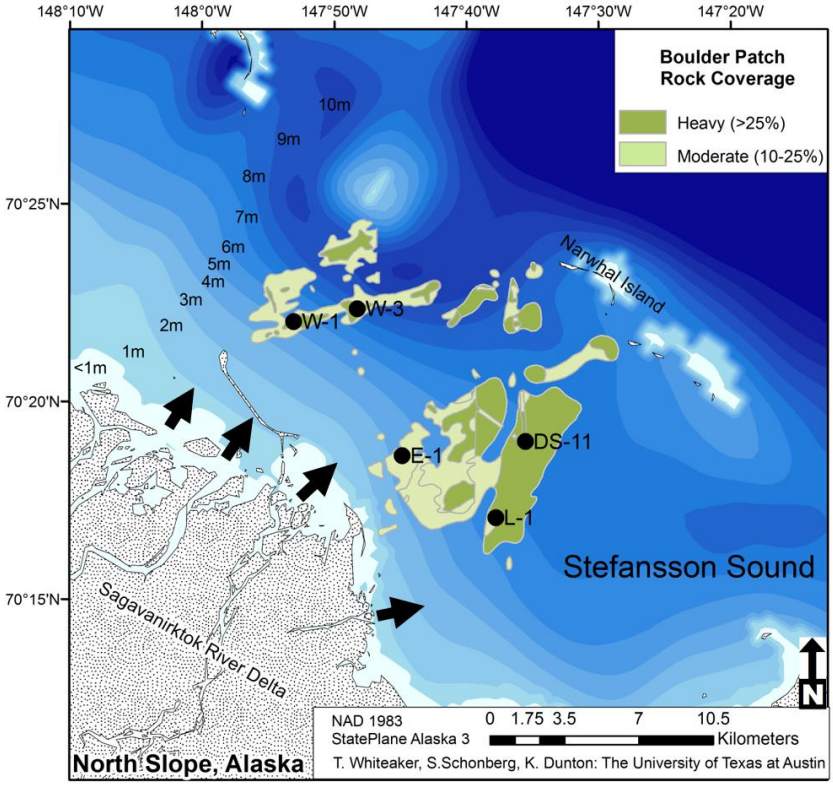

Figure 3.1: Map of study sites (W1, W3, E1, L1, and DS11) in the Boulder Patch with rock cover indicated in green. Adapted from Bonsell and Dunton, 2018. Arrows indicate channel inputs from the Sagavanirktok River.

METHODS

Study sites and environment

I used five long-term study sites that vary in their depth, distance to shore, and proximity to the mouth of the Sagavanirktok River. (Fig. 3.1). Three sites (DS11, E1, L1)

lie between a set of barrier islands (including Narwhal Island) and the mainland, while the other two sites (W1 and W3) are more exposed, located near deep channels between a shoal and barrier islands (Fig. 3.1).

Annual and seasonal means of temperature, salinity, underwater light levels (photosynthetically active radiation, PAR), and current velocity at each site were derived from Chapter 2. Briefly, *in situ* benthic loggers were deployed at each site for multiple years, bounded by the period of August 2011-August 2017 (Bonsell 2019, Chap. 2, methods described therein). Distance from each site to nearest river input (Fig. 3.1) was estimated in ArcGIS by drawing a line between each site and the nearest land boundary associated with a river channel mouth. Site depths are from Aumack et al. (2007) and Bonsell and Dunton (2018).

Benthic community structure and succession

To characterize established benthic community structure at each site, 0.05 m^2 photoquadrats were taken by a diver using a Nikon 1 AW1 waterproof digital camera in July and August 2016 and 2017. Due to the predominantly poor visibility and heterogeneous rock cover in the Boulder Patch, the diver would take the photos haphazardly while working in a spiral pattern by rising above the benthos, kicking twice and 'landing' with the photoquadrat. If rock cover within the photoquadrat appeared to be >75%, a photo was taken. Photos were analyzed for benthic percent cover to the lowest possible taxonomic group using point intercept of 56 stratified random points using the online program CoralNet (coralnet.ucsd.edu). Photos with >25% soft sediment or >20% unclear points were removed from the analysis, with 24 to 43 photos used in final analysis for each site (n: E1=36, DS11=31, L1=24, W1=43, W3=35). All data were normalized to percent rock cover in each photoquadrat.

To assess recruitment and succession patterns at each site, settlement tiles (10x10 cm fibercement) were deployed in July 2015. Each subsequent year, a subset of these tiles was removed and a new set was deployed by divers. This gave us data from plates that had

been deployed for durations of one (2015-2016, 2016-2017, and 2017-2018), two (2015-2017 and 2016-2018), and three years (2015-2018), with each plate representing an independent unit. Not all deployed plates were recovered due to loss by ice scour or adverse diving conditions (Supp. Table C1). After retrieval by divers, plates were placed in individual sealed containers with seawater and transported live to the lab where they were examined under a dissecting microscope. Organisms were identified to the lowest taxonomic level possible and counted.

Five functional groups were used to evaluate differences in community structure among sites: kelp, crustose coralline algae (hereafter abbreviated as CCA), fleshy red algae, filter feeders, and suspension feeders (Table 3.1). There are various definitions for "filter" and "suspension" feeding, and the two are sometimes used synonymously. Here, these terms are used to separate bryozoans, corals, and hydroids (suspension feeders) from sponges and ascidians (filter feeders). For the species present in this study, the former extend appendages (cilia or tentacles) into the water column to acquire food particles, while the latter actively pump water through their bodies to feed. These groups also differ in their gross morphology: the filter feeders are generally robust while the suspension feeders are more filamentous. Differences in feeding behavior and morphology may lead to differing responses to variation in flow and suspended sediments, and use of multiple traits to group biota leads to higher sensitivity when assessing differences in community composition (Bremner et al. 2003).

Data analysis

To determine differences in established benthic communities among sites, a Bray-Curtis matrix was calculated from square-root transformed percent cover data, then analyzed statistically using PERMANOVA as well as visually using an nMDS plot. Square root transformation decreased the number of pairwise differences in homogeneity, but the transformation did not change PERMANOVA results. Differences in total abundance of biota on settlement tiles within sites and within ages (one, two, and three years) was

assessed with Welsh one-way tests, or Welsh two-sample t-test, depending on the number of groups. To compare the benthic community to settlement tile communities, percent cover (photoquadrats) and abundance (tiles) data were transformed into proportional abundance of each functional group, then square-root transformed and a Bray-Curtis matrix was calculated. The trajectory of community development on the tiles was evaluated using NMDS plots that grouped mean benthic community and means of each age of tile community, as well as by plotting the Bray-Curtis dissimilarity to the benthic community over time at each site. Additionally, mean and variance in Bray-Curtis dissimilarity between one- and two-year-old tiles for each site was plotted.

The relationship between mean environmental variables and percent cover by each functional group was assessed with Spearman's rank-correlations. The use of correlations to connect the physical environment to biological characteristics is meant to springboard future field studies and experiments. While low sample number (five sites) prevents more rigorous statistical tests, I aim to characterize broad patterns which link abiotic factor to community structure, and present a baseline in the growing field of Arctic kelp bed ecology.

Table 3.1: Common species and genera from the Boulder Patch associated with each functional group category used in community analysis.

Functional group	**Common Boulder Patch examples**
Foliose red algae	*Phyllophora trucata* *Dilsea socialis* *Phycodrys rubens*
Crustose coralline algae (CCA)	*Leptophytum foecundum* *Leptophytum laevae*
Kelp	*Laminaria solidungula* *Saccharina latissimia* *Alaria esculenta*
Suspension feeders	**Phylum Bryozoa** *Alcyonidium* sp. *Eucratea loricata* **Phylum Cnidaria** *Sertularia* sp. *Calicella* sp. *Obelia* sp. *Gersemia rubiformis* **Phylum Crustacea** *Balanus* sp.
Filter feeders	**Phylum Porifera**: *Semisuberites cribrosa* *Halichondria panicea* **Phylum Urochordata** *Rhizomogula* sp.

RESULTS

Benthic community structure

Benthic community composition, as recorded by photoquadrats, varied among sites (Figs. 3.2-3.4, Tables 3.2-3.3). The community at the deep, offshore site DS11 prominently featured kelp (mostly *Laminaria solidungula*, though *Saccharina latissimia* and *Alasia esculenta* were common) and CCA (Figs. 3.3-3.4, Table 3.2). The foliose red *Dilsea*

socialis was more common at this site than at the shallower sites. *D. socialis* was also relatively common at the other deep site, W3, along with *Phyllophora truncata* and CCA. *Gersemia rubiformis* was also present in at W3, though other invertebrate groups were rare (Figs. 3.3-3.4, Table 3.2). This is in contrast to and adjacent but shallow site (W1), where *G. rubiformis*, sponges, hydroids, and bryozoans were relatively common, though the community was dominated by foliose reds (especially *Phycodrys rubens*) (Figs. 3.3-3.4, Table 3.2). The shallowest site, E1, exhibited the highest cover by foliose reds, dominated by *P. rubens*, though *P. truncata* was also abundant (Figs. 3.3-3.4, Table 3.2). This was the only site where barnacles were recorded in photoquadrats. Neither CCA nor *G. rubiformis* were recorded at this site. *Gersemia rubiformis* was also absent from L1 and DS11 photoquadrats, though it was observed at DS11. As with the other shallow sites, L1 was dominated by foliose reds, but also had the second-highest kelp cover (Figs. 3.3-3.4, Table 3.2). CCA was present, but rare at this site. All sites had >10% cover by bare rock, with sites W3 and W1 having over 30% bare rock coverage (Table 3.2).

For E1 and W1, where photoquadrats were taken over two consecutive years, community structure did not vary by year (PERMANOVA, $p>0.05$), so analysis was done by site only. Benthic community structure based on functional groups was significantly different among sites (Table 3.3, Fig. 3.2). Pairwise comparisons demonstrated that all sites were unique from each other, except E1 and L1 (Supp. Table C2).

Relationship to environmental variables

Comparisons between functional group percent cover and environmental variables at each site (Supp. Table C3) revealed only one significant relationship – a positive correlation between cover of CCA and distance from Sagavanirktok River channels ($\rho = 1.0$, $p<0.05$; Fig. 3.5A-B). Distance from river channels had stronger correlations with functional group percent cover than depth (Fig. 3.5A). There were negative, but non-significant, relationships between mean salinity and cover by both invertebrate groups (Fig. 3.5A). Temperature and velocity had no strong correlations with any functional group (Fig.

3.5A). Interestingly, PAR also had no strong correlations with any algal group, but was negatively related to filter feeder cover (Fig. 3.5A).

Settlement tiles and comparisons to benthic community

Abundance of individual biota could be extremely variable among settlement tiles (Table 3.4). In general, mean overall abundance increased over time (Table 3.4). Deployment duration had a significant effect on total abundance of tile biota at sites W1 (Welch one-way test, $F_{2,19}$=21.033, $p<0.05$) and W3 (Welch two-sample t-test, $t_{17.38}$ =-2.67, $p<0.05$). Mean abundance was greatest for tiles deployed at DS11, though not significant due to high variability (Table 3.4).

Settlement tile communities significantly varied by site and age (PERMANOVA, $p>0.05$). Within each site, tile communities significantly differed among specific years of deployment (e.g. at DS11, the community on one-year-old tiles from 2015-2016 was significantly different from one-year-old tiles from 2016-2017) as well as age (Pairwise PERMANOVAs, $p>0.05$; Fig 3.6A-E). Within durations, communities were also different among sites (PERMANOVA, $p>0.05$), except for one-year-old tiles from L1 and W1. Microscopic red algae recruits and juveniles were common on many of the tiles, though they were too small to identify species (Fig. 3.4). CCA recruits and juveniles were also fairly common on tiles at most sites, and were even present at E1 (on tiles deployed in 2017-2018 only) despite the absence of this group from the adjacent established benthic community (Fig. 3.4). Notably, no juvenile kelp ever recruited to the tiles.

At DS11, tiles were numerically dominated by CCA, while other sites were dominated by both CCA and/or red algae and suspension feeders (Fig. 3.4). A large number of filter feeders also recruited to W3 tiles in year one (Fig. 3.4). Comparison of tile communities (proportional abundance) to the benthic community (proportional percent cover) demonstrates that tile communities were generally dissimilar to the benthic community, and only became more similar to the benthic community in year two at site

W3, and in year three at W1 (Fig. 3.6F). Of all the sites, tiles at DS11 were the most similar to the benthic community, and had the least change between ages (Figs. 3.6A,F, 3.7). Tile communities at W1 and W3 were very dissimilar between years one and two, with high variation in how the community developed (Figs. 3.6D-F, 3.7).

Table 3.2: Mean and standard deviation of each functional group in the established benthic community at each site.

Site	CCA	Red algae	Kelp	Filter feeders	Suspension feeders	Rock
E1	0 ± 0	79.31 ± 0.51	2.9 ± 0.25	0.77 ± 0.11	6.12 ± 0.21	10.91 ± 0.34
L1	0.64 ± 0.06	71.67 ± 1.19	9.85 ± 0.93	0.48 ± 0.05	2.79 ± 0.21	14.57 ± 0.82
W1	0.48 ± 0.03	47.32 ± 0.76	4.4 ± 0.24	2.12 ± 0.12	14.87 ± 0.39	30.81 ± 0.59
W3	4.67 ± 0.15	58.01 ± 0.63	1.65 ± 0.14	0.77 ± 0.05	0.24 ± 0.02	34.66 ± 0.61
DS11	18.67 ± 0.46	38.01 ± 0.78	19.03 ± 0.75	0.44 ± 0.03	4.08 ± 0.19	19.77 ± 0.59

Table 3.3: PERMANOVA summary table for comparing benthic community structure by site (square-root transformed data).

	Df	Sums of Sqs	Mean Sqs	F.Model	R^2	Pr(>F)
Site	4	6.01	1.50	23.45	0.36	0.01
Residuals	164	16.51	0.06		0.64	

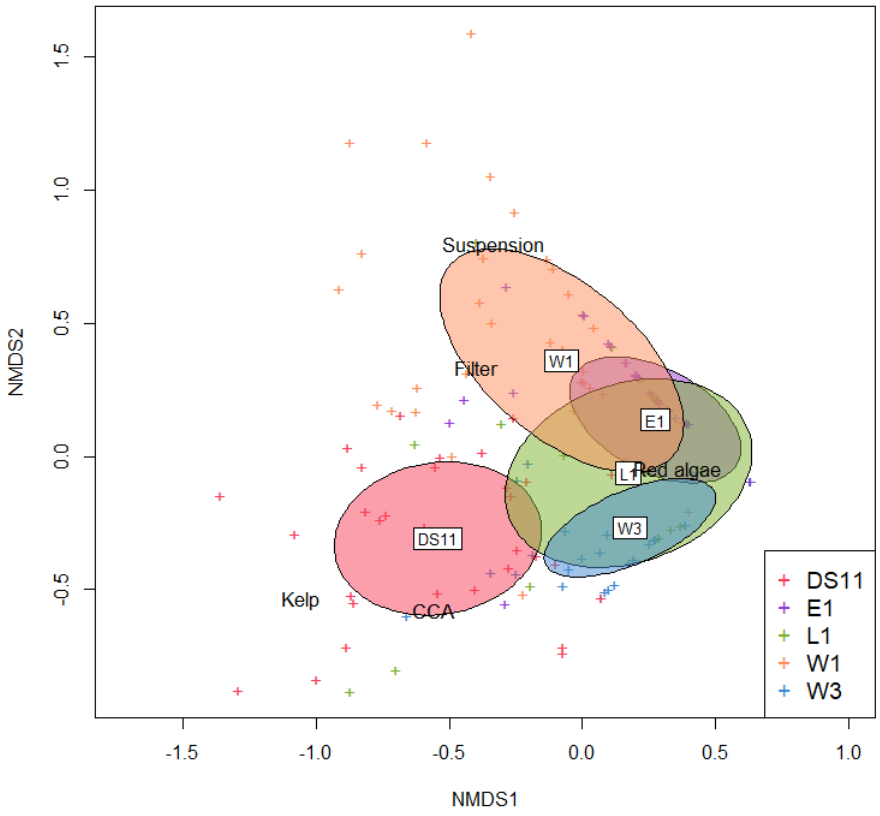

Figure 3.2: Non-metric multidementional scaling plot (Bray-Curtis matrix, square root transform) of benthic community structure by functional group at each site. Center of ellipses indicate median community structure; ellipse area indicates standard deviation. Crosses indicate individual photoquadrats. 2D stress=0.14.

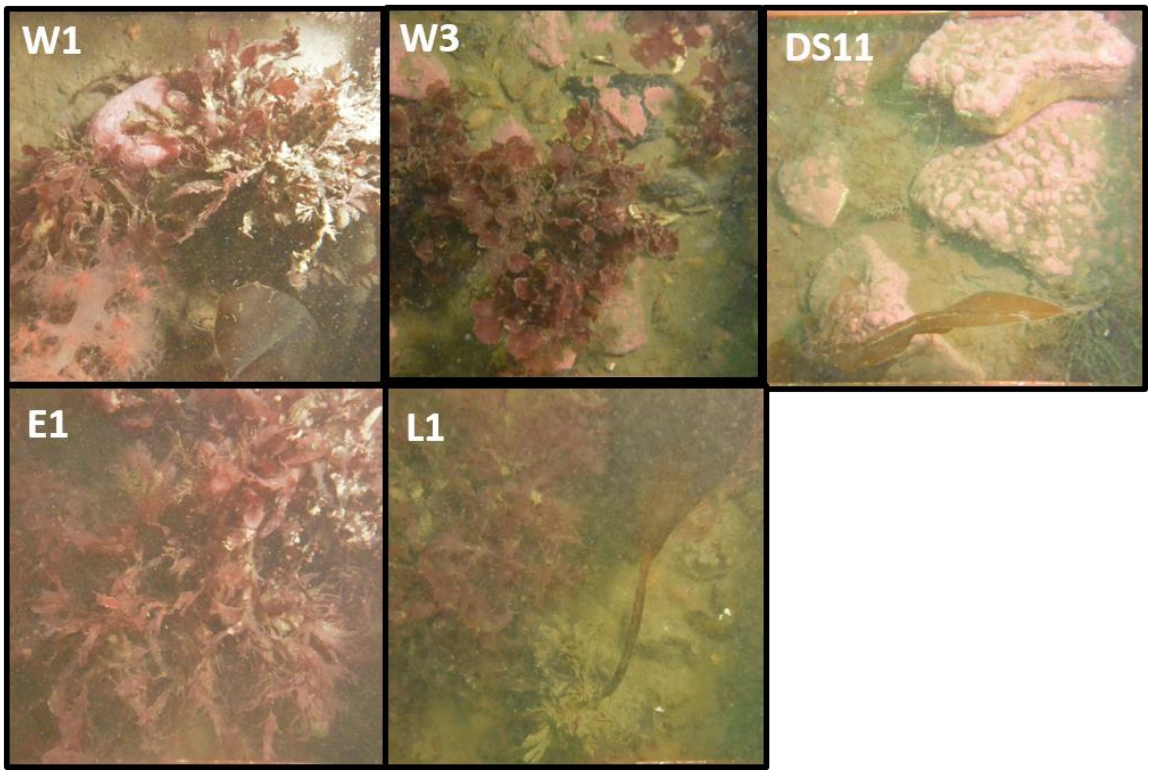

Figure 3.3: Example photoquadrats from each site.

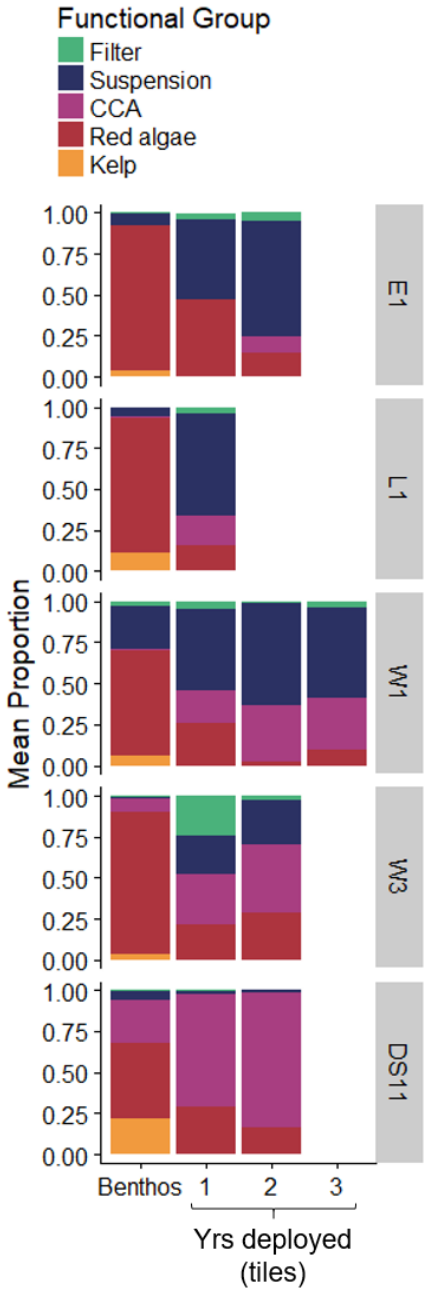

Figure 3.4: Mean proportion of each functional group at each site recorded for benthic photoquadrats and settlement tiles. This value represents proportion of total biotic percent cover for the benthic community and proportional abundance for tile communities. Note that no kelp recruited to settlement tiles.

Table 3.4: Mean total abundance (± standard deviation) of individual biota per 100 cm^2 settlement tile and number of tiles per deployment duration. * Indicates that abundances were significantly different between or among deployment durations for that site.

Site	1 Year		2 Years		3 Years	
	Mean ± SD	N	Mean ± SD	N	Mean ± SD	N
DS11	69.9 ± 61.7	24	233.0 ± 316.3	16	-	-
E1	17.8 ± 17.8	24	61.6 ± 108.5	16	-	-
L1	3.3 ± 2.1	16	-	-	-	-
W1*	15.0 ± 18.9	24	14.1 ± 4.7	8	35.9 ± 8.2	8
W3*	22.3 ± 19.6	16	42.0 ± 15.6	16	-	-

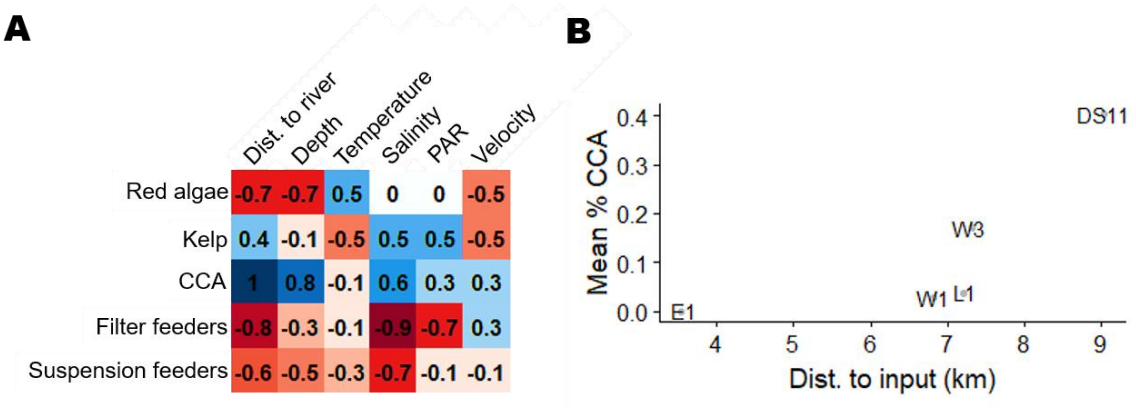

Figure 3.5: A) Correlation matrix between percent cover of functional groups and mean environmental variables at each site. Number denotes Spearman rank correlation (ρ), with ρ=1 being statistically significant in these cases (p<0.05). Color indicates correlation value, with deeper blue meaning more positively correlated and deeper red meaning more negatively correlated. B) Mean percent cover of crustose coralline algae (CCA) in the benthic community at each site compared to distance to nearest river input. See Fig. 3.1 for site locations.

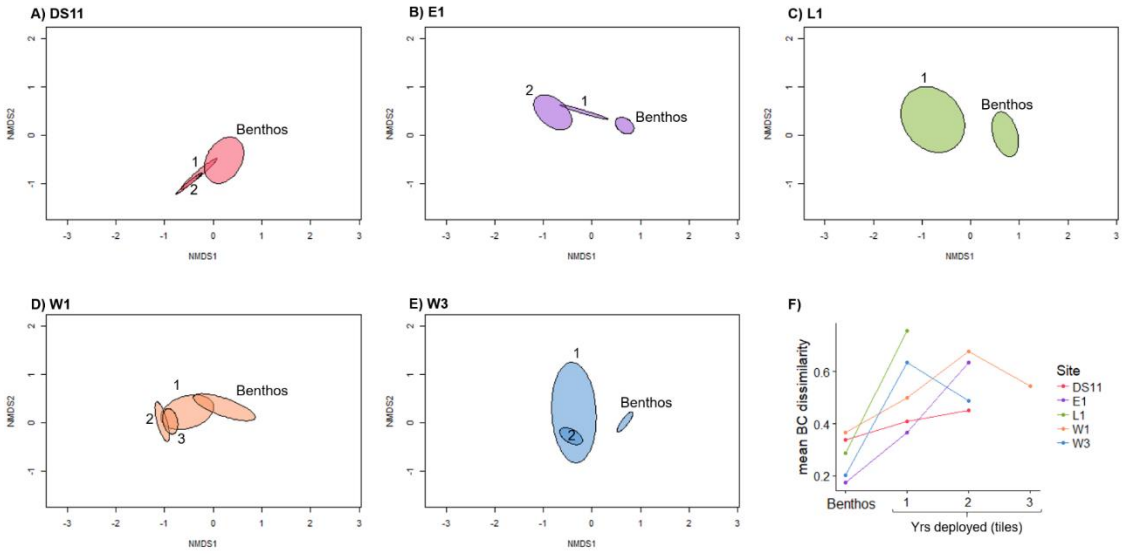

Figure 3.6: Development on tile communities over time as compared to the benthic community at each site. A-E) Non-metric multidementional scaling plot of benthic and tile communities (from Bray-Curtis matrix on square-root transformed proportional data) broken up by site showing the trajectory of community development over time. Ellipses represent the mean and standard deviation of each community. 2D stress=0.11. F) Mean development of settlement tile communities over time compared to benthos, represented as mean BC dissimilarity. The leftmost points represent the mean dissimilarity between photoquadrats within the benthic community at each site.

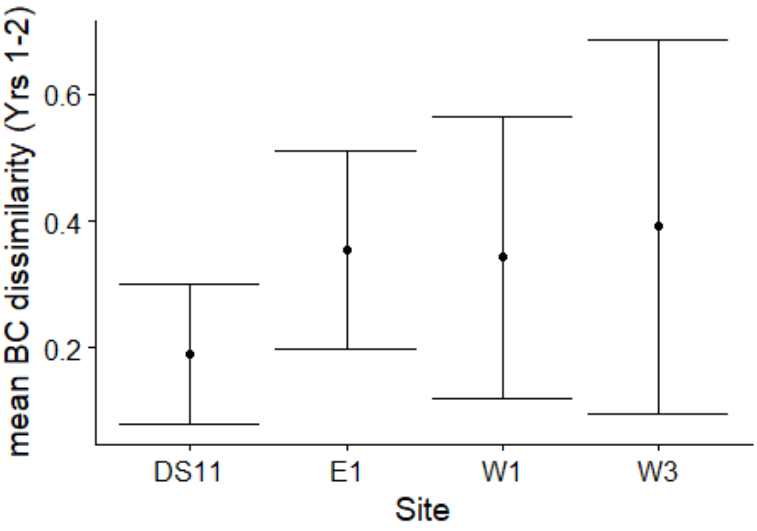

Figure 3.7: Development of settlement tile communities at each site between years one and two represented as mean (± standard deviation) Bray-Curtis dissimilarity. Standard deviation increased with distance to inter-island passes (Fig. 3.1).

DISCUSSION

Spatial heterogeneity in benthic community structure

Freshwater that flows from the Sagavanirktok River in the spring and early summer strongly influences Boulder Patch benthic community structure. In general, there were more invertebrates closer to the river and at lower mean salinities, while kelp and CCA showed the opposite pattern (Fig. 3.5A). This relationship was strongest with cover by CCA, which increased with distance from river inputs (Fig. 3.5B). During the spring freshet, Stefansson Sound can become extremely stratified (Weingartner et al. 2017), with shallow, inshore sites above the halocline (Bonsell 2019, Chap. 2). The site closest the river (E1) is distinct in its lack of CCA, relatively high cover by foliose red algae (79%), and low cover by kelp (3%) relative to the other sites. CCA are ecologically-important members of subtidal habitats (Steneck 1986; Mccoy and Kamenos 2015) and are

competitive dominants in the Boulder Patch (Konar and Iken 2005) and other Arctic epilithic communities (Beuchel and Gulliksen 2008; Kuklinski 2009), so their complete absence at E1 represents an significant ecological pattern. Although CCA are usually dominant in low light environments (Vadas and Steneck 1988), the lack of CCA at E1 does not seem to be related to light levels, as this site is comparable, or darker than other sites (Dunton et al. 2009; Bonsell and Dunton 2018; Bonsell 2019, Chap 2). The environmental data indicate that freshwater influence may preclude the establishment of CCA at this site (Fig. 3.5A-B). While CCAs are prone to low pH, Sagavanirktok River water is considerably basic (Craig and McCart 1975, Muth *pers. comm.*). Instead, low salinities may be responsible for the absence of macroscopic CCA (King and Schramm 1982; Schoenrock et al. 2018). Settlement tile data demonstrates that recruitment is not limiting, as CCA can recruit to E1 in certain years (Fig. 3.4). Furthermore, the low rate of growth of all recruited taxa prevents competitive exclusion early in succession. Instead, osmotic stress and mortality caused by exposure to the buoyant freshwater layer in certain years prevent slow-growing CCA from becoming part of the established community.

Salinity stress may also explain the low kelp abundance at E1: Karsten (2008) demonstrated that *L. solidungula* exhibits decreased photosynthetic performance after two days of exposure to salinities less than 20, conditions that often occur at E1 during the freshet (Bonsell 2019, Chap. 2). Salinity gradients structure kelp forests globally (e.g. Sundene 1953; Buschmann et al. 2004; Spurkland and Iken 2011), and low salinities resulted in the first-published instance of kelp habitat deforestation (Yendo 1914; Steneck and Erlandson 2002). In Stefansson Sound, warmer, fresher waters during the spring and summer may give a competitive advantage to red algae over CCA and kelp (King and Schramm 1982; Harley et al. 2012; Schoenrock et al. 2018), and thereby amplify the negative effect of foliose red algae on kelp (Filbee-Dexter and Wernberg 2018). This relationship is also implied by the high kelp cover observed at the site with the lowest foliose red algae cover (DS11, Table 3.2).

Current dynamics are an important structuring mechanism for benthic communities because they alter the delivery of propagules, food, and nutrients, and can cause mechanical

stress or removal of entire organisms. Current direction also determines the source of propagules delivered to any particular area. W1 had a large percent bare rock cover (31%) and a greater abundance of invertebrates (Fig. 3.4, Table 3.2). The greater current velocities from the nearby passes (Bonsell 2019, Chap. 2) may favor filter and suspension feeders by providing higher delivery rates of particulate food (e.g. Pequegnat 1964; Sebens 1984), though further investigation is needed. Community composition at L1 was not statistically different from that at E1, with both sites dominated by foliose red algae (Figs. 3.2,3.4, Table 3.2, Supp. Table C2). Although these locations experience different regimes of temperature and salinity, their seasonal current dynamics are very similar (Bonsell 2019, Chap. 2). These sites may be protected from strong currents due to their shallow position between barrier islands and the shore, which may provide a competitive advantage to algae over invertebrates (Fig. 3.1). W3 and DS11 both exhibit relatively elevated mean light levels and current speeds (Bonsell, Chapter 2), but have dissimilar benthic communities, with less CCA and kelp at W3 (Figs. 3.2,3.4, Supp. Table C2). Prominent bare rock cover at W3 (average 35%) implies that this difference may be due to more frequent disturbance. The proximity of this site to a deep channel pass into Stefansson Sound may expose it not only to stronger currents, but also to more-frequent ice-scour, a common disturbance in benthic polar habitats (Conlan et al. 1998; Beuchel and Gulliksen 2008) that has been observed extensively at W3 (*pers. obs*., Bonsell 2019, Chap. 2). This would preclude dominance by slow-growing, but competitively dominant Arctic CCA (Konar and Iken 2005; Kuklinski 2009; Schoenrock et al. 2018) and slow-to-establish kelp (this study).

The influence of light levels on benthic community composition are not straight forward, likely due to interactions between environmental variables influencing benthic biota. The most nearshore site (E1) and the most offshore site (DS11) had similar light levels, but disparate salinity regimes over the time period of data collection (Bonsell 2019, Chap. 2). Elevated light levels at DS11 in the absence of low salinities (Bonsell 2019, Chap. 2) may contribute to the abundance of kelp at this site. It is well-established – and confirmed by our results - that elevated underwater irradiance at this site supports large kelp biomass (Dunton 1990; Aumack et al. 2007; Dunton et al. 2009; Bonsell and Dunton

2018). Kelp are well-known foundation species which alter patterns of water motion (e.g. Kitching et al. 1934) and chemistry (e.g. Krause-Jensen et al. 2016), so community structure at this site could reflect the direct and indirect interspecific effects of high *L. solidungula* biomass. The negative relationship between light levels and filter feeders (Fig. 3.5A), similarly indicates that invertebrates are outcompeted by macroalgae in locations with elevated light levels. Suspended sediments in the water column, the main source of underwater light variability in the Boulder Patch, can also have strong negative effects on filter feeders by reducing feeding efficiency and pumping rate (e.g. Bell et al. 2015).

Patterns of recruitment and succession

Recruitment varied both spatially and interannually. The benthic community seems to recruit from a propagule pool generally derived from adjacent biota at certain locations (E1, W1, and DS11; Fig. 3.6F). At sites towards the edges of the main Boulder Patch area (L1 and W3; Fig. 3.6F), propagule input from other locations could result in a community of recruits that is substantially different from the established epilithic community. These spatial differences likely derive from the influence of hydrodynamic patterns across Stefansson Sound on larval transport and retention, as locations at the edge of the Boulder Patch may receive proportionally greater propagule input from adjacent soft-bottom habitats (so-called "edge effects"). Abundant recruits and juveniles at DS11 may result from elevated local propagule production due to advantageous environmental conditions, or simply enhanced priority effects (numerical dominance of local propagules leading to local recruits) due to the overall high eplithic cover at this site.

Rhodophytes dominated tile communities (Fig. 3.4). Foliose red algae, which readily settled in great numbers, appear to be key early-successional species in this community. Investigations of overgrowth interactions in the Boulder Patch demonstrated that foliose red algae often act as a substrate for bryozoan, hydroid, and sponge growth (Konar and Iken 2005). Consequently, the interactions between this group and other functional groups, including its negative effect on kelps (Filbee-Dexter and Wernberg 2018), may shape the trajectory of community development. CCA was also numerically

dominant on tiles, and was even present at E1 where adults were absent, indicating that these algae produce abundant propagules, as has been found in shallow areas of Arctic fjords (Meyer et al 2017). Also similar for these two habitats is dominance by algal recruits compared to invertebrates (Meyer et al. 2017).

Although kelp is a dominant benthic biota at these sites and readily recruits to tiles in large numbers in the lab (*pers. obs*.), it did not recruit to settlement tiles at all during the study period. In a previous study from the Boulder Patch, the first kelp to recruitment to bare boulders only occurred after seven years (Martin and Gallaway 1994). The low apparent recruitment of kelps does not prove that kelp are not present on the tiles - a "seed bank" of gametophytes may be present that have not formed sporophytes yet due to lack of some environmental cue (Carney and Edwards 2010; Carney et al. 2013). Alternatively, kelp spore chemotaxis may lead to settlement on alternative habitats in the environment (Amsler et al. 1992; Reed et al. 1992). However, if kelp are slow to recruit, establishment may be inhibited by faster-growing foliose red algae and benthic invertebrates in habitats where these groups are abiotically favored, such as turbid or high flow areas (Filbee-Dexter and Wernberg 2018, Witman and Dayton 2001).

Tile communities only become more similar to the benthic community over time at two sites, W1 and W3. However, both sites were still 40% dissimilar to the benthic community at the end of the study (Fig 3.6F). Community development at these two sites was also highly variable (Fig. 3.7). Their location adjacent to a deep pass connecting Stefansson Sound and the Beaufort Sea, and the associated strong currents at these sites (Bonsell 2019, Chap. 2) may lead to temporal patchiness in the propagule pool, contributing to the variability in the recruited community. Tiles at DS11 were the most similar to the benthic community, with the smallest shift in community between years one and two (Figs. 3.6-3.7), again indicating the importance of priority effects at this site. These results overall indicate that propagule pressure resulting from the interaction between local production and hydrodynamics leads to initial recruited community, then environmental filtering shapes the trajectory of early succession.

Succession occurred very slowly, in agreement with past studies in the Boulder Patch (Martin and Gallaway 1994; Konar 2013). Even after three years *in situ*, the large majority of individuals on the tile remined <1 mm. Consequentially, very few instances of overgrowth were observed, unlike similar studies in Arctic fjords (Beuchel and Gulliksen 2008; Meyer et al. 2017). Overall, community development in the Boulder Patch appears to be very slow, which makes it difficult to parse out successional patterns over timescales less than a decade (Martin and Gallaway 1994; Beuchel and Gulliksen 2008; Konar 2013; Meyer et al. 2017). These results bolster conclusions that the Boulder Patch community would be very sensitive to any catastrophic disturbance event (Konar 2013).

Scaling up: links to Arctic climate

Understanding the links between climatic changes and shifts in Arctic kelp bed community structure and distribution requires knowing the connections between climate, the abiotic environment, and biota. The body of research surrounding Arctic kelp ecology is small compared to that of lower latitudes, but drawing upon knowledge of the physical environment of Arctic coasts can illuminate relationships between climate and community structure (Fig. 3.8). The majority of the proposed relationships shown in Figure 3.8B have not been empirically tested. Rather, I present them as hypotheses for future scientific inquiry.

First, coastal salinity reflects freshwater inputs from both Arctic rivers and sea ice melt. Downwelling winds entrain freshwater along Arctic inner shelves, while upwelling winds advect it offshore and bring in cool, salty oceanic water (Sellmann et al. 1992; Weingartner et al. 2017). Low salinities exert considerable influence on community structure by causing osmotic stress in certain algal groups, particularly CCA (King and Schramm 1982; Schoenrock et al. 2018), which is reflected in Boulder Patch community structure (Fig. 3.4). Through the negative effect of CCAs on invertebrate groups and foliose red algae (Konar and Iken 2005; Kortsch et al. 2012; Beuchel and Gulliksen 2008; Kuklinski 2009), low salinity can give a competitive advantage to these groups. The adverse effects of salinity on kelp (Karsten 2007; Fredersdorf et al. 2009) is amplified by

the negative effects of red algae on kelp (Filbee-Dexter and Wernberg 2018). As the Arctic Ocean freshens due to runoff and sea ice melt (McClelland et al. 2006; McPhee et al. 2009; Morison et al. 2012), kelp beds in shallow, river-influenced areas may face increasingly adverse conditions for kelps and CCA to persist. However, intensification of easterly winds, such as what is occurring along the Beaufort Sea coast (Wood et al. 2013, 2015) may ameliorate salinity conditions through upwelling.

Second, fluvial inputs and coastal erosion introduce suspended sediments to nearshore habitats, which increases light attenuation (Van Duin et al. 2001; Aumack et al. 2007; Fritz et al. 2017). Wind-driven currents and mixing in the open-water season resuspend benthic sediments on Arctic inner shelves, and further degrade the underwater light environment (Aumack et al. 2007; Bonsell and Dunton 2018). While all algae need light to grow, Arctic kelps are particularly sensitive to low light conditions caused by sediment resuspension (Dunton 1990; Aumack et al. 2007; Bartsch et al. 2016; Bonsell and Dunton 2018), while red algae are generally more tolerant of low-light conditions (Vadas and Steneck 1988). Sediments also have a negative effect on filter feeders (Fig. 3.4B), such as sponges (Bell et al. 2015). Identical to freshwater inputs, downwelling winds entrain water masses with high concentrations of suspended sediments along the coastal margin (Dunton et al. 2006). Climate-driven lengthening of the open water season, intensified coastal erosion, and increased fluvial sediment inputs would thereby have a negative effect on abundance and persistence of nearshore kelps and filter feeders (Fig. 3.8).

Finally, wind dynamics can considerably impact patterns of benthic recruitment by altering the speed and direction of prevalent current flow. Faster currents and currents that advect water masses out of the coastal zone decrease local propagule retention (e.g. Gaylord et al. 2012). The community of recruits would potentially be more varied (Fig. 3.6), and the established community would reflect the relative ability of each individual to withstand the local environment (Leibold et al. 2004). The resultant decrease in priority effects (wherein current community composition strongly influences future composition by dominating the propagule pool) would strengthen the importance of abiotic effects on benthic community structure (Fig. 3.8).

The community structure of Arctic kelp beds reflects an integration of local environmental conditions over decadal timescales due to the long successional cycle and longevity of many of the taxa. While this study highlights the effects of seasonal abiotic variation on benthic community structure, it also demonstrates that variability within a single year (or even >5 years) cannot account for the spatial distribution of benthic biota. Researchers must account for long-term environmental variability to fully comprehend and predict the impact of climate variation on kelp bed structure and distribution.

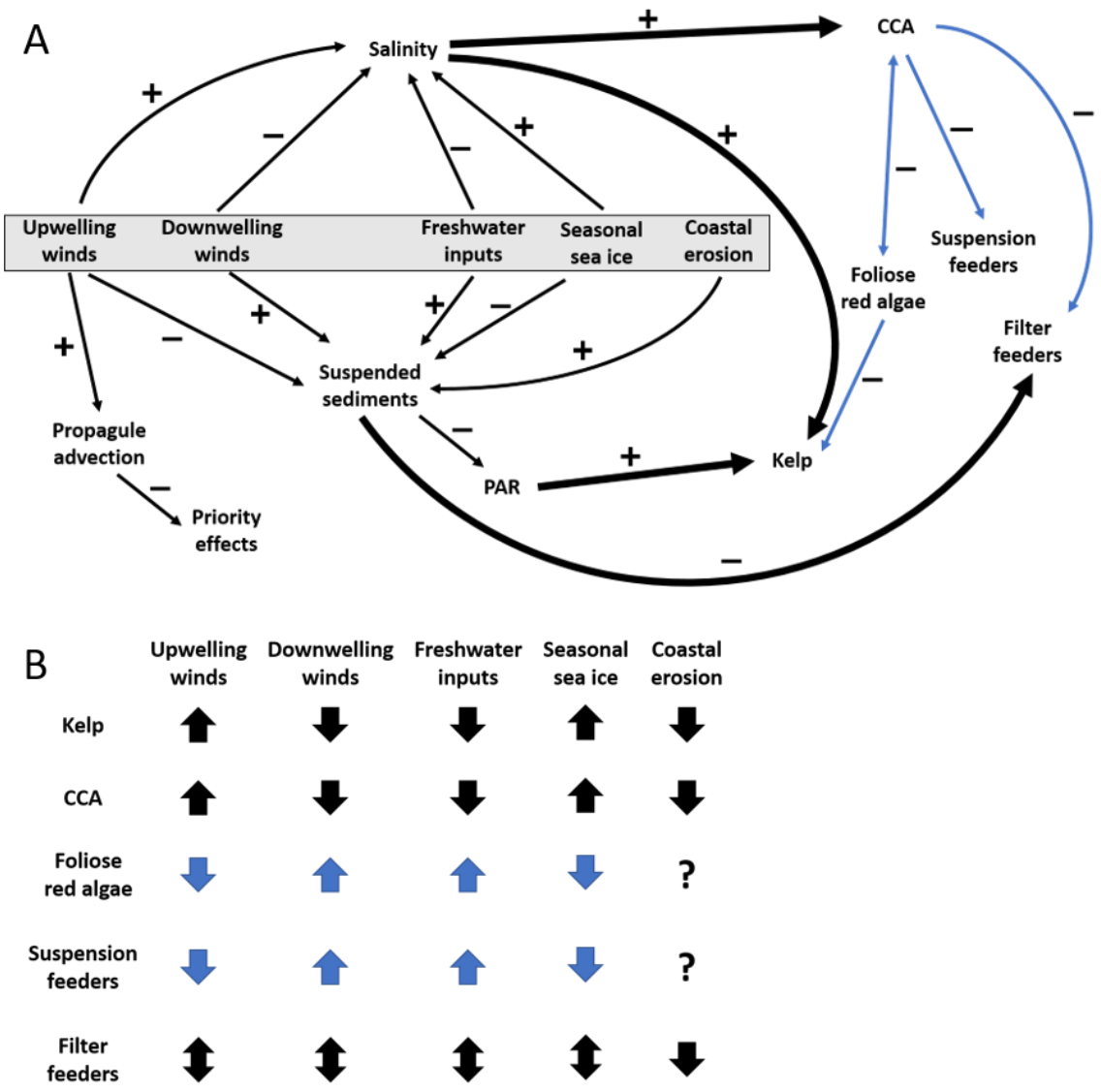

Figure 3.8: A) Positive and negative impacts (represented as arrows) of climatic drivers (in grey box) on environmental parameters/processes and functional groups on Arctic inner shelves. Biotic interactions are represented by blue arrows. A decrease in priority effects would strengthen the impacts of abiotic variables on functional group abundance (bolded arrows). See in-text citations. B) Overall effect of climatic drivers on functional group abundance. Indirect effects that occur through biological interactions are in blue.

Chapter Four: Within- and between-basin population connectivity in the Arctic endemic kelp *Laminaria solidungula*

ABSTRACT

Pathways of dispersal and post-glacial recolonization patterns across the Arctic Ocean may provide insight into climate-driven borealization of Arctic ecosystems. To assess connectivity and dispersal in this rapidly-changing region, we analyzed population genetic structure in the Arctic endemic kelp *Laminaria solidungula* at two scales: 1) among populations in the Alaskan Beaufort Sea using microsatellites, and 2) among populations from across the Arctic using ribosomal large sub-unit (LSU) sequence data. The Beaufort Sea populations appear to be largely panmictic (global F_{ST}: 0.01), though sampling stations as close as 6 km could exhibit significant pairwise differentiation. Apparent inbreeding was extremely low ($F_{IS}<0$) and genetic diversity was high ($H_e>0.5$) at all well-sampled stations, indicative of rare self-recruitment. These results suggest that sub-polar benthic species migrating into the Beaufort Sea will quickly spread across the Alaskan Arctic coast, likely assisted by alongshore transport during fall storms. Conversely, LSU analysis revealed two genotypes that represent strong population differentiation between Beaufort Sea *L. solidungula* and those from the Canada and Svalbard, indicating that phylogeography of this species reflects Arctic recolonization after the Last Glacial Maximum. LSU topology within Laminariales demonstrates that this partition represents a significant subdivision within *L. solidungula*.

CHAPTER GLOSSARY

Microsatellites: DNA loci containing repeated short sequences of nucleotides. In genetic studies, comparisons are made using microsatellite length.

LSU: The ribosomal large sub-unit. In Phaeophyceae, the LSU has a size of 26S. In genetics studies, comparisons are made between LSU ribosomal DNA sequences (which code for the ribosomal RNA that makes up the LSU).

H_o: Observed heterozygosity.

H_e: Expected heterozygosity.

F_{ST}: Fixation index. The mean reduction in heterozygosity of subpopulations compared to the total population. Subopulations that are not differentiated have a value close to zero and subpopulations that are completely differentiated have a value closer to 1. If F_{ST} is significantly different from 0, then there is significant (sub)population differentiation.

G_{ST}: Similar to F_{ST}, but explicitly developed for >2 alleles. However, G_{ST} can never reach 1 if there are >2 alleles.

F_{IS}: Inbreeding coefficient. Mean reduction of individual heterozygosity due to inbreeding within a subpopulation. Has a value of 1 if all individuals are homozygous (an indication of inbreeding), and -1 if all individuals are heterozygous.

G_{IS}: Similar to F_{IS}, but explicitly developed for >2 alleles.

INTRODUCTION

Contemporary dispersal pathways and post-glacial recolonization into and across the Arctic are not well understood (Hardy et al. 2010), but are necessary to quantitatively forecast Arctic ecosystem changes (Krause-Jensen and Duarte 2014). The Arctic is warming at a faster rate than any other region in the world (IPCC 2014). As a result, a suite of ecosystem changes are occurring, including changes in species distributions (Bluhm et al. 2011; Grebmeier 2012; Michel et al. 2012). Northward range shifts of certain diatoms (Reid et al. 2007), bivalves (Berge et al. 2005), and fish demonstrates that "the coming Arctic invasion" (Vermeij and Roopnarine 2008) is occurring across many taxonomic groups. These changes reflect increases in suitable habitats for subpolar species, but invasion success also requires adequate vectors to disperse individuals to new areas (Sakai et al. 2001). These vectors are changing as well, since ships traversing the increasingly navigable Northwest Passage transport non-native species into Arctic waters (Smith and Stephenson 2013; Chan et al. 2016). The spatial spread of species moving poleward as the Arctic warms will likely reflect the dispersal pathways used by contemporary Arctic species (Vermaij and Roopnarine 2008). Understanding how populations are connected

through the region allows for accurate prediction and sound management of species' persistence and the borealization of polar ecosystems

In the changing Arctic, dispersal among populations and the resultant genetic connectivity can determine a population's capacity to withstand change or recover from disturbance. Healthy populations, with sufficient genetic diversity, can be self-sustaining (Hamilton 2009). However, immigration from outside populations may play an important role in "rescuing" populations dwindled by ecosystem change or decimated by disturbance (Brown and Kodric-Brown 1977). Persistence of foundation species (sensu Dayton 1972), such as kelps, in the face of warmer temperatures, increased turbidity, and lower salinities is central to the redistribution of habitats and ecosystem functions in the emerging Arctic.

In rocky subtidal Arctic areas, kelps provide habitat and a source of primary production that can increase local biodiversity and production, and alter local biogeochemistry (Dunton et al. 1982; Dunton and Schell 1987; Krause-Jensen et al. 2016; Filbee-Dexter et al. 2019). Shifts in kelp distributions are occurring globally (Krumhansl et al. 2016), and are recorded in a few Arctic areas (Bartsch et al. 2016). Sub-polar kelps are expected to expand their range northward due to increasing temperatures and alleviated underwater light conditions (Müller et al. 2009; Krause-Jensen and Duarte 2014). However, baseline understanding of Arctic kelp biology and ecology is limited, making it challenging to predict and anticipate change under future climate and development scenarios (Filbee-Dexter et al. 2019). Currently, fourteen species of kelp inhabit the Arctic region (Filbee-Dexter et al. 2019). Only one of these species, *Laminaria solidungula*, is defined as an "Arctic endemic" due to its evolutionary history and its association with dark, freezing-temperature waters. This species is also common in deep waters of cold, subarctic areas, including Svalbard (Lüning 1990). Consequently, the distributional pattern of *L. solidungula* provides a valuable opportunity to examine mechanisms of physical dispersal and kelp evolutionary history, due to the trans-Arctic spread of Laminariales into the Atlantic Ocean from the North Pacific (Stam et al. 1988). Furthermore, as this species represents the most cold-tolerant kelp (tom Dieck 1993), it is of interest for comparative biogeography studies and predicting future kelp distributions.

Due to their requirement of rocky substrate, *L. solidungula* can exist in patches separated by 100s of kms, as they do in the Alaskan Beaufort Sea (Dunton et al. 1982) (Fig. 4.1). Genetic data indicate that marine macroalgae disperse on scales of 100s to 1000s of m $year^{-1}$ on average, either through their free-swimming microscopic stage or their macroscopic stage via drift (Kinlan and Gaines 2003). A lack of habitat continuity may limit the amount of genetic exchange between *L. solidungula* patches, and decreased within-patch genetic diversity, as shown in other kelp species (Alberto et al. 2010; Durrant et al. 2018). Genetic diversity of a population can be linked to the probability that a declining population could be "rescued" by migration from other populations, as well as linked to the capacity of a population to adapt to change or disturbance (Brown and Kodric-Brown 1977; Sakai et al. 2001). Recently, work by Wernberg et al (2018) highlighted the link between higher genetic diversity (expected heterozygosity) in temperate kelp populations and their resilience to extreme climatic events – kelp forests with higher genetic diversity showed greater capacity to regrow after experimental disturbance and a marine heatwave. Genetic diversity, therefore, may then provide an important measure to evaluate the vulnerability of Beaufort Sea *L. solidungula* populations to the environmental perturbations associated with climate change and coastal development.

Spatial genetic data can be used to infer information about dispersal and population connectivity. Closely related populations of individuals are generally characterized by having higher connectivity through propagule dispersal. The timescale of connectivity conferred by genetic data varies by genetic marker. For example, microsatellite markers, which evolve relatively quickly, are used to infer population connectivity over scales of decades to thousands of years while mitochondrial cytochrome C oxidase subunit I gene (COI), internal transcribed spacer (ITS), and other ribosomal markers are used to infer population connectivity and species relationships over longer periods, from tens of thousands to millions of years. Mitochondrial and ribosomal markers have been used to infer the recolonization history of the Arctic by macroalgae after the Last Glacial Maximum (McDevit and Saunders 2010; Coyer et al. 2011; Bringloe and Saunders 2018).

However, data from more than a few high Arctic sites within these studies are rare (but see Nieva et al. 2018).

The aim of this study is to evaluate genetic connectivity of *Laminaria solidungula* populations across two different scales in the Arctic: 1) among stations within the Alaskan Beaufort Sea, including six stations within the Stefansson Sound Boulder Patch, Camden Bay, and Barter Island, and 2) among sites in the Western Arctic Basin, including the Beaufort Sea, Arctic Canada, Newfoundland, and Svalbard. We used two different markers, corresponding to each scale. For the regional-scale study, we used microsatellite markers to infer population connectivity and genetic diversity in the Alaskan Beaufort Sea. These are putatively neutral and rapidly evolving, often used to determine population differentiation across geographic scales of 10s-1000s of m. For the basin-scale assessment, we sequenced the D1/D2 region of the large sub unit (26S) ribosomal RNA gene (rDNA). The 26S rDNA sequence is generally highly conserved in Phaeophyceae and has been used in combination with other molecular markers to resolve taxonomic relationships in brown algae at the level of order and above (Phillips et al 2008, Lane 2006), but its use in determining genetic divergence within kelp species is limited. However, the more divergent D1/D2 hypervariable regions within the LSU rDNA gene, which have been excluded from large phylogenetic analysis of Phaeophyceae due to high variability (Draisma et al 2001), are often used to barcode species of taxa such as dinoflagellates (Scholin et al. 1994) and ciliates (Stoeck et al. 2014) and have been suggested as a barcode gene for all metazoans (Sonnenberg et al. 2007). We therefore expected subspecies-level variability in the D1/D2 region within Laminariales, reflecting population differentiation over longer timescales than microsatellites.

METHODS

Adult sporophytes of *L. solidungula* were collected from six sites: Stefansson Sound Boulder Patch (Beaufort Sea), Camden Bay (Beaufort Sea), Barter Island (Beaufort Sea), Finlayson Islands (Canadian Archipelago), Bonne Bay (Newfoundland), and Kongsfjorden (Svalbard) (Fig. 1). Within the Beaufort Patch there were six distinct

sampling stations: B1, DS11, E1, L1, W1, and W3 (Fig. 4.1). Therefore, there were eight Beaufort Sea stations total, among three sites. Stefansson Sound, Bonne Bay, and Kongsfjorden samples were collected by divers. Camden Bay samples were obtained by dragging for plant material. Barter Island samples were collected from fresh drift algae. Finlayson Island samples were acquired incidentally via benthic trawl. Tissue samples were collected from the meristem (when possible), then dried in silica desiccant and frozen at -80 ^{o}C.

For DNA extraction, ~10-20 mg of dry material from each sporophyte was ground using an MPBio FastPrep tissue lyser (Lysing Matrix A). Extraction was carried out using a cetyltri-methylammonium bromide (CTAB) protocol (Zuccarello and Lokhorst 2005). Briefly, ground kelp material was added to a microcentrifuge tube with 500-700 µL of CTAB extraction buffer, and incubated overnight at 65 ^{o}C with gentle shaking. Chloroform : isoamyl alcohol (24:1) was added then briefly vortexed, and the phases were separated by certifugation at 12000 X g for 10 min. The aqueous phase was removed to a new centrifuge tube, and the extraction step was repeated in that tube. The twice-extracted aqueous phase was again placed in a new tube along with an equal volume of 100% isoproponal, then mixed by inversion. The sample was incubated at room temperature for 30 min to 1 hr. Precipitated nucleic acids were collected by centrifugation for 30 min at 12000 X g at 20 ^{o}C, after which the supernatant was decanted. The DNA pellet was washed in 70% ethanol, concentrated by centrifugation for 5 min at 12000 X g, drained, and air-dried. Depending on the size of the pellet, I added 50-150 µL of 0.1 X TE buffer (145 M Tris, 1 µM EDTA). Samples were frozen at -20 ^{o}C.

Microsatellite analysis

From population genetic studies in other kelp species, we selected five primer pairs that amplified microsatellite sequences in *L. solidungula* sampled in the Boulder Patch (Table 4.1, Supp. Table D1). PCR reactions consisted of 0.25 mM dNTPs, 0.5 mM MgCl, 1X Dream Taq buffer, 2U Dream Taq polymerase, 0.4 µM of each reverse primer and fluorescently-labelled forward primer, and 1 µL DNA template (10-20 ng) in 20µL total

volume. Capillary electrophoresis fragment analyses were performed at Texas A&M University Corpus Christi Genomics Core Lab on an Advanced Analytical Fragment Analyzer. Peaks were scored in Geneious (http://geneious.com).

Microsatellite loci only amplified consistently for samples collected in Beaufort Sea, so this analysis excluded the other sites. Data were filtered to only include samples with one or fewer missing loci. We used MICRO-CHECKER (Van Oosterhout et al. 2004) to scan for evidence of null alleles and scoring errors. Per locus F_{ST} and F_{IS} were determined in GENEPOP (Rousset 2008), along with tests for linkage disequilibrium, deviations from Hardy Weinberg equilibrium, and heterozygote excess. We used Fisher's exact test in GENEPOP to determine pairwise population differentiation on genotypes. Per population F statistics and AMOVA were analyzed using GENODIVE (Meirmans and Van Tienderen 2004). All other data analysis and visualization for microsatellite DNA variation was carried out in R (R Core Team 2016).

To assess the role of environmental factors on genetic differentiation among stations within the Boulder Patch, we compared biotic and abiotic environmental variables (Bonsell 2019, Chaps. 2-3) to genetic diversity using a distance-based redundancy analysis (db-RDA) (Legendre and Anderson 1999). Benthic percent cover data of functional groups (kelp, crustose coralline algae, foliose red algae, filter feeders, suspension feeders) were arcsine transformed. To homogenize the mean and standard deviation for all environmental data for the db-RDA, including benthic cover, raw values were normalized by subtracting the grand mean and dividing by the standard deviation. Dissimilarity between kelp stations based on microsatellite data were calculated using a principal coordinate analysis (PCoA, R package adgenet; Jombart 2008). The relationship between PCoA coordinates and normalized environmental variables was determined using a db-RDA, with a step-wise model building approach (R package vegan; Oksanen et al. 2016). Differences among stations were assessed using one-way ANOVAs on each environmental variable, with posthoc Tukey HSD tests.

Ribosomal large subunit (LSU) DNA

The lack of microsatellite amplification in individuals collected outside of the Beaufort Sea necessitated the use of a different marker to investigate population differences among geographic regions in the Western Arctic Ocean Basin. Partial sequences of LSU ribosomal RNA genes cvering the D1/D2 region (~550 bp) were aquired for samples from Boulder Patch stations DS11 (n=4) and B1 (n=5), Barter Island (n=3), Camden Bay (n=8), Newfoundland (n=3), Svalbard (n=7), and the Finlayson Islands (n=4). Amplification was carried out in 20 µL total volume using 0.4 µM D1R/D2C primers (Scholin et al. 1994), 1X Myfi mix (Bioline), and 10-20 ng DNA. Cycling conditions consisted of 2 min at 94^{o}, then 30 cycles of 1 min at 94 ^{o}, 40 sec at 51 ^{o}, 1.5 min at 72 ^{o}, with a final elongation step of 5 min at 72 ^{o}.

Sequences were visually inspected, trimmed, and aligned using Geneious. To assess the relative phylogenetic significance of variation in the LSU, we aligned *L. solidungula* sequences with other sequences from the Order Laminariales available on GenBank (Table 4.2). A neighbor-joining algorithm was used to visualize LSU variation within and between species.

Table 4.1: Information for loci used in this study. *Marker development reference

Locus	AT	Sequence motif	*L. solidungula* fragment length	Cross amplification species	References
Ld-3	51	(aag)6	251-263	*S. japonica, L. hyperborea*	Liu et al. 2012*
Ld-13	54	(ggaa)10	159-231	*S. japonica*	Liu et al. 2012*
Ld2/520	53	(at)6(gt)7	366-388	*L. digitata, L. nigrecens*	Billot et al. 1998*, Martinez et al. 2015
LolVVIV-15	60	(aac)21	102-144	*L. hyperborea, L. ochroleuca*	Coelho et al. 2014*
LolVVIV -23	60	(aac)14	105-111	*L. digitata, L. hyperborea, L. ochroleuca*	Coelho et al. 2014*

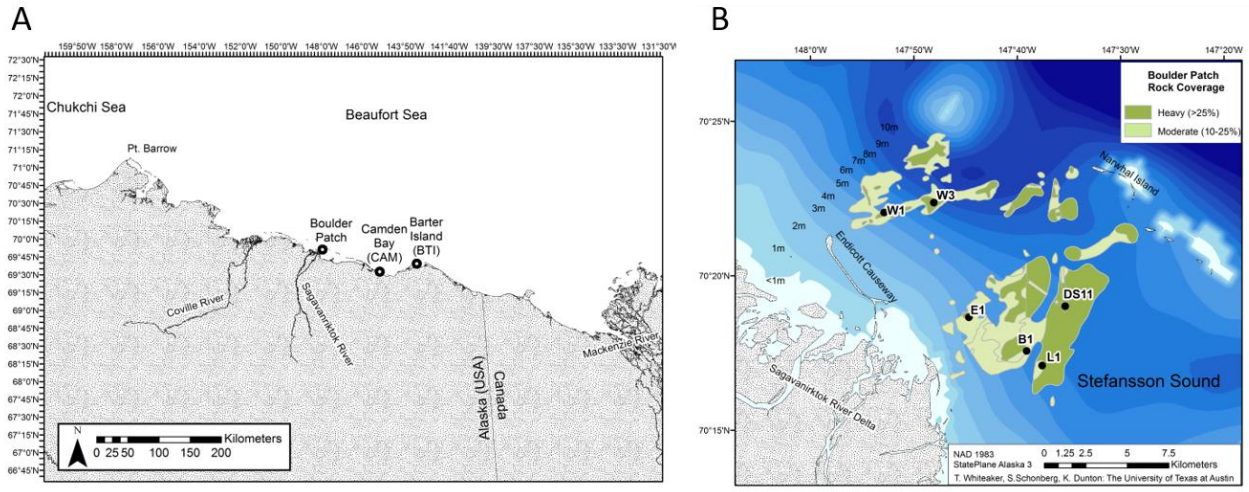

Figure 4.1: A) Location of three Beaufort Sea sampling sites. B) Location of sampling stations within the Boulder Patch. Benthic cover and long term environmental data exists for sites DS11, E1, L1, W1, and W3.

Table 4.2: List of samples used for LSU analysis and accession numbers

Species	Collection information	No. samples	LSU Genbank and reference
Laminaria solidungula	Boulder Patch, AK, USA (collector: C. Bonsell)	9	
	Camden Bay, AK, USA (collectors: J. Dunton and T. Dunton)	8	
	Barter Island, AK, USA (collector: C. Bonsell)	3	
	Bonne Bay, NL, Canada (collector: G. Bishop)	3	
	Hansneset, Svalbard, Norway (collector: I. Bartsch)	7	
	Finlayson Islands, NU, Canada (collector: B. Bluhm)	4	
Laminaria yezoensis	L. Druehl culture	1	AY851518 (Lane et al. 2006)
Laminaria sinclarii	Mud Cove, Bamfield, BC, Canada	1	AY851516 (Lane et al. 2006)
Laminaria ochroleuca	Roscoff, Brit., France	1	AF071154 (Rousseau et al. 2000)
Laminaria digitata	Roscoff, Brit., France	1	AF071153 (Rousseau and De Reviers 1999)
	Green Pt., Lepreau, NB, Canada	1	AY851517 (Lane et al. 2006)
	Hornbaek, Sjaelland, Denmark	1	AY441778 (Erting et al. 2004)
Laminaria hyperborea	Roscoff, Brit., France	1	AF071155 (Rousseau and De Reviers 1999)
	Deget, Denmark	1	AY441779 (Erting et al. 2004)
Saccharina sessilis	Cape Beale, Bamfield, BC, Canada	1	AY851513 (Lane et al. 2006)
Saccharina nigripes	Green Pt., Lepreau, SB, Canada	1	AY851514 (Lane et al. 2006)
Saccharina latissima	Helsinborg, Denmark	1	AY441780 (Erting et al. 2004)
	Hirsholm, Denmark	1	AY441781 (Erting et al. 2004)
	Drelnes, Denmark	1	AY441782 (Erting et al. 2004)

Table 4.2, cont.

Saccharina gyrata	L. Druehl culture	1	AY851526 (Lane et al. 2006)
Saccharina augustata	L. Druehl culture	1	AY851515 (Lane et al. 2006)
Cymathaere triplicata	Wiffen Spit, Sooke, BC Canada	1	AY851519 (Lane et al. 2006)
Egregia menziezii	Boiler Bay, OR, USA	1	AY851506 (Lane et al. 2006)
Lessonia corrugata	Gov. Is. Reserve, Tas., Australia	1	AY851532 (Lane et al. 2006)
Lessonia flavicans	Rookery Bay, Falkland Islands	1	AY851531 (Lane et al. 2006)
Lessonia nigrescens	Las Cruces, Chile	1	AY851530 (Lane et al. 2006)

RESULTS

Microsatellite analyses: Beaufort Sea populations

For the 119 individuals analyzed, the five polymorphic loci had a total of 49 alleles, ranging from 5 to 13 alleles per locus (Table 4.3). No significant linkage disequilibrium was detected ($p<0.05$). Heterozygosity varied among loci, and overall heterozygosity was moderate (H_o=0.67, Table 4.3). No difference between observed and expected heterozygosity was observed (Bartlett's K^2=0.217, $p>0.05$). Three out of five loci deviated significantly from Harvey-Weinberg Equilibrium ($p<0.05$, Table 4.3). Genetic diversity (number of alleles per individual) varied among sites, depending on sample size (Table 4.4).

The likely total number of alleles per individual for these stations and loci is ~1.5. Overall heterozygosity at each station (H_o) was moderate to high (0.625-0.800, Table 4.4). There were significant departures from Hardy-Weinberg Equilibrium at three out of the eight sampling stations, and overall ($F_{IS}\neq0$; Tables 4.4-4.5). Chi-squared tests demonstrated that heterozygote excess was present at two sites, as well as within the global

population (Table 4.4). There was no significant population structure given by sites (AMOVA, $p<0.05$). Similarly, overall population differentiation (F_{ST} = 0.010, 0.006 excluding Camden Bay samples, Table 4.5) and pairwise F_{ST} (0-0.107, Table 4.6) were low, meaning that populations are not well differentiated by site. However, some pairwise genetic differentiation was statistically significant, with site DS11 showing the most consistent genetic differentiation from the other sites (Table 4.6). DS11 had significantly higher kelp cover than the other sites ($\alpha=0.05$; one way ANOVA: $F_{(1,4)}=9.70$, Supp. Tables D2-D3) and comparison to environmental parameters via dbRDA revealed that benthic cover by kelp significantly influenced the genetic differences between sites (Table 4.7, Fig. 4.2).

LSU analysis: *Laminaria solidungula* across the Western Arctic Ocean Basin and comparisons to other Laminariales

LSU rDNA sequences were ~550 bases long after trimming, with two variable sites: C-T polymorphism and a G-A polymorphism. All individuals had either the C and G or T and A combination, resulting in two genotypes. One genotype was found exclusively in the Beaufort Sea individuals, and the other was restricted to the Canadian/Atlantic Arctic, with a single exception in Camden Bay (Fig 4.3). The Beaufort Sea genotype was 1 base different from the *L. yezoensis* genotype (Fig. 4.4). These two species had fewer deviations from *Saccharina* species and *C. triplicata* than from other Laminaria species (Fig. 4).

Table 4.3: Summary statistics for microsatellite loci. Bold indicates significant deviance from Harvey-Weinberg Equilibrium ($p<0.05$). * indicates significant deviance from HWE after Bonferroni correction.

Locus	**# alleles**	**H_o**	**H_e**	**F_{is}**	**F_{st}**
Ld-3	8	0.75	0.66	**-0.132**	0.001
Ld-13	13	0.25	0.24	-0.018	0.016
Ld2/520	12	0.85	0.72	**-0.188**	0.006
LolVVIV-15	11	0.82	0.68	**-0.208***	0.017
LolVVIV - 23	5	0.80	0.49	-0.636	0.013
global		0.69	0.56	**-0.244***	0.010

Table 4.4: Genetic summary statistics for samples from each sampling location. Bold indicates sig after Bonferroni correction.

Site or Station	**N**	**# alleles/ind**	**Effective # of alleles**	**H_o**	**H_e**	**F_{is}**	***p* (Heterozygote excess)**
BTI	12	2.083	2.61	0.627	0.533	**-0.138**	0.766
CAM	2	6.000	2.47	0.625	0.425	0.167	1.000
Boulder Patch Stations:							
B1	16	1.438	2.66	0.689	0.537	-0.240	0.091
DS11	19	1.421	2.45	0.800	0.571	**-0.378**	**0.000**
E1	13	1.692	2.40	0.662	0.517	-0.243	0.258
L1	18	1.389	2.71	0.696	0.569	**-0.198**	0.741
W1	20	1.450	2.39	0.667	0.530	-0.227	0.010
W3	19	1.421	2.50	0.703	0.547	-0.260	**0.004**

Table 4.5: Overall differentiation statistics for Beaufort Sea stations. Values in brackets include the two Camden Bay individuals. *statistically significant.

F_{st}	0.006 (0.010*)
F_{is}	-0.248 (-0.243)
G_{st}	0.005 (0.028*)
G_{is}	-0.200* (-0.241*)

Table 4.6: Pairwise F_{ST} values between Beaufort Sea sampling locations. Sampling sites are in bold, sampling stations within the Boulder Patch site are in normal font. * indicates significant differentiation ($p<0.05$). **indicates significant differentiation after Bonferroni correction.

	CAM	B1	DS11	E1	L1	W1	W3
BTI	0.059	0	0.019*	0.009	-0.008	-0.002	0
CAM		0.18*	0.1*	0.107*	0.052	0.089	0.069
B1			0.022*	0.014	-0.003	-0.004	0
DS11				0.031**	0.003	0.019*	0.016**
E1					0.009	0.005	-0.006
L1						-0.003	-0.001
W1							-0.01

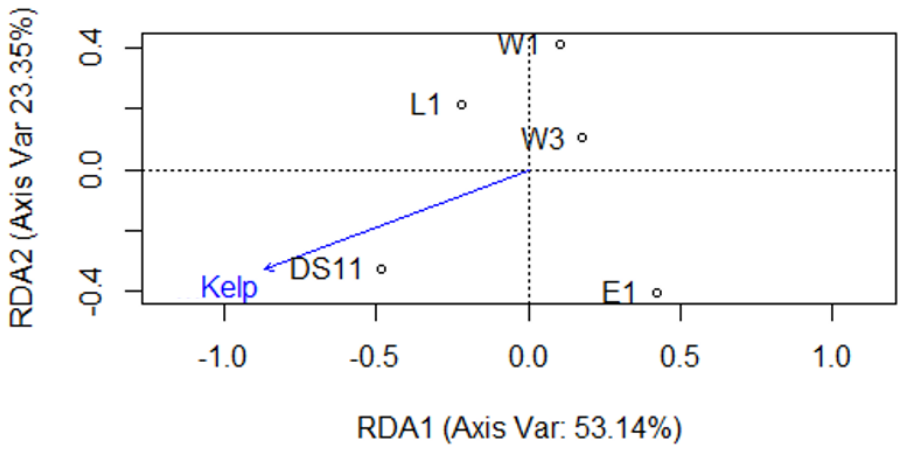

Figure 4.2: Ordination plot of stations within the Boulder Patch based on genetic distance compared to kelp cover.

Table 4.7: Stepwise model building results for the effect of environmental variables on the distance between stations given by PCoA on genetic data. **Bold** indicates significance. Units: Temperature, daily mean (°C); Light (photons m^{-2} day^{-1}); Salinity, daily mean; Current velocity, daily mean (cm sec^{-1})

	Df	**AIC**	**F**	***p***
% Kelp cover	1	-15.705	4.7264	0.025
% CCA cover	1	-13.585	2.057	0.15
Temperature (Ice cover)	1	-13.131	1.6179	0.2333
Temperature (Year-round)	1	-13.355	1.829	0.2417
Light (Open water)	1	-12.64	1.1858	0.3833
Temperature (Open water)	1	-12.9	1.4095	0.3917
% Red algae cover	1	-12.573	1.1298	0.4167
Light (Year-round)	1	-12.617	1.1664	0.425
Salinity (Open water)	1	-12.157	0.8	0.5417
Salinity (Year-round)	1	-12.173	0.8124	0.575
% Filter feeder cover	1	-11.957	0.6516	0.6167
Salinity (Ice break-up)	1	-12.048	0.7185	0.6333
Temperature (Ice break-up)	1	-11.914	0.6202	0.6583
Salinity (Ice freeze-up)	1	-11.608	0.4055	0.75
Salinity (Ice cover)	1	-11.517	0.3436	0.7833
Current velocity (Ice break-up)	1	-11.339	0.227	0.8083
Current velocity (Ice cover)	1	-11.341	0.2282	0.825
Current velocity (Ice freeze-up)	1	-11.301	0.2021	0.9
Temperature (Ice freeze-up)	1	-11.037	0.0377	0.9083
% Suspension feeder cover	1	-11.135	0.0978	0.9167
Current velocity (Open water)	1	-11.108	0.0811	0.9417
Current velocity (Year-round)	1	-11.023	0.0292	1

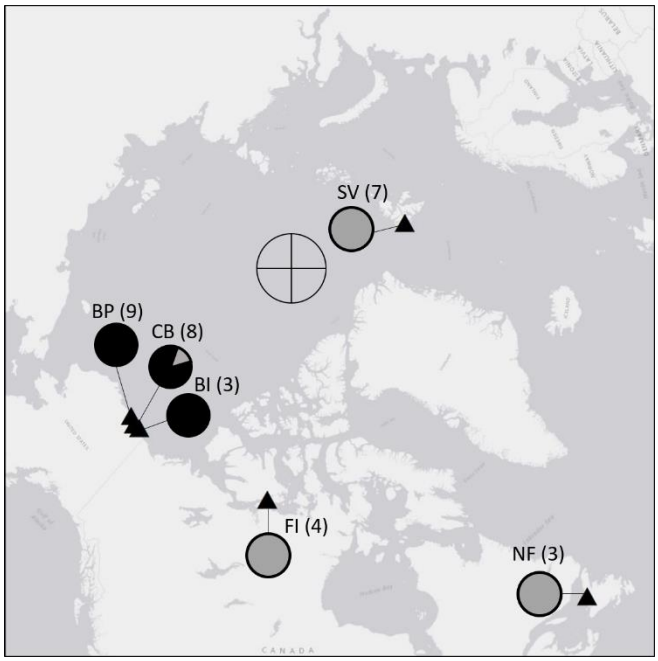

Figure 4.3: Map of *L. solidungula* sampling locations (triangles) and percent of LSU genotypes, represented as pie graphs. Black = "Beaufort" genotype, grey = "Atlantic Arctic" genotype. Number of samples in parentheses. Cross shows location of the pole.

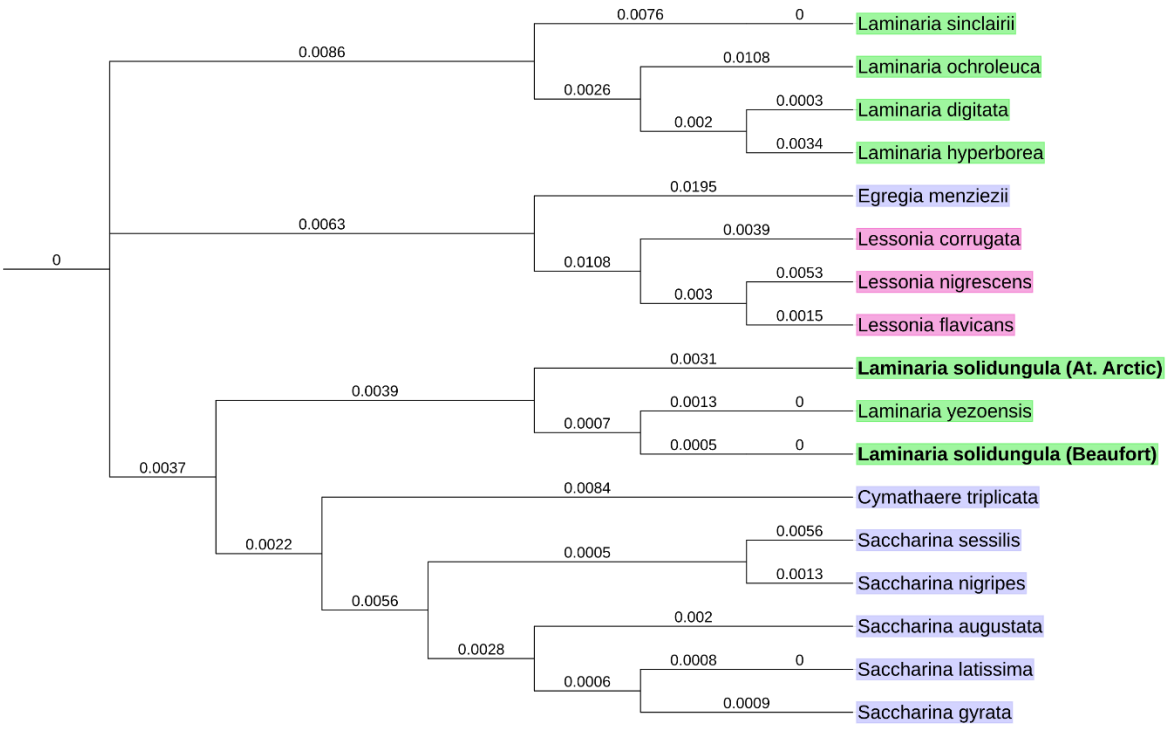

Figure 4.4: Topology of LSU sequences from kelps in the families Arthromenceae (blue), Lessonaceae (pink), and Laminaraceae (green). *Laminaria solidungula* sequences, generated in this study are bolded. All other sequences from GenBank (Table 2). Branch numbers indicate percent difference between sequences. Adding the differences along the path between any two species will give the total percent difference in sequence between those two species. This tree does not represent a phylogeny.

DISCUSSION

Evidence for panmixia in the Beaufort Sea

When compared to other microsatellite studies on kelps, the level of population differentiation (F_{ST}) we found in the Beaufort Seas corresponds to the low end of

differentiation found over scales of <20 km (Billot et al. 2003; Alberto et al. 2010; Robuchon et al. 2014; Brennan et al. 2014). As the majority of our samples came from within the Boulder Patch, our results fit into the model of weak differentiation over smaller scales for most kelp species (Billot et al. 2003; Coleman et al. 2011; Brennan et al. 2014). However, we found that drift kelp on Barter Island were not differentiated from attached kelp within the Stefansson Sound Boulder Patch, approximately 150 km away. This indicates that the Beaufort Sea population of *Laminaria solidungula* has the capacity for panmixia (random mating within the region), despite the lack of habitat continuity. Other studies have reported strong differentiation over similar spatial scales, which was attributed to complex coastline or hydrographic barriers (Billot et al. 2003; Breton et al. 2018; Durrant et al. 2018). Coleman et al (2011) demonstrated that genetic connectivity of kelps is related to the strength of currents that connects those systems. The lack of genetic structure in the Beaufort Sea indicates high connectivity among habitats, which may be assisted by the regional circulation regime.

Kelp dispersal in the nearshore Beaufort Sea is likely enhanced by fall storm events, which can transport large numbers of reproductive individuals, as evidenced by the extensive biomass that can wash onshore after a large wind event (Fig. 4.5). Experiments with seabed drifters show that neutrally buoyant, near bottom drift (which would transport kelp), can transport materials alongshore by 10s of km under ice cover and 100s of km in the summer (Barnes and Reimnitz 1982). Summer circulation patterns along the Alaska Arctic coast, including over the Boulder Patch, are wind-driven and primarily alongshore, with dominant westward flows (Barnes and Reimnitz 1982; Weingartner et al. 2017; Bonsell 2019, Chap. 2). In the Beaufort Sea, *L. solidungula* releases meiospores under the cover of 1.8 m thick landfast sea ice in late winter or early spring (Dunton, *pers.comm.*). Currents are minimal during this time, so the transport of mature adults during the summer and fall is more important for maintaining population connectivity, since kelp meiospores – whose small size exposes them to boundary layer effects - can only travel 10s of m without the aid of strong currents (Gaylord et al. 2006). The low pairwise genetic differentiation demonstrates that each sampling site is highly connected to the others. The

fact that this population exhibits low genetic differentiation among geographically distinct locations suggests that range expansion by boreal species may occur rather quickly within the Beaufort Sea, given suitable habitat.

Additional evidence of a panmictic *L. solidungula* population in the Beaufort Sea is high observed heterozygosity, as well as heterozygote excess at two Boulder Patch stations (DS11 and L1, Table 4.4), and negative inbreeding coefficients (F_{IS}<0, Tables 4.4-4.5). Outbreeding is rare in kelps (Valero et al. 2001) and isolated kelp patches should display prominent selfing and inbreeding (Gaylord et al. 2012). However, despite the habitat isolation of the Boulder Patch, the kelp are apparently not isolated genetically. While connectivity to a wider kelp population is not unexpected, the level of heterozygosity in the Beaufort Sea population is unusual. Interestingly, this suggests that very little sexual reproduction occurs within the Boulder Patch itself; in other words, the Boulder Patch is not self-recruiting. Concurrent observations in the Boulder Patch show that sporophyte recruitment happens over spans of >5 yrs (Martin and Gallaway 1994; Konar 2013; Bonsell 2019, Chap. 3). Furthermore, kelp establishment on hard substrate - rather than to algae or invertebrates that will become dislodged - is extraordinarily rare considering the relative availability of rock surface (Bonsell and Muth *unpub. data*). Additionally, *L solidungula* in the Boulder Patch can be considerably long-lived: Dunton (1990) was able to relocate individuals more than two decades after they had been tagged for growth measurements. The genetic structure may reflect establishment in the Boulder Patch by drift kelp from various sources and breeding populations followed by little to no self-recruitment. Submergence of the Beaufort Sea coast after the last glacial maximum, and subsequent recruitment of kelp to the Boulder Patch, may have effectively occurred relatively recently compared to the apparent long *L. solidungula* generation time. As a result, Boulder Patch genetic structure may show heterozygote excess associated with recent population mixing (i.e. isolate breaking). This may act in combination with a selective benefit to heterozygosity, as seen in other kelp species (Raimondi et al. 2004; Johansson et al. 2013).

Heterozygote excess and high variability in inter-locus F_{IS} (Table 4.3) are also an indicator of clonal reproduction (Balloux et al. 2003). However, the kelp haploid-diploid

life cycle would require apomeiosis and the production of diploid zoospores instead of the normal haploid to increase population heterozygosity. Regular production of diploid zoospores has only been reported from a single wild subpopulation of *L. digitata* (Oppliger et al. 2014). In that case, the irregular zoospores did not significantly contribute to population dynamics. Therefore, it would be extremely unusual if our results reflected *L. solidungula* clonal reproduction

Smaller-scale differentiation within the Beaufort Sea mainly consisted of pairwise differentiation of the Boulder Patch station DS11 compared to other stations. This station has the highest kelp density (Supp. Table D2; Dunton and Iken *unpubl. data*), and high annual kelp growth (Dunton et al. 2009; Bonsell and Dunton 2018). It is notable that there was significant differentiation between kelps from DS11 and W3, which have comparable depths and environmental regimes (Bonsell 2019, Chap. 2), similar levels of genetic diversity, and similarly high heterozygosity (Fig. 4.2, Table 4.4). Ordination analysis also revealed high dissimilarity among three spatially adjacent stations: E1, L1, and DS11 (Figs. 4.1-4.2). These stations all have distinct environmental regimes (Bonsell 2019, Chap. 2); however, ordination analysis indicated that genetic dissimilarity between sites was related to kelp cover rather than to any particular abiotic factor (Table 4.7). Given the long-lived nature of *L. solidungula*, our multi-year environmental data may not have covered enough timespan to capture selective forces, such as multidecadal disturbance and environmental variability. Furthermore, spatial patterns in benthic cover are related to environmental variables in the Boulder Patch (Bonsell 2019, Chap. 3). Significant outbreeding at DS11 and at W3 suggest that these areas may exhibit high genetic exchange. These two sites exhibit especially strong along-shore currents during the open-water season (Bonsell 2019, Chap. 2). Flow patterns demonstrate regular physical connectivity with areas outside the Boulder Patch. The deeper, offshore areas of the Boulder Patch could therefore function as sources of *L. solidungula* propagules or entrap kelp drift from the eastern Beaufort Sea and act as sinks.

Divergence between Arctic basins: outcome of glacial cycles

Despite the high connectivity within the Beaufort Sea, LSU sequences indicated that there is far less gene flow occurring between the Canadian Arctic and the Alaskan Arctic. Two distinct genotypes were identified, which occurred almost exclusively in different basins with the exception of one Canadian genotype present in Camden Bay. The dominance of one genotype in each basin indicates long-term evolutionary divergence between *L. solidungula* lineages from the Canadian and Alaskan Artic. This observation is supported by results from sequencing for COI in the same species collected from the North American Arctic (McDevit and Saunders 2009; Bringloe 2018, Fig E58). It also resembles the pattern in *Saccharina latissima*, a circumpolar species, which shows strong population differentiation between Pacific and Atlantic populations, with the Canadian Arctic as an area of interbreeding (McDevit and Saunders 2010). Based on various lines of genetic evidence, *S. latissima* recolonized the Arctic after the Last Glacial Maximum from at least two different populations, likely from a Pacific and Atlantic population, or a local refuge population (McDevit and Saunders 2010; Bringloe and Saunders 2018). We propose that a similar process occurred for *L. solidungula* – recolonization from allopatric source populations, with mixing between the two occurring in the eastern Beaufort. The population structure of *S. latissima* displays within-basin admixture at high Arctic sites (Neiva et al. 2018). This reflects our microsatellite analysis findings of admixture within the Beaufort population of *L. solidungula* and suggests that cross-basin range expansion by boreal species will occur much more slowly than within-basin.

Polymorphism within *L. solidungula* LSU is interesting given the lack of within-species variation in other investigated kelp species (*L. digitata*, *S. latissima*), and the overall low genetic divergence among kelp species. Whole LSU sequences are <3% divergent among species in the Laminariales, while other markers (ITS, RUBISCO, mitochondrial) are much more variable (Lane et al. 2006). Significant divergence, beyond the LSU locus, may also explain why microsatellite markers developed from Boulder Patch samples failed to amplify in all samples from outside the Beaufort Sea, and most samples from Camden Bay. The degree of genetic (COI) differentiation in *S. latissima* among Arctic

basins led Nieva et al. (2018) to conclude that the phylogenetic lineages represented incipient species. Although our work only involves one genetic marker, the scale of genetic differentiation within the Laminariales suggests similar emerging divergence for *L. solidungula.* *L. solidungula* is hypothesized to have first colonized the Arctic after the opening of the Bering Strait ~ 5.32 mya (Rothman et al. 2017). Glacial growth and retreat then lead to allopatric divergence and phylogeographic population structure (McDevit and Saunders 2010; Neiva et al. 2018).

Relationship to other kelp species

LSU topology grouped *L. solidungula* with *L. yezoensis*, separate from other Laminaria, in agreement with the findings of Rothman et al. (2017) for concatenated alignment of rbcL and ITS. McDevit and Saunders (2010) also found high relatedness of *L. solidungula* and *L. yezoensis* based on COI sequences, though neither study included Beaufort Sea samples. Interestingly, the divergence between Beaufort *L. solidungula* and *L. yezoensis* is less than the divergence between Beaufort and Atlantic Arctic genotypes of *L. solidungula* (Fig. 4.4). The rbcL topology of Rothman et al. (2017) placed Canadian *L. solidungula* between *L. yezoensis* from Japan and *L. yezoensis* from British Columbia. Their time-calibrated phylogeny indicated that these two species started diverging 16.4 to 5.6 mya, but these species are not monophyletic for LSU (this study) or rbcL (Rothman et al. 2017). These two species may have continued to interbreed during glacial maxima when *L. solidungula* would have been pushed south of the Arctic basin. The genetic relationships within and between these two species would be an interesting investigation based on the priorities to resolve kelp phylogenies with molecular data (e.g. Lane et al. 2006; McDevit and Saunders 2009; Jackson et al. 2016; Rothman et al. 2017). Taxonomic investigation of *L. solidungula* and *L. yezoensis* may uncover hidden diversity in the Arctic and North Pacific and unravel Pacific-Atlantic migration histories in Laminaria.

Conclusions

The phylogeographic history of kelp and the origin of kelp in the Arctic remains highly debated (Adey et al. 2008; Bolton 2010; Rothman et al. 2017). Our LSU results reveal significant and previously unknown subspecies diversity in *L. solidungula*, the only Arctic endemic kelp. Further investigation via multiple genetic markers may uncover whether the two genotypes require taxonomic consideration. *L. solidungula*, an Arctic endemic with relatively wide distribution, but distinct substrate requirements, is a model organism for testing the various hypothesis of recolonization and potential glacial refugia. Significant subspecies differentiation, tied to geography, demonstrate the substantial impact of glacial cycles on current Arctic diversity. While our results shed some light upon those processes, additional details of trans-Arctic population connectivity could be elucidated with further genetic investigation.

Kelp are thought to be poor dispersers in their zoospore stage (Santelices 1990, Norton 1992; Gaylord et al. 2006), but as sporophytes they can dislodged by storms carried long distances (e.g. Saunders 2014). In the Alaskan Beaufort Sea, fall storm cause large masses of kelp to wash ashore along exposed area of the coast, from Pt. Barrow to Demarcation Bay (Fig 4). These storms coincide with the time that the local kelp develop reproductive structures and become fecund, and may therefore be a key mechanism for kelp dispersal within the Beaufort Sea and contribute to the high gene flow shown in this study. As the timing of sea ice freeze-up becomes later due to warming, dislodgement by waves and transport by storm-driven currents will become more frequent (Thomson et al. 2016). This would enhance the connectivity of existing Arctic benthic populations, as well as potentially assist the spread of boreal species.

The genetic structure of *Laminaria solindnugla* in the Beaufort Sea suggests that this area is one of high gene flow and genetic diversity. However, it also indicates that the Boulder Patch kelps are not self-seeding, but are instead a part of a large, mixed population in the Beaufort Sea. This may be connected to relatively recent population mixing in the current inter-glacial period compared to long *L. solidungula* generation times. Along with the low apparent recruitment of kelps (Dunton et al. 1982; Konar 2013; Bonsell 2019,

Chap. 2), it appears that kelp removal or die off would be followed by a decade or more of recovery, with kelp recruiting from the larger regional population. While the Boulder Patch is the largest kelp bed in the Beaufort Sea, kelp inhabiting alternative habitats are clearly important to regional genetic patterns and population persistence. In the face of further development in the nearshore Beaufort Sea, more work is needed to investigate the spatial distribution, size, and mating patterns of the regional kelp population to accurately assess the consequences of anthropogenic modification to kelp habitats such as the Boulder Patch.

Figure 4.5: Reproductive *Laminaria solidungula* (main species), *Saccharina latissima*, and *Alaria esculenta* drift algae on the northwest side of Endicott Causeway. 15 August 2017.

Appendices

APPENDIX A

Table A1: Lightmeter deployment sites and dates (dd/mm/yy) per year. * = data recorded is 1 hr averages; all others recorded 3 hour averages.

	DS11	**E1**	**E2**	**E3**	**L1**	**W1**	**W2**	**W3**	**Eastdock /Endicott**
1984	12/08/84-26/08/84	09/08/84-20/08/84				09/08/84-26/08/84			
1986	07/08/86-23/08/86	10/08/86-22/08/86	11/08/86-20/08/86	10/08/86-23/08/86		18/08/86-23/08/86	07/08/86-18/08/86		11/08/86-21/08/86
1986-87	23/08/86-06/088/7	21/1/87-26/6/87*	23/08/86-07/08/87			12/10/8-14/6/87*	25/08/86-05/08/87 *	25/08/86-03/02/87	01/09/86-31/08/87
1987-88	06/08/87-21/08/88	07/08/87-01/04/88 *, 07/08/88-18/08/88	08/08/87-18/08/88	06/08/87-18/08/88		08/08/87-16/04/88 *, 09/08/88-21/08/88	05/08/87-21/08/88	05/08/87-17/08/88	30/05/87-22/08/88
1988-89	21/08/88-20/08/89	18/08/88-19/08/89	18/08/88-06/08/89, 13/08/89-22/08/89	18/08/88-21/08/89		08/08/88-19/08/89	08/08/88-12/07/89, 11/08/89-19/08/89	08/08/88-19/08/89	22/08/88-18/08/89
1989-90	21/08/89-21/08/90	19/08/89-21/08/90	22/08/89-01/08/90	2/08/89-1/08/90		19/08/89-01/08/90	19/08/89-02/08/90	19/08/89-31/07/90	25/08/89-31/07/90
1990-91	11/08/90-18/08/91	22/08/90-18/08/91	01/08/90-10/04/91, 3/08/91-18/08/91	01/08/90-23/10/91, 2/08/91-18/08/91		01/08/90-23/10/91, 10/08/91-18/08/91	02/08/90-18/08/91	02/08/90-18/08/91	01/08/90-20/08/91
1991-92	19/08/91-16/08/92								22/08/91-16/04/92
2002	28/07/02-8/08/02								26/07/02-10/08/02
2004	25/07/04-12/08/04	25/07/04-13/08/04				26/07/04-12/08/04			3/08/04-14/08/04
2005	22/07/05-9/08/05		22/07/05-9/08/05				22/07/05-9/08/05		19/07/05-26/07/05
2006	27/07/06-9/08/06		24/07/06-9/08/06				27/07/06-9/08/06		24/07/06-09/08/06

2007	26/07/07-16/08/07	26/07/07-16/08/07							26/07/07-17/08/07

Table A1, cont.

2012-13	28/07/12-19/07/13								
2013-14	20/07/13-22/08/14	26/07/13-22/08/14							21/07/13-23/08/14
2014-15	23/08/14-17/07/15				22/08/14-18/07/15	23/08/14-18/07/15		23/08/14-18/07/15	25/08/14-12/07/15
2015-16	26/07/15-21/07/16	26/07/15-22/07/16			25/07/15-26/07/16	25/07/15-26/07/16			13/07/15-18/07/16

Table A2: Estimated TSS concentrations (mg/L) for each site under given wind conditions (from Trefry et al. 2009, Aumack & Dunton unpublished data)

Site	< 5 knots	5-10 knots	10-20 knots
B1	2.0	4.0	7.6
DS11	1.4	2.8	5.2
E1	4.0	8.0	15.0
E2	3.4	6.8	12.7
E3	2.4	4.8	9.1
L1	2.0	3.9	7.4
L2	1.2	2.4	4.4
W1	1.4	2.8	5.3
W2	1.4	2.8	5.3
W3	1.3	2.5	4.7

Table A3: Summary of ice events and trends over time, 1979-2016. * Indicates statistically significant change over time (linear model, α=0.05).

Feature	Mean date or duration	Trend (days/decade)	R^2
Freeze up start*	October 14	2.67	0.37
Freeze up end*	October 28	3.82	0.42
Freeze up duration*	15 days	1.15	0.12
Break up start*	June 17	-2.37	0.22
Break up end*	July 26	-2.29	0.17
Break up duration	39 days	0.08	<0.01
Break up end to freeze up start*	80 days	4.95	0.34
Break up start to freeze up end*	133 days	6.22	0.50

APPENDIX B

Table B1: Results table for comparing each abiotic factor among sites via a blocked ANOVA (blocked by day) for the entire data record.

Season		**Variable**	**Sig diff.s by site?**
All		Temperature	Yes
	Sum Sq.	**DF**	**F**
Intercept	153.0	1	37.08
Site	188.5	4	11.42
Day	210.3	1	50.95
Residuals	30295.3	7340	
Season		**Variable**	**Sig diff.s by site?**
Ice-covered winter		Temperature	Yes
	Sum Sq.	**DF**	**F**
Intercept	12.62	1	1326.85
Site	2.21	4	58.18
Day	0.15	1	15.77
Residuals	29.01	3051	
Season		**Variable**	**Sig diff.s by site?**
Spring break-up		Temperature	Yes
	Sum Sq.	**DF**	**F**
Intercept	2.38	1	19.29
Site	18.51	4	37.57
Day	0.03	1	0.24
Residuals	149.55	1214	
Season		**Variable**	**Sig diff.s by site?**
Open-water summer		Temperature	Yes
	Sum Sq.	**DF**	**F**
Intercept	137.8	1	27.90
Site	486.5	4	24.62
Day	82.2	1	16.65
Residuals	8802.7	1782	
Season		**Variable**	**Sig diff.s by site?**
Fall freeze-up		Temperature	No
	Sum Sq.	**DF**	**F**
Intercept	20.17	1	22.17
Site	2.72	4	0.75
Day	8.88	1	9.76
Residuals	1160.22	1275	
Season		**Variable**	**Sig diff.s by site?**
All		Salinity	Yes
	Sum Sq.	**DF**	**F**
Intercept	4886	1	364.16

Table B1, cont.

Site	3278	4	61.08
Day	171	1	12.72
Residuals	73888	5507	
Season		**Variable**	**Sig diff.s by site?**
Ice-covered winter		Salinity	Yes
	Sum Sq.	**DF**	**F**
Intercept	3738.8	1	2016.10
Site	609.3	4	82.14
Day	24.2	1	13.06
Residuals	4066.9	2193	
Season		**Variable**	**Sig diff.s by site?**
Spring break-up		Salinity	Yes
	Sum Sq.	**DF**	**F**
Intercept	519.9	1	46.53
Site	1600.5	4	35.81
Day	116.6	1	10.43
Residuals	10437.6	934	
Season		**Variable**	**Sig diff.s by site?**
Open-water summer		Salinity	Yes
	Sum Sq.	**DF**	**F**
Intercept	2367.7	1	211.53
Site	1432.7	4	31.97
Day	133.8	1	11.94
Residuals	17408.8	1554	
Season		**Variable**	**Sig diff.s by site?**
Fall freeze-up		Salinity	Yes
	Sum Sq.	**DF**	**F**
Intercept	2060.6	1	428.57
Site	131.2	4	6.82
Day	191.1	1	39.74
Residuals	3885.0	808	
Season		**Variable**	**Sig diff.s by site?**
All		PAR	No
	Sum Sq.	**DF**	**F**
Intercept	0.01	1	0.01
Site	4.81	4	1.46
Day	0.27	1	0.33
Residuals	3000.75	3654	
Season		**Variable**	**Sig diff.s by site?**
Ice-covered winter		PAR	No
	Sum Sq.	**DF**	**F**
Intercept	0.0005	1	0.60
Site	0.0030	3	1.28
Day	0.0001	1	0.09

Table B1, cont.

Residuals	1.1660	1507	
Season		**Variable**	**Sig diff.s by site?**
Spring break-up		PAR	No
	Sum Sq.	**DF**	**F**
Intercept	0.04	1	1.37
Site	0.02	3	0.30
Day	0.02	1	0.70
Residuals	16.16	605	
Season		**Variable**	**Sig diff.s by site?**
Open-water summer		PAR	Yes
	Sum Sq.	**DF**	**F**
Intercept	9.29	1	3.40
Site	61.27	4	5.60
Day	15.10	1	5.52
Residuals	2491.96	911	
Season		**Variable**	**Sig diff.s by site?**
Fall freeze-up		PAR	No
	Sum Sq.	**DF**	**F**
Intercept	0.045	1	29.19
Site	0.003	3	0.70
Day	0.460	1	26.60
Residuals	0.940	615	
Season		**Variable**	**Sig diff.s by site?**
All		Current velocity	Yes
	Sum Sq.	**DF**	**F**
Intercept	3835	1	243.08
Site	6335	4	100.38
Day	3353	1	212.49
Residuals	54293	3441	
Season		**Variable**	**Sig diff.s by site?**
Ice-covered winter		Current velocity	Yes
	Sum Sq.	**DF**	**F**
Intercept	10.40	1	14.78
Site	198.55	4	70.58
Day	5.97	1	8.49
Residuals	953.65	1356	
Season		**Variable**	**Sig diff.s by site?**
Spring break-up		Current velocity	Yes
	Sum Sq.	**DF**	**F**
Intercept	21.55	1	32.73
Site	91.89	4	34.90
Day	17.24	1	26.19
Residuals	357.47	543	
Season		**Variable**	**Sig diff.s by site?**

Table B1, cont.

Open-water summer		Current velocity	Yes
	Sum Sq.	**DF**	**F**
Intercept	160.8	1	9.65
Site	2097.0	4	31.45
Day	78.8	1	4.72
Residuals	15235.2	914	
Season		**Variable**	**Sig diff.s by site?**
Fall freeze-up		Current velocity	Yes
	Sum Sq.	**DF**	**F**
Intercept	2.8	1	0.08
Site	2680.2	4	18.81
Day	25.3	1	0.71
Residuals	21733.6	610	

APPENDIX C

Table C1: Number of tiles (and tile pieces) retrieved from each site for each deployment period. *indicates plates lost to ice scour.

Site	One year			Two years		Three years
	2015-2016	2016-2017	2017-2018	2015-2017	2016-2018	2015-2018
DS11	10	8	8	8	8	0*
E1	8	8	8	8	8	0
L1	0	0	8	0	0	0
W1	8	8	8	8	0	8
W3	0*	8	8	0*	8	0*

Table C2: Pairwise PERMANOVA summary table for comparing benthic community structure at each site (square-root transformed data). *Denotes significant difference.

	Df	SS	MS	F.Model	R2	Pr(>F)
DS11|E1* N:31|36						
Site	1	3.23	3.23	69.59	0.52	0.01
Residuals	65	3.02	0.05		0.48	
DS11|L1* N:31|24						
Site	1	1.91	1.91	26.83	0.34	0.01
Residuals	53	3.76	0.07		0.66	
DS11|W1* N:31|43						
Site	1	2.67	2.67	29.80	0.29	0.01
Residuals	72	6.45	0.09		0.71	
DS11|W3* N:31|35						
Site	1	1.71	1.71	30.45	0.32	0.01
Residuals	64	3.58	0.06		0.68	
E1|L1 N:36|24						
Site	1	0.11	0.11	2.42	0.04	0.12
Residuals	58	2.57	0.04		0.96	
E1|W1* N:36|43						
Site	1	0.89	0.89	12.98	0.14	0.01
Residuals	77	5.26	0.07		0.86	
E1|W3* N:36|35						
Site	1	0.98	0.98	28.23	0.29	0.01
Residuals	69	2.40	0.03		0.71	
L1|W1* N:24|43						
Site	1	0.82	0.82	8.91	0.12	0.01
Residuals	65	6.00	0.09		0.88	
L1|W3* N:24|35						
Site	1	0.44	0.44	8.06	0.12	0.01

Table C2 cont.

Residuals	**57**	**3.14**	**0.06**		**0.87**	
W1|W3* N:43|35						
Site	1	2.00	2.00	26.14	0.26	0.01
Residuals	76	5.83	0.08		0.74	

Table C3: Environmental characteristics of each site (Bonsell, Chapter 2). Values for physiochemical parameters represent mean±SD.

Site	Lat. (DD)	Long. (DD)	Depth (m)	Dist. to river input (km)	Temp. (°C)	Salinity	Current velocity (cm s^{-1})	PAR (mol photons m^{-2} day^{-1})
DS11	70.32228	-147.579	6.1	9.03	-0.78 ±1.96	32 ±3	4.4 ±5.3	0.271 ±1.013
E1	70.31495	-147.732	4.4	3.54	-0.41 ±2.50	31 ±4	2.8 ±3.2	0.208 ±0.925
L1	70.28993	-147.613	5.5	7.20	-0.82 ±1.89	33 ±4	1.9 ±2.7	0.194 ±0.756
W1	70.37003	-147.873	6.0	3.54	-0.95 ±1.84	30 ±4	4.3 ±5.4	0.102 ±0.236
W3	70.37627	-147.794	6.6	7.31	-0.80 ±1.88	32 ±3	4.8 ±4.6	0.184 ±0.700

APPENDIX D

Table D1: All microsatellite primers tested, species for which there are multiple alleles at that locus, and citations.

Primers	Species	Citation
Lo4-24	L. ochroleuca, L. hyperborea	Coelho et al 2014
LoIVVIV-13 F	L. ochroleuca, L. hyperborea, L. digitata	Coelho et al 2014
LoIVVIV-15 F	L. ochroleuca, L. hyperborea	Coelho et al 2014
LoIVVIV-17 F	L. ochroleuca, L. hyperborea, L. digitata	Coelho et al 2014
LoIVVIV-23 F	L. ochroleuca, L. hyperborea, L. digitata	Coelho et al 2014
LoIVVIV-24 F	L. ochroleuca, L. hyperborea, L. digitata	Coelho et al 2014
LoIVVIV-27 F	L. ochroleuca	Coelho et al 2014
LoIVVIV-28 F	L. ochroleuca, L. hyperborea, L. digitata	Coelho et al 2014
Ld1-124 F	L. digitata, Lessonia nigrescens	Billot et al 1998, Martinez et al 2005
Ld2-148 F	L. digitata, L. hyperborea, Lessonia nigrescens	Billot et al 1998, Martinez et al 2005, Robuchon et al 2014
Ld2-158 F	L. digitata, L. hyperborea, Lessonia nigrescens	Billot et al 1998, Martinez et al 2005, Robuchon et al 2014
Ld2-167 F	L. digitata, L. hyperborea, Lessonia nigrescens	Billot et al 1998, Martinez et al 2005, Robuchon et al 2014
Ld2-371 F	L. digitata, Lessonia nigrescens	Billot et al 1998, Martinez et al 2005
Ld2-520 F	L. digitata, Lessonia nigrescens	Billot et al 1998, Martinez et al 2005
Ld2-531 F	L. digitata, Lessonia nigrescens	Billot et al 1998, Martinez et al 2005
Ld2-704 F	L. digitata, Lessonia nigrescens	Billot et al 1998, Martinez et al 2005
Ld-2 F	S. japonica	Liu et al 2012
Ld-3 F	S. japonica, L. hyperborea	Liu et al 2012, Evankow 2015
Ld-6 F	S. japonica, L. hyperborea	Liu et al 2012, Evankow 2015
Ld13-F	S. japonica	Liu et al 2012

Table D2: Daily, year-round mean (±SD) benthic environmental conditions (originally from Bonsell 2019, Chap 2) and mean benthic percent cover of functional groups (originally from Bonsell 2019, Chap 3) at each site. Bold indicates significant differences between sites (Supp. Table 3). Superscripts indicate grouping from Tukey HSD test.

Site	**Temp. (ºC)**	**Sal.**	**Current vel. (cm s^{-1})**	PAR (mol photons m^{-2} day^{-1})	**Crustose coralline algae**	**Foliose red algae**	**Kelp**	**Filter feeders**	**Suspension feeders**
DS11	**-0.78 ±1.96^{a}**	**32 ±3^{a}**	**4.4 ±5.3^{a}**	0.271 ±1.013	**18.67 ± 0.46^{a}**	**38.01 ± 0.78^{a}**	**19.03 ± 0.75^{a}**	**0.44 ± 0.03^{ab}**	**4.08 ± 0.19^{a}**
E1	**-0.41 ±2.50^{b}**	**31 ±4^{b}**	**2.8 ±3.2^{b}**	0.208 ±0.925	**0± 0^{b}**	**79.31 ± 0.51^{b}**	**2.9 ± 0.25^{b}**	**0.77 ± 0.11 ^{b}**	**6.12 ± 0.21^{a}**
L1	**-0.82 ±1.89 ^{a}**	**33 ±4^{a}**	**1.9 ±2.7^{c}**	0.194 ±0.756	**0.64 ± 0.06^{c}**	**71.67 ± 1.19^{bc}**	**9.85 ± 0.93^{b}**	**0.48 ± 0.05 ^{ab}**	**2.79 ± 0.21^{ab}**
W1	**-0.95 ±1.84^{a}**	**30 ±4^{c}**	**4.3 ±5.4^{a}**	0.102 ±0.236	**0.48 ± 0.03^{d}**	**47.32 ± 0.76^{ad}**	**4.4 ± 0.24^{b}**	**2.12 ± 0.12 ^{a}**	**14.87 ± 0.39^{d}**
W3	**-0.80 ±1.88^{a}**	**32 ±3^{b}**	**4.8 ±4.6^{a}**	0.184 ±0.700	**4.67 ± 0.15^{a}**	**58.01 ± 0.63^{cd}**	**1.65 ± 0.14^{b}**	**0.77 ± 0.05 ^{ab}**	**0.24 ± 0.02^{c}**

Table D3: Results table for comparing benthic cover by each functional group among sites via ANOVA. *Indicates significant differences among sites (α=0.05).

Variable: Crustose coralline algae % cover*			
	Sum Sq.	**DF**	**F**
Intercept	5.55	1	472.18
Site	4.00	4	84.99
Residuals	1.93	164	
Variable: Foliose red algae % cover*			
	Sum Sq.	**DF**	**F**
Intercept	2.06	1	199.01
Site	0.51	4	12.43
Residuals	1.70	164	
Variable: Kelp % cover*			
	Sum Sq.	**DF**	**F**
Intercept	4.16	1	74.30
Site	2.17	4	9.70
Residuals	9.19	164	
Variable: Filter feeder % cover*			
	Sum Sq.	**DF**	**F**
Intercept	0.031	1	3.65
Site	0.085	4	2.49
Residuals	1.393	164	
Variable: Suspension feeder % cover*			
	Sum Sq.	**DF**	**F**
Intercept	0.20	1	22.40
Site	0.64	4	17.78
Residuals	1.48	164	

References

Adey, W. H., S. C. Lindstrom, M. H. Hommersand, and K. M. Müller. 2008. the Biogeographic Origin of Arctic Endemic Seaweeds: a Thermogeographic View 1. J. Phycol. 44: 1384–1394.

Agardh, J. G. 1862. Om Spetsbergens alger.

Agostinelli, C. and U. Lund. 2017. R package 'circular': Circular Statistics (version 0.4-93). https://r-forge.r-project.org/projects/circular/.

Alberto, F., P. Raimondi, and D. Reed. 2010. Habitat continuity and geographic distance predict population genetic differentiation in giant kelp. Ecology 91: 49–56.

Alkire, M. B., and J. H. Trefry. 2006. Transport of spring floodwater from rivers under ice to the Alaskan Beaufort Sea. J. Geophys. Res. Ocean. 111: 1–12.

Amsler, C., D. Reed, and M. Neushul. 1992. The microclimate inhabited by macroalgal propagules. Br. Phycol. J. 37–41.

Anthony, K. R. N., P. V Ridd, A. R. Orpin, P. Larcombe, J. Lough, S. Connolly, and D. Anthony. 2004. Temporal variation of light availability in coastal benthic habitats: Effects of clouds, turbidity, and tides. Limnol. Oceanogr. 49: 2201–2211.

Aumack, C. F., K. H. Dunton, A. B. Burd, D. W. Funk, and R. A. Maffione. 2007. Linking light attenuation and suspended sediment loading to benthic productivity within an Arctic kelp-bed community 1. J. Phycol. 43: 853–863.

Balloux, F., L. Lehmann, and T. De Meeûs. 2003. The population genetics of clonal and partially clonal diploids. Genetics 164: 1635–1644.

Barnes, P. W. and Reimnitz, E. 1982. Net flow of near-bottom waters on the inner Beaufort Sea Shelf as Determined from Seabed Drifters. USGS Report.

Barry, R. G., R. E. Moritz, and J. C. Rogers. 1979. The fast ice regimes of the Beaufort and Chukchi Sea coasts, Alaska. Cold Reg. Sci. Technol. 1: 129–152.

Bartsch, I., M. Paar, S. Fredriksen, M. Schwanitz, C. Daniel, H. Hop, and C. Wiencke. 2016. Changes in kelp forest biomass and depth distribution in Kongsfjorden, Svalbard, between 1996–1998 and 2012–2014 reflect Arctic warming. Polar Biol. 39: 2021–2036.

Bell, J. J., E. McGrath, A. Biggerstaff, T. Bates, H. Bennett, J. Marlow, and M. Shaffer. 2015. Sediment impacts on marine sponges. Mar. Pollut. Bull. 94: 5–13.

Berge, J., G. Johnsen, F. Nilsen, B. Gulliksen, and D. Slagstad. 2005. Ocean temperature oscillations enable reappearance of blue mussels Mytilus edulis in Svalbard after a 1000 year absence. Mar. Ecol. Prog. Ser. 303: 167–175.

Bertness, M. D., and R. Callaway. 1994. Positive interactions in communities. Trends Ecol. Evol. 9: 27–29.

Beuchel, F., and B. Gulliksen. 2008. Temporal patterns of benthic community development in an Arctic fjord (Kongsfjorden, Svalbard): Results of a 24-year manipulation study. Polar Biol. 31: 913–924.

Beuchel, F., B. Gulliksen, and M. L. Carroll. 2006. Long-term patterns of rocky bottom macrobenthic community structure in an Arctic fjord (Kongsfjorden, Svalbard) in relation to climate variability (1980–2003). J. Mar. Syst. 63: 35–48.

Billot, C., C. R. C. Engel, S. Rousvoal, B. Kloareg, and M. Valero. 2003. Current patterns, habitat discontinuities and population genetic structure: the case of the kelp Laminaria digitata in the English Channel. Mar. Ecol. Prog. Ser. 253: 111–121.

Bluhm, B., A. Gebruk, and R. Gradinger. 2011. Arctic marine biodiversity: an update of species richness and examples of biodiversity change. Oceanogr. … 24: 232–248.

Bolton, J. J. 2010. The biogeography of kelps (Laminariales, Phaeophyceae): a global analysis with new insights from recent advances in molecular phylogenetics. Helgol. Mar. Res. 64: 263–279.

Bonsell, C., and K. H. Dunton. 2018. Long-term patterns of benthic irradiance and kelp production in the central Beaufort sea reveal implications of warming for Arctic inner shelves. Prog. Oceanogr. 162: 160–170.

Bremner, J., S. Rogers, and C. Frid. 2003. Assessing functional diversity in marine benthic ecosystems: a comparison of approaches. Mar. Ecol. Prog. Ser. 254: 11–25.

Brennan, G., L. Kregting, G. E. Beatty, C. Cole, B. Elsasser, G. Savidge, and J. Provan. 2014. Understanding macroalgal dispersal in a complex hydrodynamic environment: a combined population genetic and physical modelling approach. J. R. Soc. Interface 11: 20140197–20140197.

Breton, T. S., J. C. Nettleton, B. O'Connell, and M. Bertocci. 2018. Fine-scale population genetic structure of sugar kelp, Saccharina latissima (Laminariales, Phaeophyceae), in eastern Maine, USA. Phycologia 57: 32–40. .

Bringloe, T.T. 2018 The biogeographic history and contemporary origins of North American Arctic marine macroalgae. Doctoral Dissertation.

Bringloe, T. T., and G. W. Saunders. 2018. Mitochondrial DNA sequence data reveal the origins of postglacial marine macroalgal flora in the Northwest Atlantic. Mar. Ecol. Prog. Ser. 589: 45–58.

Brown, J. H. J. H., and A. Kodric-Brown. 1977. Turnover rates in insular biogeography: effect of immigration on extinction. Ecology 58: 445–449. doi:10.2307/1935620

Buschmann, A. H., J. A. Vasquez, P. Osorio, E. Reyes, L. Filun, M. C. Hernandez-Gonzalez, and A. Vega. 2004. The effect of water movement, temperature and salinity on abundance and reproductive patterns of Macrocystis spp. (Phaeophyta) at different latitudes in Chile. Mar. Biol. 145: 849–862.

Carmack, E., and R. Macdonald. 2002. Oceanography of the Canadian Shelf of the Beaufort Sea: a setting for marine life. Arctic 55: 29–45.

Carmack, E., and P. Wassmann. 2006. Food webs and physical-biological coupling on pan-Arctic shelves: Unifying concepts and comprehensive perspectives. Prog. Oceanogr. 71: 446–477.

Carney, L. T., A. J. Bohonak, M. S. Edwards, and F. Alberto. 2013. Genetic and experimental evidence for a mixed-age, mixed-origin bank of kelp microscopic stages in southern California. Ecology 94: 1955–65.

Carney, L. T., and M. S. Edwards. 2010. Role of nutrient fluctuations and delayed development in gametophyte reproduction by Macrocystis pyrifera (phaeophyceae) in Southern California. J. Phycol. 46: 987–996.

Chan, F. T., H. J. MacIsaac, and S. A. Bailey. 2016. Survival of ship biofouling assemblages during and after voyages to the Canadian Arctic. Mar. Biol. 163: 1–14.

Chapman, A., and J. Lindley. 1980. Seasonal growth of Laminaria solidungula in the Canadian High Arctic in relation to irradiance and dissolved nutrient concentrations. Mar. Biol. 5: 1–5.

Christie, H., K. Norderhaug, and S. Fredriksen. 2009. Macrophytes as habitat for fauna. Mar. Ecol. Prog. Ser. 396: 231–243.

Clark, G. F., J. S. Stark, E. L. Johnston, J. W. Runcie, P. M. Goldsworthy, B. Raymond, and M. J. Riddle. 2013. Light-driven tipping points in polar ecosystems. Glob. Chang. Biol. 19: 3749–3761.

Coleman, M. A., M. Roughan, H. S. Macdonald, S. D. Connell, B. M. Gillanders, B. P. Kelaher, and P. D. Steinberg. 2011. Variation in the strength of continental boundary currents determines continent-wide connectivity in kelp. J. Ecol. 99: 1026–1032.

Conlan, K. E., H. S. Lenihan, R. G. Kvitek, and J. S. Oliver. 1998. Ice scour disturbance to benthic communities in the Canadian High Arctic. Mar. Ecol. Prog. Ser. 166: 1–16.

Cowen, R. K., and S. Sponaugle. 2009. Larval Dispersal and Marine Population Connectivity. Ann. Rev. Mar. Sci. 1: 443–466.

Coyer, J. a., G. Hoarau, J. Van Schaik, P. Luijckx, and J. L. Olsen. 2011. Trans-Pacific and trans-Arctic pathways of the intertidal macroalga Fucus distichus L. reveal multiple glacial refugia and colonizations from the North Pacific to the North Atlantic. J. Biogeogr. 38: 756–771.

Craig, P. C., and P. J. McCart. 1975. Classification of Stream Types in Beaufort Sea Drainages between Prudhoe Bay , Alaska , and the Mackenzie Delta, N. W. T., Canada. Arct. Alp. Res. 7: 183–198.

Delille, B., A. V Borges, and D. Delille. 2009. Influence of giant kelp beds (Macrocystis pyrifera) on diel cycles of pCO2 and DIC in the Sub-Antarctic coastal area. Estuar. Coast. Shelf Sci. 81: 114–122.

Devinny, J., and L. Volse. 1978. Effects of sediments on the development of Macrocystis pyrifera gametophytes. Mar. Biol. 348: 343–348.

Van Duin, E. H. S., G. Blom, F. J. Los, R. Maffione, R. Zimmerman, C. F. Cerco, M. Dortch, and E. P. H. Best. 2001. Modeling underwater light climate in relation to sedimentation, resuspension, water quality and autotrophic growth. Hydrobiologia 444: 25–42.

Dunton, K. H. 1985. Growth of Dark-exposed Laminaria saccharina (L.) Lamour. and Laminaria solidungula J. Ag. (Laminariales : Phaeophyta) in the Alaskan Beaufort Sea. J. Exp. Mar. Bio. Ecol. 94: 181–189. doi:10.1016/0022-0981(85)90057-7

Dunton, K. H. 1990. Growth and production in Laminaria solidungula: relation to continuous underwater light levels in the Alaskan High Arctic. Mar. Biol. 106: 297–304.
Dunton, K. H., and C. M. Jodwalis. 1988. Photosynthetic performance of Laminaria solidungula measured in situ in the Alaskan High Arctic. Mar. Biol. 98: 277–285.
Dunton, K. H., E. R. K. Reimnitz, and S. Schonberg. 1982. An Arctic Kelp Community in the Alaskan Beaufort Sea. Arctic 35: 465–484. doi:10.14430/arctic2355
Dunton, K. H., and D. M. Schell. 1987. Dependence of consumers on macroalgal (Laminaria solidungula) carbon in an arctic kelp community: d 13 C evidence. Mar. Biol. 93: 615–625.
Dunton, K.H., and S. V. Schonberg. 2000. The benthic faunal assemblage of the Boulder Patch kelp community, p. 371–397. In The Natural History of an Arctic Oil Field. Academic Press.
Dunton, K. H., S. V. Schonberg, and D. W. Funk. 2009. Interannual and spatial variability in light attenuation: evidence from three decades of growth in the arctic kelp, Laminaria solidungula, p. 271–284. In Smithsonian at the Poles/Contributions to International Polar Year Science.
Dunton, K. H., S. V Schonberg, L. R. Martin, and G. S. Mueller. 1992. Seasonal and Annual Variations in the underwater light environment of an Arctic kelp community. Diving Sci. 83–92.
Dunton, K. H., T. Weingartner, and E. C. Carmack. 2006. The nearshore western Beaufort Sea ecosystem: Circulation and importance of terrestrial carbon in arctic coastal food webs. Prog. Oceanogr. 71: 362–378.
Durrant, H. M. S., N. S. Barrett, G. J. Edgar, M. A. Coleman, and C. P. Burridge. 2018. Seascape habitat patchiness and hydrodynamics explain genetic structuring of kelp populations. Mar. Ecol. Prog. Ser. 587: 81–92.
Erlandson, J. M., M. H. Graham, B. J. Bourque, D. Corbett, J. a. Estes, and R. S. Steneck. 2007. The Kelp Highway Hypothesis: Marine Ecology, the Coastal Migration Theory, and the Peopling of the Americas. J. Isl. Coast. Archaeol. 2: 161–174.
Erting, L., N. Daugbjerg, and P. M. Pedersen. 2004. Nucleotide diversity within and between four species of Laminaria (Phaeophyceae) analysed using partial LSU and ITS rDNA sequences and AFLP. Eur. J. Phycol. 39: 243–256.
Evankow, A. M. 2015. Genetics of Norwegian kelp forests: Microsatellites reveal the genetic diversity, differentiation, and structure of two foundation kelp species in Norway. Master's Thesis.
Filbee-Dexter, K., and T. Wernberg. 2018. Rise of Turfs: A New Battlefront for Globally Declining Kelp Forests. Bioscience 68: 64–76.
Filbee-Dexter, K., T. Wernberg, S. Fredriksen, K. M. Norderhaug, and M. F. Pedersen. 2019. Arctic kelp forests: Diversity, resilience and future. Glob. Planet. Change 172: 1–14.
Fredersdorf, J., R. Müller, S. Becker, C. Wiencke, and K. Bischof. 2009. Interactive effects of radiation, temperature and salinity on different life history stages of the Arctic kelp Alaria esculenta (Phaeophyceae). Oecologia 160: 483–492.

Fredriksen, S. 2003. Food web studies in a Norwegian kelp forest based on stable isotope (δ13C and δ15N) analysis. Mar. Ecol. Prog. Ser. 260: 71–81.
Frey, K. E., G. W. K. Moore, L. W. Cooper, and J. M. Grebmeier. 2015. Divergent patterns of recent sea ice cover across the Bering, Chukchi, and Beaufort seas of the Pacific Arctic Region. Prog. Oceanogr. 136: 32–49.
Fricke, A., M. Molis, C. Wiencke, N. Valdivia, and A. S. Chapman. 2008. Natural succession of macroalgal-dominated epibenthic assemblages at different water depths and after transplantation from deep to shallow water on Spitsbergen. Polar Biol. 31: 1191–1203.
Fritz, M., J. E. Vonk, and H. Lantuit. 2017. Collapsing Arctic coastlines. Nat. Clim. Chang. 7: 6–7.
Gaylord, B., K. J. Nickols, and L. Jurgens. 2012. Roles of transport and mixing processes in kelp forest ecology. J. Exp. Biol. 215: 997–1007.
Gaylord, B., D. C. Reed, P. T. Raimondi, and L. Washburn. 2006. Macroalgal spore dispersal in coastal environments: Mechanistic insights revealed by theory and experiment. Ecol. Monogr. 76: 481–502.
Gaylord, B., J. H. Rosman, D. C. Reed, and others. 2013. Spatial patterns of flow and their modification within and around a giant kelp forest. Limnol. Ocean. 52: 100–100.
Gibbs, A. E., and B. M. Richmond. 2015. National assessment of shoreline change—Historical shoreline change along the north coast of Alaska, U.S.–Canadian border to Icy Cape: U.S. Geological Survey Open-File Report 2015–1048,.
Gordeev, V. V. 2006. Fluvial sediment flux to the Arctic Ocean. Geomorphology 80: 94–104.
Grebmeier, J. M. 2012. Shifting Patterns of Life in the Pacific Arctic and Sub-Arctic Seas. Ann. Rev. Mar. Sci. 4: 63–78.
Grebmeier, J. M., J. E. Overland, S. E. Moore, and others. 2006. A major ecosystem shift in the Northern Bering Sea. Science (80-.). 311: 1461–1465.
Gunther, F., P. P. Overduin, I. A. Yakshina, T. Opel, A. V. Baranskaya, and M. N. Grigoriev. 2015. Observing Muostakh disappear: permafrost thaw subsidence and erosion of a ground-ice-rich island in response to arctic summer warming and sea ice reduction. Cryosphere 9: 151–178.
Hardy, S. M., C. M. Carr, M. Hardman, D. Steinke, E. Corstorphine, and C. Mah. 2010. Biodiversity and phylogeography of Arctic marine fauna: insights from molecular tools. Mar. Biodivers. 41: 195–210.
Harley, C. D. G., K. M. Anderson, K. W. Demes, J. P. Jorve, R. L. Kordas, T. a. Coyle, and M. H. Graham. 2012. Effects of Climate Change on Global Seaweed Communities. J. Phycol. 48: 1064–1078.
Harris, C. M., J. W. McClelland, T. L. Connelly, B. C. Crump, and K. H. Dunton. 2017. Salinity and Temperature Regimes in Eastern Alaskan Beaufort Sea Lagoons in Relation to Source Water Contributions. Estuaries and Coasts 40: 50–62.
Harris, C. M., N. D. McTigue, J. W. McClelland, and K. H. Dunton. 2018. Do high Arctic coastal food webs rely on a terrestrial carbon subsidy? Food Webs 15.

Henley, W., and K. Dunton. 1995. A seasonal comparison of carbon, nitrogen, and pigment content in Laminaria solidungula and L. saccharina (Phaeophyta) in the Alaskan Arctic. J. Phycol. 331: 325–331.

Holmes, R. M., J. W. McClelland, P. A. Raymond, B. B. Frazer, B. J. Peterson, and M. Stieglitz. 2008. Lability of DOC transported by Alaskan rivers to the Arctic Ocean. Geophys. Res. Lett. 35: 3–7.

Jackson, C., E. D. Salomaki, C. E. Lane, and G. W. Saunders. 2016. Kelp transcriptomes provide robust support for interfamilial relationships and revision of the little know Arthrothamnaceae (Laminariales). J. Phycol. 1–6.

Jackson, G. A., and C. D. Winant. 1983. Effect of a kelp forest on coastal currents. Cont. Shelf Res. 2: 75–80.

Ji, R., M. Jin, and Ø. Varpe. 2013. Sea ice phenology and timing of primary production pulses in the Arctic Ocean. Glob. Chang. Biol. 19: 734–741.

Johansson, M. L., P. T. Raimondi, D. C. Reed, N. C. Coelho, E. a Serrão, and F. a Alberto. 2013. Looking into the black box: simulating the role of self-fertilization and mortality in the genetic structure of Macrocystis pyrifera. Mol. Ecol. 22: 4842–54.

Jombart, T. 2008. adegenet: a R package for the multivariate analysis of genetic markers, Bioinformatics. 24:1403–1405.

Jones, B. M., C. D. Arp, M. T. Jorgenson, K. M. Hinkel, J. A. Schmutz, and P. L. Flint. 2009. Increase in the rate and uniformity of coastline erosion in Arctic Alaska. Geophys. Res. Lett. 36: 1–5.

Jones, B. M., K. M. Hinkel, C. D. Arp, and W. R. Eisner. 2008. Modern erosion rates and loss of coastal features and sites, Beaufort Sea coastline, Alaska. Arctic 61: 361–372.

Kahru, M., V. Brotas, M. Manzano-Sarabia, and B. G. Mitchell. 2011. Are phytoplankton blooms occurring earlier in the Arctic? Glob. Chang. Biol. 17: 1733–1739.

Karsten, U. 2007. Research note: Salinity tolerance of Arctic kelps from Spitsbergen. Phycol. Res. 55: 257–262.

Karsten, U., K. Bischof, and C. Wiencke. 2001. Photosynthetic performance of arctic macroalgae after transplantation from deep to shallow waters. Oecologia 127: 11–20.

Kasper, J. L., and T. J. Weingartner. 2015. The Spreading of a Buoyant Plume Beneath a Landfast Ice Cover. J. Phys. Oceanogr. 45: 478–494.

Kempema, E. W., E. Reimnitz, and P. W. Barnes. 1989. Sea Ice Sediment Entrainment and Rafting in the Arctic. J. Sediment. Petrol. 59: 308–317.

King, R. J., and W. Schramm. 1982. Calcification in the Maerl Coralline Alga Phymatolithon-Calcareum - Effects of Salinity and Temperature. Mar. Biol. 70: 197–204.

Kinlan, B., and S. Gaines. 2003. Propagule dispersal in marine and terrestrial environments: a community perspective. Ecology 84: 2007–2020.

Kitching, J. A., T. T. Macan, and H. C. Gilson. 1934. Studies in Sublittoral Ecology. I. A Submarine Gully in Wembury Bay, South Devon. J. Mar. Biol. Assoc. United Kingdom 19: 677–705.
Kjellman, F. R. 1883. The Algae of the Arctic Sea.
Konar, B. 2013. Lack of recovery from disturbance in high-arctic boulder communities. Polar Biol. 36: 1205–1214.
Konar, B., and K. Iken. 2005. Competitive dominance among sessile marine organisms in a high Arctic boulder community. Polar Biol. 29: 61–64.
Kortsch, S., R. Primicerio, F. Beuchel, P. E. Renaud, J. Rodrigues, O. J. Lønne, and B. Gulliksen. 2012. Climate-driven regime shifts in Arctic marine benthos. Proc. Natl. Acad. Sci. U. S. A. 109: 14052–7.
Krause-Jensen, D., and C. M. Duarte. 2014. Expansion of vegetated coastal ecosystems in the future Arctic. Front. Mar. Sci. 1: 1–10.
Krause-Jensen, D., N. Marbà, B. Olesen, and others. 2012. Seasonal sea ice cover as principal driver of spatial and temporal variation in depth extension and annual production of kelp in Greenland. Glob. Chang. Biol. 18: 2981–2994.
Krause-Jensen, D., N. Marbà, M. Sanz-Martin, I. E. Hendriks, J. Thyrring, J. Carstensen, M. K. Sejr, and C. M. Duarte. 2016. Long photoperiods sustain high pH in Arctic kelp forests. Sci. Adv. 2: e1501938.
Kroeker, K. J., M. C. Gambi, and F. Micheli. 2013. Community dynamics and ecosystem simplification in a high-CO2 ocean. Proc. Natl. Acad. Sci. U. S. A. 110: 12721–6.
Kroeker, K. J., F. Micheli, and M. C. Gambi. 2012. Ocean acidification causes ecosystem shifts via altered competitive interactions. Nat. Clim. Chang. 2: 1–4. 0
Krumhansl, K. A., D. K. Okamoto, A. Rassweiler, and others. 2016. Global patterns of kelp forest change over the past half-century. Proc. Natl. Acad. Sci. 113: 13785–13790.
Kuklinski, P. 2009. Ecology of stone-encrusting organisms in the Greenland Sea-a review. Polar Res. 28: 222–237.
Kuklinski, P., J. Berge, L. McFadden, K. Dmoch, M. Zajaczkowski, H. Nygård, K. Piwosz, and A. Tatarek. 2013. Seasonality of occurrence and recruitment of Arctic marine benthic invertebrate larvae in relation to environmental variables. Polar Biol. 36: 549–560.
Lane, C. E., C. Mayes, L. D. Druehl, and G. W. Saunders. 2006. a Multi-Gene Molecular Investigation of the Kelp (Laminariales, Phaeophyceae) Supports Substantial Taxonomic Re-Organization1. J. Phycol. 42: 493–512.
Lantuit, H., P. P. Overduin, N. Couture, and others. 2012. The Arctic Coastal Dynamics Database: A New Classification Scheme and Statistics on Arctic Permafrost Coastlines. Estuaries and Coasts 35: 383–400.
Legendre, P., and M. J. Anderson. 1999. Distance-Based Redundancy Analysis: Testing Multispecies Responses in Multifactorial Ecological Experiments. Ecol. Monogr. 69: 1.
Leibold, M. a., M. Holyoak, N. Mouquet, and others. 2004. The metacommunity concept: a framework for multi-scale community ecology. Ecol. Lett. 7: 601–613.

Lind, A. C., and B. Konar. 2017. Effects of abiotic stressors on kelp early life-history stages. Algae 32: 223–233.
Lüning, K., and M. J. Dring. 1979. Continuous underwater light measurement near Helgoland (North Sea) and its significance for characteristic light limits in the sublittoral region. Helgolander Wiss. Meeresunters 32: 403–424.
Macdonald, R. W., and Y. Yu. 2006. The Mackenzie Estuary of the Arctic ocean. Handb. Environ. Chem. Vol. 5 Water Pollut. 5: 91–120.
Mahoney, A. R., H. Eicken, A. G. Gaylord, and R. Gens. 2014. Landfast sea ice extent in the Chukchi and Beaufort Seas: The annual cycle and decadal variability. Cold Reg. Sci. Technol. 103: 41–56.
Markus, T., J. C. Stroeve, and J. Miller. 2009. Recent changes in Arctic sea ice melt onset, freezeup, and melt season length. J. Geophys. Res. Ocean. 114: 1–14.
Martin, L., and B. Gallaway. 1994. The effects of the Endicott Development Project on the Boulder Patch, an arctic kelp community in Stefansson Sound, Alaska. Arctic 47: 54–64.
Matthews, J. B. 1981a. Observations of under-ice circulation in a shallow lagoon in the Alaskan Beaufort Sea. Ocean Manag. 6: 223–234.
Matthews, J. B. 1981b. Observations of surface and bottom currents in the Beaufort Sea near Prudhoe Bay, Alaska. J. Geophyisical Res. 86: 6653–6660.
McClelland, J. W., S. J. Déry, B. J. Peterson, R. M. Holmes, and E. F. Wood. 2006. A pan-arctic evaluation of changes in river discharge during the latter half of the 20th century. Geophys. Res. Lett. 33: 2–5.
McClelland, J. W., R. M. Holmes, K. H. Dunton, and R. W. Macdonald. 2012. The Arctic Ocean Estuary. Estuaries and Coasts 35: 353–368.
McClelland, J. W., A. Townsend-Small, R. M. Holmes, F. Pan, M. Stieglitz, M. Khosh, and B. J. Peterson. 2014. River export of nutrients and organic matter from the North Slope of Alaska to the Beaufort Sea. Water Resour. Res. 50: 1823–1839.
Mccoy, S. J., and N. A. Kamenos. 2015. Coralline algae (Rhodophyta) in a changing world: Integrating ecological, physiological, and geochemical responses to global change. J. Phycol. 51: 6–24.
McDevit, D. C., and G. W. Saunders. 2009. On the utility of DNA barcoding for species differentiation among brown macroalgae (Phaeophyceae) including a novel extraction protocol. Phycol. Res. 57: 131–141.
McDevit, D., and G. Saunders. 2010. A DNA barcode examination of the Laminariaceae (Phaeophyceae) in Canada reveals novel biogeographical and evolutionary insights. Phycologia 49: 235–248.
McMeans, B. C., K. S. McCann, M. Humphries, N. Rooney, and A. T. Fisk. 2015. Food web structure in temporally-forced ecosystems. Trends Ecol. Evol. 30: 662–672.
McPhee, M. G., A. Proshutinsky, J. H. Morison, M. Steele, and M. B. Alkire. 2009. Rapid change in freshwater content of the Arctic Ocean. Geophys. Res. Lett. 36: 1–6.

Meirmans, P. G., and P. H. Van Tienderen. 2004. GENOTYPE and GENODIVE: Two programs for the analysis of genetic diversity of asexual organisms. Mol. Ecol. Notes 4: 792–794.
Meyer, K. S., A. K. Sweetman, P. Kuklinski, and others. 2017. Recruitment of benthic invertebrates in high Arctic fjords: Relation to temperature, depth, and season. Limnol. Oceanogr. 62: 2732–2744.
Michel, C., B. Bluhm, V. Gallucci, and others. 2012. Biodiversity of Arctic marine ecosystems and responses to climate change. Biodiversity 13: 200–214.
Michel, C., R. G. Ingram, and L. R. Harris. 2006. Variability in oceanographic and ecological processes in the Canadian Arctic Archipelago. Prog. Oceanogr. 71: 379–401.
Morison, J., R. Kwok, C. Peralta-Ferriz, M. Alkire, I. Rigor, R. Andersen, and M. Steele. 2012. Changing Arctic Ocean freshwater pathways. Nature 481: 66–70.
Müller, R., T. Laepple, I. Bartsch, and C. Wiencke. 2009. Impact of oceanic warming on the distribution of seaweeds in polar and cold-temperate waters. Bot. Mar. 52: 617–638.
Neiva, J., C. Paulino, M. M. Nielsen, and others. 2018. Glacial vicariance drives phylogeographic diversification in the amphi-boreal kelp Saccharina latissima. Sci. Rep. 8: 1–12.
Norton, T. 1992. Dispersal by macroalgae. Br. Phycol. J. 27: 293–301.
O'Brien, M. C., R. W. Macdonald, H. Melling, and K. Iseki. 2006. Particle fluxes and geochemistry on the Canadian Beaufort Shelf: Implications for sediment transport and deposition. Cont. Shelf Res. 26: 41–81.
Oksanen, O., Blanchet, F.G., Kindt, R., et al. 2016. Vegan Community Ecology Package. R Package Version 2.3-5
Van Oosterhout, C., W. F. Hutchinson, D. P. M. Wills, and P. Shipley. 2004. MICRO-CHECKER: Software for identifying and correcting genotyping errors in microsatellite data. Mol. Ecol. Notes 4: 535–538.
Overeem, I., R. S. Anderson, C. W. Wobus, G. D. Clow, F. E. Urban, and N. Matell. 2011. Sea ice loss enhances wave action at the Arctic coast. Geophys. Res. Lett. 38: 1–6.
Parkinson, C. L. 2014. Spatially mapped reductions in the length of the Arctic sea ice season. Geophys. Res. Lett. 41: 4316–4322.
Pequegnat, W. E. 1964. The epifauna of a California siltstone reef. Ecology 45: 272–283.
Pessarrodona, A., A. Foggo, and D. A. Smale. 2018. Can ecosystem functioning be maintained despite climate-driven shifts in species composition? Insights from novel marine forests. J. Ecol. 91–104.
Polis, G. A., and S. D. Hurd. 1996. Linking Marine and Terrestrial Food Webs: Allochthonous Input from the Ocean Supports High Secondary Productivity on Small Islands and Coastal Land Communities. Am. Nat. 147: 396–423.
Post, E., U. S. Bhatt, C. M. Bitz, and others. 2013. Ecological consequences of sea-ice decline. Science 341: 519–24.

Probyn, T. A., and C. D. McQuaid. 1985. In-situ measurements of nitrogenous nutrient uptake by kelp (Ecklonia maxima) and phytoplankton in a nitrate-rich upwelling environment. Mar. Biol. 88: 149–154.

R Core Team R: A language and environment for statistical computing 2016 R Foundation for Statistical Computing Vienna, Austria<https://www.R-project.org/>.

Raimondi, P. T. P. T., D. C. C. Reed, B. Gaylord, and L. Washburn. 2004. Effects of self-fertilization in the giant kelp, Macrocystis pyrifera. Ecology 85: 3267–3276.

Reed, D., C. Amsler, and A. Ebeling. 1992. Dispersal in kelps: factors affecting spore swimming and competency. Ecology 73: 1577–1585.

Reid, P. C., D. G. Johns, M. Edwards, M. Starr, M. Poulin, and P. Snoeijs. 2007. A biological consequence of reducing Arctic ice cover: arrival of the Pacific diatom Neodenticula seminae in the North Atlantic for the first time in 800 000 years. Glob. Chang. Biol. 13: 1910–1921.

Reimnitz, E. 2000. Interactions of river discharge with sea ice in proximity of arctic deltas: A review. Polarforschung 70: 123–134.

Reimnitz, E., S. M. Graves, and P. W. Barnes. 1988. Beaufort Sea coastal erosion, shoreline evolution, and sediment flux. US Department of the Interior, Geological Survey.

Robuchon, M., L. Le Gall, S. Mauger, and M. Valero. 2014. Contrasting genetic diversity patterns in two sister kelp species co-distributed along the coast of Brittany, France. Mol. Ecol. 23: 2669–2685.

Rothman, M. D., L. Mattio, R. J. Anderson, and J. J. Bolton. 2017. A phylogeographic investigation of the kelp genus Laminaria (Laminariales, Phaeophyceae), with emphasis on the South Atlantic Ocean. J. Phycol. 53: 778–789.

Rousseau, F., B. de-Reviers, M. C. Leclerc, A. Asensi, and R. Delepine. 2000. Adenocystaceae fam. nov. (Phaeophyceae) based on morphological and molecular evidence. Eur. J. Phycol. 35: 35–43.

Rousseau, F., and B. De Reviers. 1999. Phylogenetic relationships within the fucales (phaeophyceae) based on combined partial ssu + lsu rdna sequence data. Eur. J. Phycol. 34: 53–64.

Rousset, F., 2008. Genepop'007: a complete reimplementation of the Genepop software for Windows and Linux. Mol. Ecol. Resources 8: 103-106.

Sakai, A. K., F. W. Allendorf, J. S. Holt, and others. 2001. The Population Biology of Invasive Species. Annu. Rev. Ecol. Syst. 32: 305–332.

Santelices, B. (2014). Patterns of reproduction, dispersal and recruitment inseaweeds. Ocean. Mar Biol. 28: 177-276

Saunders, G. W. 2014. Long distance kelp rafting impacts seaweed biogeography in the Northeast Pacific: the kelp conveyor hypothesis. J. Phycol. 50: 968–974.

Schoenrock, K. M., M. Bacquet, D. Pearce, B. R. Rea, J. E. Schofield, J. Lea, D. Mair, and N. Kamenos. 2018. Influences of salinity on the physiology and distribution of the Arctic coralline algae, Lithothamnion glaciale (Corallinales, Rhodophyta). J. Phycol. 702: 690–702.

Scholin, C. A., M. Herzog, M. Sogin, and D. M. Anderson. 1994. Identification of group - and strain - specific genetic markersfor globally distributed Alexandrium (Dinophyceae) II. Sequenceanalysis of a fragment of the LSU rRNA gene. J. Phycol. 30: 999–1011.
Sebens, K. P. 1984. Water flow and coral colony size: Interhabitat comparisons of the octocoral Alcyonium siderium. Proc. Natl. Acad. Sci. 81: 5473–5477.
Sellmann, P. V., A. J. Delaney, E. J. Chamberlain, and K. H. Dunton. 1992. Seafloor temperature and conductivity data from Stefansson Sound, Alaska. Cold Reg. Sci. Technol. 20: 271–288.
Serreze, M. C., and J. C. Stroeve. 2015. Arctic sea ice trends, variability and implications for seasonal ice forecasting. Philos. Trans. R. Soc. A Math. Phys. Eng. Sci. 373: 20140159.
Smith, L. C., and S. R. Stephenson. 2013. New Trans-Arctic shipping routes navigable by midcentury. Proc. Natl. Acad. Sci. U. S. A. 110: E1191-5.
Sonnenberg, R., A. Nolte, and D. Tautz. 2007. An evaluation of LSU rDNA D1-D2 sequences for their use in species identification. Front. Zool. 4: 1–12.
Spurkland, T., and K. Iken. 2011. Kelp Bed Dynamics in Estuarine Environments in Subarctic Alaska. J. Coast. Res. 275: 133–143.
Stam, W. T., P. V. M. Bot, S. A. Boele-Bos, J. M. van Rooij, and C. van den Hoek. 1988. Single-copy DNA-DNA hybridizations among five species of Laminaria (Phaeophyceae): Phylogenetic and biogeographic implications. Helgoländer Meeresuntersuchungen 42: 251–267.
Steneck, R. 1986. The Ecology of Coralline Algal Crusts: Convergent Patterns and Adaptative Strategies. Annu. Rev. Ecol. Syst. 17: 273–303.
Steneck, R. S., M. H. Graham, B. J. Bourque, D. Corbett, J. M. Erlandson, J. A. Estes, and M. J. Tegner. 2002. Kelp forest ecosystems: biodiversity, stability, resilience and future. Environ. Conserv. 29.
Stoeck, T., E. Przybos, and M. Dunthorn. 2014. The D1-D2 region of the large subunit ribosomal DNA as barcode for ciliates. Mol. Ecol. Resour. 14: 458–468.
Stroeve, J. C., T. Markus, L. Boisvert, J. Miller, and A. Barrett. 2014. Changes in Arctic melt season and implifications for sea ice loss. Geophys. Res. Lett. 41: 1216–1225.
Sundene, O., 1953. The algal vegetation of Oslofjord.Skr. Nor. Videnak. Akad 2:244 p.
Teagle, H., S. J. Hawkins, P. J. Moore, and D. A. Smale. 2017. The role of kelp species as biogenic habitat formers in coastal marine ecosystems. J. Exp. Mar. Biol. Ecol. Spec. Issue.
Thomson, J., Y. Fan, S. Stammerjohn, and others. 2016. Emerging trends in the sea state of the Beaufort and Chukchi seas. Ocean Model. 105: 1–12.
tom Dieck, I. 1993. Temperature tolerance and survival in darkness of kelp gametophytes (Laminariales, Phaeophyta) - Ecological and biogeographical implications. Mar. Ecol. Prog. Ser. 100: 253–264.
Traiger, S. B., and B. Konar. 2017. Supply and survival: Glacial melt imposes limitations at the kelp microscopic life stage. Bot. Mar. 60: 603–617. Vadas, R. L., and R. S.

Steneck. 1988. Zonation of Deep Water Benthic Algae in the Gulf of Maine. J. Phycol. 24: 338–346.
Vadas, R. L., and R. S. Steneck. 1988. Zonation of Deep Water Benthic Algae in the Gulf of Maine. J. Phycol. 24: 338–346.
Valero, M., C. Engel, C. Billot, B. Kloareg, and C. Destombe. 2001. Concepts and issues of population genetics in seaweeds. Cah. Biol. Mar. 42: 53–62.
Vergés, A., C. Doropoulos, H. A. Malcolm, and others. 2016. Long-term empirical evidence of ocean warming leading to tropicalization of fish communities, increased herbivory, and loss of kelp. 1–6.
Vermeij, G. J., and P. D. Roopnarine. 2008. The Coming Arctic Invasion. Science. 321: 780–781.
Vetter, E. 1995. Detritus-based patches of high secondary production in the nearshore benthos. Mar. Ecol. Prog. Ser. 120: 251–262.
Walker, T. R., J. Grant, P. Cranford, D. G. Lintern, P. Hill, P. Jarvis, J. Barrell, and C. Nozais. 2008. Suspended sediment and erosion dynamics in Kugmallit Bay and Beaufort Sea during ice-free conditions. J. Mar. Syst. 74: 794–809.
Wassmann, P. 2011. Arctic marine ecosystems in an era of rapid climate change. Prog. Oceanogr. 90: 1–17.
Wassmann, P., C. M. Duarte, S. Agustí, and M. K. Sejr. 2011. Footprints of climate change in the Arctic marine ecosystem. Glob. Chang. Biol. 17: 1235–1249.
Wassmann, P., and M. Reigstad. 2011. Future Arctic Ocean Seasonal Ice Zones and Implications for Pelagic-Benthic Coupling. Oceanography 24: 220–231.
Wegner, C., J. A. Hölemann, I. Dmitrenko, S. Kirillov, K. Tuschling, E. Abramova, and H. Kassens. 2003. Suspended particulate matter on the Laptev Sea shelf (Siberian Arctic) during ice-free conditions. Estuar. Coast. Shelf Sci. 57: 55–64.
Weingartner, T. J., S. L. Danielson, R. A. Potter, J. H. Trefry, A. Mahoney, M. Savoie, C. Irvine, and L. Sousa. 2017. Circulation and water properties in the landfast ice zone of the Alaskan Beaufort Sea. Cont. Shelf Res. 148: 185–198.
Wernberg, T., S. Bennett, R. C. Babcock, and others. 2016. Climate-driven regime shift of a temperate marine ecosystem. Science. 353: 169–172.
Wiencke, C., M. N. Clayton, I. Gómez, and others. 2006. Life strategy, ecophysiology and ecology of seaweeds in polar waters. Rev. Environ. Sci. Bio/Technology 6: 95–126.
Witman, J. & Dayton, P. (2001) Rocky subtidal communities. In: Marine Community Ecology, ed. M. Bertness, S. Gaines & M. Hay, pp. 339–366. Sunderland, MA, USA: Sinauer Press.
Wood, K. R., N. A. Bond, S. L. Danielson, J. E. Overland, S. A. Salo, P. J. Stabeno, and J. Whitefield. 2015. A decade of environmental change in the Pacific Arctic region. Prog. Oceanogr. 136: 12–31.
Wood, K. R., J. E. Overland, S. A. Salo, N. A. Bond, W. J. Williams, and X. Dong. 2013. Is there a “new normal” climate in the Beaufort Sea? Polar Res. 32: 1–9.
Yendo, K. 1914. On the cultivation of seaweeds, with special accounts of their ecology. Economic Proceedings of the Royal Dublin Society 2: 105–122

Zacher, K., M. Bernard, I. Bartsch, and C. Wiencke. 2016. Survival of early life history stages of Arctic kelps (Kongsfjorden, Svalbard) under multifactorial global change scenarios. Polar Biol. 39: 2009–2020.

Zuccarello, G., and G. Lokhorst. 2005. Molecular phylogeny of the genus Tribonema (Xanthophyceae) using rbc L gene sequence data: monophyly of morphologically simple algal species. Phycologia 44: 384–392.